The Structure of Carbon Dioxide Adsorbed on a Sodium Chloride(001) Surface

Mohammad-Ali Saberi

A Thesis
in
The Department
of
Chemistry and Biochemistry

Presented in Partial Fulfilment of the Requirements
for the Degree of Master of Science at
Concordia University
Montreal, Quebec, Canada

August 1996

ISBN 0-612-18435-8

Canada

Name Mohammad-Ali Saberi

Dissertation Abstracts International is arranged by broad, general subject categories. Please select the one subject which most nearly describes the content of your dissertation. Enter the corresponding four-digit code in the spaces provided.

Physical Chemistry — SUBJECT TERM

0495 — SUBJECT CODE

UMI

Subject Categories

THE HUMANITIES AND SOCIAL SCIENCES

COMMUNICATIONS AND THE ARTS

Architecture 0729
Art History 0377
Cinema 0900
Dance 0378
Fine Arts 0357
Information Science 0723
Journalism 0391
Library Science 0399
Mass Communications 0708
Music 0413
Speech Communication 0459
Theater 0465

EDUCATION

General 0515
Administration 0514
Adult and Continuing 0516
Agricultural 0517
Art 0273
Bilingual and Multicultural 0282
Business 0688
Community College 0275
Curriculum and Instruction 0727
Early Childhood 0518
Elementary 0524
Finance 0277
Guidance and Counseling 0519
Health 0680
Higher 0745
History of 0520
Home Economics 0278
Industrial 0521
Language and Literature 0279
Mathematics 0280
Music 0522
Philosophy of 0998
Physical 0523
Psychology 0525
Reading 0535
Religious 0527
Sciences 0714
Secondary 0533
Social Sciences 0534
Sociology of 0340
Special 0529
Teacher Training 0530
Technology 0710
Tests and Measurements 0288
Vocational 0747

LANGUAGE, LITERATURE AND LINGUISTICS

Language
- General 0679
- Ancient 0289
- Linguistics 0290
- Modern 0291

Literature
- General 0401
- Classical 0294
- Comparative 0295
- Medieval 0297
- Modern 0298
- African 0316
- American 0591
- Asian 0305
- Canadian (English) 0352
- Canadian (French) 0355
- English 0593
- Germanic 0311
- Latin American 0312
- Middle Eastern 0315
- Romance 0313
- Slavic and East European 0314

PHILOSOPHY, RELIGION AND THEOLOGY

Philosophy 0422
Religion
- General 0318
- Biblical Studies 0321
- Clergy 0319
- History of 0320
- Philosophy of 0322

Theology 0469

SOCIAL SCIENCES

American Studies 0323
Anthropology
- Archaeology 0324
- Cultural 0326
- Physical 0327

Business Administration
- General 0310
- Accounting 0272
- Banking 0770
- Management 0454
- Marketing 0338

Canadian Studies 0385
Economics
- General 0501
- Agricultural 0503
- Commerce-Business 0505
- Finance 0508
- History 0509
- Labor 0510
- Theory 0511

Folklore 0358
Geography 0366
Gerontology 0351
History
- General 0578
- Ancient 0579
- Medieval 0581
- Modern 0582
- Black 0328
- African 0331
- Asia, Australia and Oceania 0332
- Canadian 0334
- European 0335
- Latin American 0336
- Middle Eastern 0333
- United States 0337

History of Science 0585
Law 0398
Political Science
- General 0615
- International Law and Relations 0616
- Public Administration 0617

Recreation 0814
Social Work 0452
Sociology
- General 0626
- Criminology and Penology 0627
- Demography 0938
- Ethnic and Racial Studies 0631
- Individual and Family Studies 0628
- Industrial and Labor Relations 0629
- Public and Social Welfare 0630
- Social Structure and Development 0700
- Theory and Methods 0344

Transportation 0709
Urban and Regional Planning 0999
Women's Studies 0453

THE SCIENCES AND ENGINEERING

BIOLOGICAL SCIENCES

Agriculture
- General 0473
- Agronomy 0285
- Animal Culture and Nutrition 0475
- Animal Pathology 0476
- Food Science and Technology 0359
- Forestry and Wildlife 0478
- Plant Culture 0479
- Plant Pathology 0480
- Plant Physiology 0817
- Range Management 0777
- Wood Technology 0746

Biology
- General 0306
- Anatomy 0287
- Biostatistics 0308
- Botany 0309
- Cell 0379
- Ecology 0329
- Entomology 0353
- Genetics 0369
- Limnology 0793
- Microbiology 0410
- Molecular 0307
- Neuroscience 0317
- Oceanography 0416
- Physiology 0433
- Radiation 0821
- Veterinary Science 0778
- Zoology 0472

Biophysics
- General 0786
- Medical 0760

EARTH SCIENCES

Biogeochemistry 0425
Geochemistry 0996
Geodesy 0370
Geology 0372
Geophysics 0373
Hydrology 0388
Mineralogy 0411
Paleobotany 0345
Paleoecology 0426
Paleontology 0418
Paleozoology 0985
Palynology 0427
Physical Geography 0368
Physical Oceanography 0415

HEALTH AND ENVIRONMENTAL SCIENCES

Environmental Sciences 0768
Health Sciences
- General 0566
- Audiology 0300
- Chemotherapy 0992
- Dentistry 0567
- Education 0350
- Hospital Management 0769
- Human Development 0758
- Immunology 0982
- Medicine and Surgery 0564
- Mental Health 0347
- Nursing 0569
- Nutrition 0570
- Obstetrics and Gynecology 0380
- Occupational Health and Therapy 0354
- Ophthalmology 0381
- Pathology 0571
- Pharmacology 0419
- Pharmacy 0572
- Physical Therapy 0382
- Public Health 0573
- Radiology 0574
- Recreation 0575
- Speech Pathology 0460
- Toxicology 0383

Home Economics 0386

PHYSICAL SCIENCES

Pure Sciences

Chemistry
- General 0485
- Agricultural 0749
- Analytical 0486
- Biochemistry 0487
- Inorganic 0488
- Nuclear 0738
- Organic 0490
- Pharmaceutical 0491
- Physical 0494
- Polymer 0495
- Radiation 0754

Mathematics 0405
Physics
- General 0605
- Acoustics 0986
- Astronomy and Astrophysics 0606
- Atmospheric Science 0608
- Atomic 0748
- Electronics and Electricity 0607
- Elementary Particles and High Energy 0798
- Fluid and Plasma 0759
- Molecular 0609
- Nuclear 0610
- Optics 0752
- Radiation 0756
- Solid State 0611

Statistics 0463

Applied Sciences

Applied Mechanics 0346
Computer Science 0984
Engineering
- General 0537
- Aerospace 0538
- Agricultural 0539
- Automotive 0540
- Biomedical 0541
- Chemical 0542
- Civil 0543
- Electronics and Electrical 0544
- Heat and Thermodynamics 0348
- Hydraulic 0545
- Industrial 0546
- Marine 0547
- Materials Science 0794
- Mechanical 0548
- Metallurgy 0743
- Mining 0551
- Nuclear 0552
- Packaging 0549
- Petroleum 0765
- Sanitary and Municipal 0554
- System Science 0790

Geotechnology 0428
Operations Research 0796
Plastics Technology 0795
Textile Technology 0994

PSYCHOLOGY

General 0621
Behavioral 0384
Clinical 0622
Developmental 0620
Experimental 0623
Industrial 0624
Personality 0625
Physiological 0989
Psychobiology 0349
Psychometrics 0632
Social 0451

ABSTRACT

The Structure of Carbon Dioxide Adsorbed
on a Sodium Chloride(001) Surface

Mohammad-Ali Saberi

Two sets of parameters and potential energy surfaces for a single CO_2 molecule adsorbed on the (001) face of a uniform semi-infinite crystal of NaCl were developed and tested using the Steepest Descent method. When the CO_2 molecule attains the absolute minimum of the potential energy it was found, for both parameter sets, to lie parallel to the surface at height z= 2.5 Å above the connection line of two adjacent Na^+ ions (along the <110> direction) at 1.994 Å from Na^+ (C to Na^+); *i.e.* the carbon atom is directly above the midpoint between two sodium ions. The values of the potential energy were found to be E_{min}= -7.643 kcal/mol and E_{min}= -8.000 kcal/mol for parameters set I and set II respectively. Saddle points in the potential energy surfaces were found to exist above the connection line between Na^+ and Cl^- (the <100> direction). The position of this point correspond to a lateral sodium to carbon distance of 0.92 Å and a carbon height of z=2.95 Å above the surface for parameter set I. At this position the molecule is tilted by an angle of 35° from surface (55° from the surface normal). The potential energy at this point was found to be E_{sad} = -5.723 kcal/mol which yielded an estimated diffusion barrier energy of E_{diff} = 1.918 kcal/mol. The parameter set II was examined the similar results was obtained.

The single molecule surface potential which was developed was then used within the Metropolis Monte Carlo method to examine monolayer, bilayer and trilayer configurations of CO_2 on an NaCl(001) surface. In particular, the average potential energy, position, and orientation of the molecules were calculated. The results show that the monolayer and multilayer systems have a stable $p(2\times1)$ structure (herringbone-like pattern) with two CO_2 molecules in each unit cell related via a glide plane. For a monolayer the average potential energy at 90 K was found to be -8.021 kcal/mol which is consistent with the experimental heat of adsorption of -8.51±0.31 kcal/mol. The molecules were found to sit in the saddle point sites at an angle of 60° from the surface normal.

In the bilayer system, both layers adopted a stable $p(2\times1)$ structure (both in a herringbone-like pattern) with the second layer offset from the first layer. Once again the molecules were tilted by 60°. The trilayer system was found to be unstable and showed evidence of the emergence of a $c(2\times2)$ structure at the expense of the less compact $p(2\times1)$ structure. Four layer and five layer systems were similarly found to be unstable.

ACKNOWLEDGEMENTS

Many thanks to Dr. D. Jack, my research supervisor. I have greatly benefited from his comments and constructive criticisms. I would also like to thank the members of my Research Committee, Dr. M. Lawrence and Dr. G. Dénés, whose advice and interest were helpful towards the completion of this thesis. Thanks to Thanh Vu, Araz Jakalian and Wei Hu for being helpful to me in my studies.

TABLE OF CONTENTS

LIST OF FIGURES

LIST OF TABLES

1. INTRODUCTION

The determination of adsorbate structure and heats of adsorption are important aspects of surface science. The theoretical interpretation is important for understanding processes such as the collision of molecules with surfaces, the adsorption-desorption of physisorbed species, and the mobility of adlayers or films [1]. The physisorption of small molecules on alkali halide single crystal surfaces is of interest from both the experimental and theoretical point of view. Because not much is known about the symmetry and structure of adsorbates on insulator surfaces. Also solid carbon dioxide and alkali halides such as NaCl, LiF have a cubic unit cell with similar lattice constants and thus form convenient systems for the study of gas-solid phase transition, epitaxial growth and the structure of the monolayer and multilayers.

The interactions between adsorbate and substrate are electrostatic and van der Waals in nature, and largely consist of two-body type interactions. Since these interactions are better understood than the interactions in analogous metal systems, the alkali halides are ideal substrates for studying the structure and dynamics of the adsorbate and their phase transitions. The principal means of studying these systems is through the use of neutral beams like helium atoms and infrared radiation. These methods give good results because there is no surface charging problem as in Low Energy Electron Diffraction (LEED). The structure and dynamics of CO_2 on NaCl(001) surface have been studied during the last few decades using Fourier Transform Infrared Spectroscopy (FTIR),

Helium Atom Scattering (HAS) and other methods.

The CO_2/NaCl(001) system is ideal for surface science studies because the admolecules are only slightly perturbed by the presence of the surface. This is due to the physisorptive nature of the adsorbate-substrate interaction and the fact that the substrate and adsorbate have similar crystallographic structures with lattice constants which differ by only 1.26% (dCO_2 =5.575 Å and dNaCl= 5.646 Å). As a result, the substrate can act as a template on which ordered adlayers can nucleate and subsequently grow epitaxially. This system is therefore amenable to examination, by theoretical and experimental means, of a number of issues of both academic and technological interest. Among these are:

1) Thermodynamics of adsorption.
2) 2-D phase transitions (2D-gas to 2D-solid).
3) Adlayer nucleation and growth modes.
4) Molecular interaction potentials.

Information obtained from the examination of these topics is important for understanding more complex systems and processes such as:

1) Heterogeneous catalysis.
2) Photodissociation and photoinduced reactions at surfaces.
3) Adsorption of gases on granular substrates (*e.g.* graphite, zeolites).
4) Interfacial structures and properties.
5) Organic and biomolecules at surfaces *e.g.* SAMs and biosensors.

For the CO_2/NaCl(001) system, we decided to calculate the binding energy, position of the adsorption site, and the orientation of a single CO_2 molecule as well as the structure and stability of a monolayer and multilayers on the NaCl(001) surface.

1.1 Historical background

The infrared spectrum of carbon dioxide on a sodium chloride film was first reported by Kozirovski and Folman[2]. Based on coverage behaviour of the bending doublet they reported that there is only one kind of adsorption site, and that carbon dioxide has a non-perpendicular orientation with respect to the surface[2]. The heat of adsorption of an isolated molecule has been experimentally measured by Hayakawa to be 6.07 kcal/mol and estimated from calculations to be 5.42 kcal/mol[3].

The monolayer structure of carbon dioxide on sodium chloride surface has been studied by Ewing's group using infrared spectroscopy. They mentioned that there are two tilted molecules per unit cell, arranged in herringbone fashion and tilted by an angle of 68° from the surface normal[4]. Schaich's group did calculations[5] for the asymmetric stretch of adsorbed monolayer carbon dioxide on sodium chloride surface for s- and p-polarized radiation and obtained agreement with Ewing's experimental results.

Heidberg's group did Fourier Transform Infrared Spectroscopy (FTIR) using different isotopes of carbon dioxide on sodium chloride surface. They studied 2D gas-solid transition by changing the pressure of CO_2 and they found the structure of adsorbed monolayer CO_2 on NaCl(001) surface. They reported that there are two molecules in each unit cell arranged in herringbone fashion related via a glide plane. The angle between the projection of molecular axes is 80°±5° and the angle between each molecular axis and the surface normal is 56°±5°. They found that monolayer CO_2 has a $p(2\times 1)$ structure. They also did calculations of the surface potential of a single CO_2 molecule on sodium chloride surface and found an absolute potential minimum with V_{min}=-16.85 kJ/mol=-4.03 kcal/mol which roughly is half of the measured value q_{st}=32.4±1.1 kJ/mol=7.74±0.26 kcal/mol[7]. The CO_2 molecule was found to lie above the center of the connection line between two adjacent Na^+ ions with the molecular axis parallel to the surface. A second minimum with V_{min}=-15.56 kJ/mol=-3.72 kcal/mol was found above the connection line between Na^+ and Cl^- ions with CO_2 molecule tilted by 41.2° from the surface normal[6-9].

Scoles' group used low-energy helium diffraction to study CO_2 overlayers physisorbed on NaCl(001). They reported a $(2\sqrt{2}\times 2\sqrt{2})$ **R**45° structure for monolayer and multilayer systems and $p(2\times 1)$ structure for submonolayer system[10,11]. Toennies' group studied the structure and dynamics of CO_2 on NaCl(001) by helium atom scattering, they reported a $p(2\times 1)$ structure for the monolayer system and a $c(2\times 2)$ structure for multilayer systems[12].

In order to determine which of these experimental findings' is correct our laboratory did energy minimization of a single CO_2 molecule on NaCl(001) surface and Monte Carlo simulations of monolayer and multilayer structures. These results are described in this thesis.

1.2 Adsorption

There are two types of adsorption phenomena: chemical adsorption and physical adsorption. Chemical adsorption (chemisorption) occurs with electron transfer between adsorbate and substrate to form a chemical bond. The adsorbed molecules are held to the surface by covalent forces of the same general type as those occurring between bound atoms in molecules. The heat evolved per mole for this type of adsorption is usually comparable to that evolved in chemical bonding, namely 100 to 500 kJ. The adsorption of oxygen, sulfur dioxide and carbon monoxide on some metals are of the chemical adsorption type.

In physical adsorption, the forces are of a physical nature; namely, of the electrostatic and van der Waals type. As a results, the adsorption bond is relatively weak. The heat evolved when a mole of gas becomes physisorbed is typically less than 50 kJ and often less than 20 kJ. This type of adsorption plays only a minor role in catalysis, except for certain special types of reactions involving free atoms or radicals. The adsorption of carbon dioxide, carbon monoxide and hydrogen molecule on alkali halide surface are examples of physisorption[13].

In order to obtain the adsorption potential energy of carbon dioxide on a sodium chloride surface, molecule-surface and molecule-molecule interactions must be considered. Fortunately these interactions can be regarded as the sum of two body interactions. The total adsorption potential of a central molecule on the surface is the sum of the molecule - surface interaction and the molecule - molecule interaction.

1.2.1. Adsorption energy

The adsorption energy is the energy required to carry a gas molecule with energy equal to H_g into the most favorable adsorption site with the surface binding energy E_0 at T=0 K. The adsorption energy q_{st} (isosteric heat of adsorption) can be expressed as below[14,15,16],

$$H_g = \frac{n}{2} k_B T + PV = \left(\frac{n+2}{2}\right) k_B T \tag{1.2.1}$$

$$H_s = E_0 + \sum_{\alpha=1}^{n} \frac{\hbar\omega_\alpha}{2} \coth\left(\frac{\hbar\omega_\alpha}{2k_B T}\right) \tag{1.2.2}$$

$$q_{st} = H_g - H_s = \left(\frac{n+2}{2}\right) k_B T - E_0 - \sum_{\alpha=1}^{n} \frac{\hbar\omega_\alpha}{2} \coth\left(\frac{\hbar\omega_\alpha}{2k_B T}\right) \tag{1.2.3}$$

where H_g is the enthalpy of the 3-D gas phase, H_s is the enthalpy of the 2-D gas phase on the surface and n is the number of degrees of freedom of the molecule k_B is the Boltzmann constant, T is the absolute temperature, ω_α is the frequency for the αth degree of freedom (vibration or libration on the surface). For CO_2 molecules in both the 3-D gas phase

and 2-D gas phase on the surface, $n = 5$ (3 translations + 2 rotations for 3-D and 3 vibrations with respect to the surface + 2 librations for 2-D), assuming the internal vibrational modes of the molecule are ignored.

In high temperature limit, *i.e* $\frac{\hbar\omega_\alpha}{2k_BT} << 1$ so that $\coth\left(\frac{\hbar\omega_\alpha}{2k_BT}\right) \approx \frac{2k_BT}{\hbar\omega_\alpha}$, equation (1.2.3) becomes.

$$q_{st} = \left(\frac{n+2}{2}\right) k_BT - E_0 - nk_BT \tag{1.2.4}$$

or,

$$q_{st} = -E_0 - \left(\frac{n-2}{2}\right) k_BT \tag{1.2.5}$$

If $n = 5$ then equation (1.2.5) will be as below.

$$q_{st} = -E_0 - \frac{3}{2} k_BT \tag{1.2.6}$$

Using equation (1.2.6) and the experimental value of the isosteric heat of adsorption at 90 K (32.4 ±1.1 kJ/mol)[7], the isosteric heat of adsorption at 0 K was estimated to be 33.5±1.1 kJ/mol=8±0.26 kcal/mol.

1.3. Molecule - molecule interaction

The interaction of two molecules, separated by distance r, may be expressed in terms of the interaction potential energy U(r). The interaction potential energy is the sum of electrostatic (coulombic), repulsion (Pauli exclusion) and dispersion interactions and orientation dependent terms. These interactions are considered to be of the two body type so that the total potential is the sum of all two body interactions. Since this interaction is short-ranged it is convenient to arrange that the potential energy U take zero value at infinite distance. In general, intermolecular energies and forces depend on the relative orientation of the two interacting molecules and their separation. But for spherically symmetric molecules they depend only on the separation r. The intermolecular potential U(r) is equal to the work done to bring the two molecules together to distance r from infinite separation. The intermolecular force F(r) and energy U(r) are given by[17]:

$$F(r) = -\frac{dU(r)}{dr} \tag{1.3.1}$$

$$U(r) = \int_r^\infty F(r)dr \tag{1.3.2}$$

The general form of an intermolecular potential for two interacting inert gas atoms is shown in Figure 1.3.1. The principal features of the potential function is characterized by a small number of parameters. These parameters are:

σ, the collision diameter, the separation at which $U(r) = 0$;

r_m, the separation at which the energy has the minimum value of $-\varepsilon$.

If r is greater than r_m ($r > r_m$) then the intermolecular force is attractive; F(r) has a negative value. If r is smaller than r_m ($r < r_m$) then the intermolecular force is repulsive; F(r) has a positive value. In the region $\sigma < r < r_m$ the intermolecular force is repulsive, but the energy is negative. Potentials of this form have been used to describe molecular interactions in low density gases where collisions between molecules are rare and the molecules spend little time in close contact with each other. In the condensed phase such a simple potential has little chance of accurately describing the molecular interactions; the molecules are always in intimate contact with nearby molecules and are keenly sensitive to the structure and relative orientation of their neighbours.

To obtain a more accurate representation of the intermolecular potential energy of polyatomic molecules like CO, CO_2, NO_2,...*etc.* it is convenient to assume that the molecule-molecule interactions can be expressed as the sum of atom-atom interactions. As a result, attention must be made to the potential function and parameters which characterize the various atom-atom interactions.

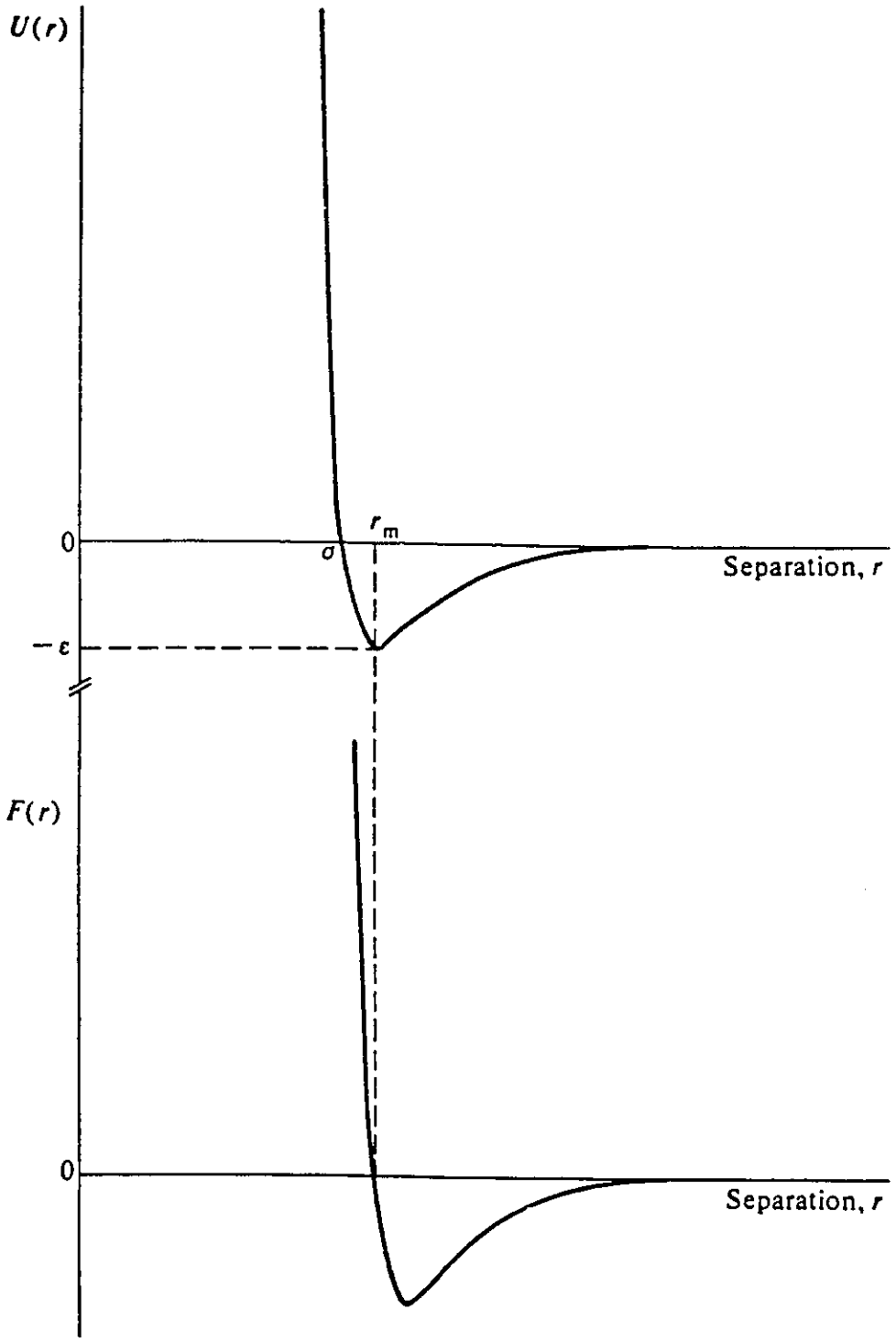

FIGURE 1.3.1. THE INTERMOLECULAR POTENTIAL ENERGY FUNCTION OF TWO INTERACTING INERT GAS ATOMS (*i.e.* He,Ne...) (From ref.[17]).

1.4. Molecule-surface (gas-solid) interaction

A discrete model that is frequently used for molecule-surface interactions considers the surface to consist of a rigid planar array of atoms, ions or molecules having the same characteristics (spacing, symmetry, composition) as the bulk solid. As mentioned previously, pairwise additivity is assumed so that the interaction energy between a single adsorbed molecule and the surface may be evaluated by summing over all the interactions between the constituent atoms of the admolecule and the ions of the solid substrate, *i.e.*

$$U_s(\boldsymbol{r}) = \sum_i U_{gs}(\boldsymbol{r} - \boldsymbol{R}_i) = \sum_i U_{gs}(\boldsymbol{r}_i) \qquad (1.4.1)$$

where $\boldsymbol{R}_i$ is the lattice vector of solid, $U_{gs}(\boldsymbol{r}_i)$ is the interaction energy between the gas-phase molecule and the ith ion in the solid separated by a distance $\boldsymbol{r}_i$ (Figure. 1.4.1)[17]. As suggested by Figure1.4.1, the surface potential can be expressed in terms of a Fourier series as shown below[18,19,20].

$$U_s(x,y,z) = \sum_{n,m} U_{n,m}(z) \cos(\frac{2\pi n}{a}x) \cos(\frac{2\pi m}{a}y) \qquad (1.4.2)$$

where z is the perpendicular distance of the gas molecule from the surface and $n,m = 0,1,2,$ .... defines an infinite series. Usually equation 1.4.2 is truncated at the $n + m = 2$ level.

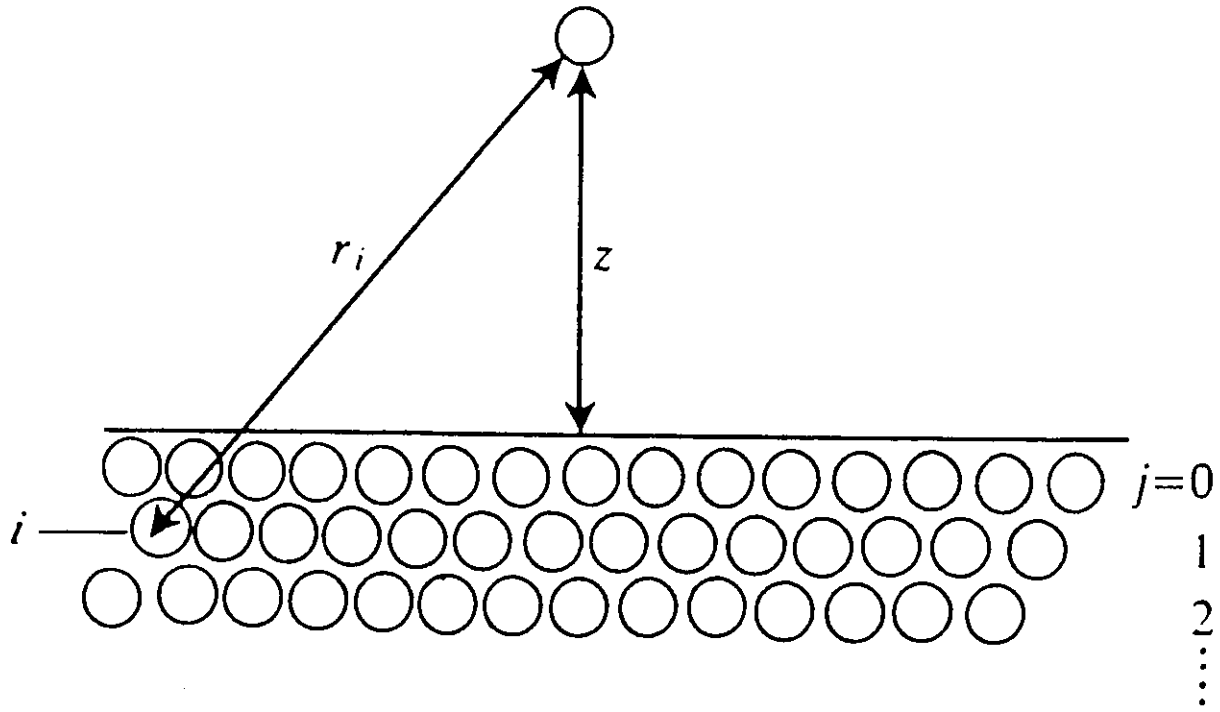

FIGURE 1.4.1 COORDINATES FOR GAS-SURFACE INTERACTION POTENTIAL (From ref.[17]).

2. POTENTIAL FUNCTIONS

The form of the potential functions used in this work are similar to those used by Polanyi's group[18,19]. The potential energy functions of a carbon dioxide molecule adsorbed on a sodium chloride surface is considered to be the pairwise sum of electrostatic, repulsion and dispersion (van der Waals) interactions. This assumption allows the potential interaction to be expressed in terms of two body interactions.

The electrostatic energy of the molecule-surface interactions may be calculated if we know the charge distribution of the molecule and the form of the electrostatic potential and electric field at the solid surface. The electric field $\mathbf{E}(\mathbf{r})$ at the (001) face of a NaCl ionic crystal (face centered-cubic) may be obtained from the electrostatic potential $\Phi(\mathbf{r})$ as follows[18,19,21].

$$\mathbf{E}(\mathbf{r}) = -\nabla\Phi(\mathbf{r}) \tag{2.1}$$

$$\Phi(\mathbf{r}) = \frac{4e}{a}\left[\frac{\exp\left(-\frac{2\pi z}{a}\right)}{1+\exp\left(-\sqrt{2}\pi\right)}\right]\left[\cos\left(\frac{2\pi x}{a}\right)+\cos\left(\frac{2\pi y}{a}\right)\right] \tag{2.2}$$

where a is the lattice constant of the NaCl crystal and e is the magnitude of the electronic charge on an individual ion. The coordinate system of the position vector $\mathbf{r}$=(x,y,z) has its origin on the surface at an Na^+ site. The z axis is perpendicular to the surface plane, while the x and y axes are in the surface plane pointing toward adjacent Na^+ sites along the <110> and <110> directions of the NaCl unit cell.

The charge distribution of the CO_2 molecule may be represented by a partial negative charge on each of the O atoms and a compensating partial positive charge on the C atom which represents the charge transfer between atoms when the molecule is formed. In addition, point dipoles are assigned to each of the oxygen atoms (pointing in opposite directions) to represent the polar nature of the C=O bond. The partial charges are coupled with the electrostatic potential $\Phi(\mathbf{r})$ while the point dipoles are coupled with the electric field $\mathbf{E}(\mathbf{r})$ at the NaCl surface (see Equation 2.3 below). The point dipoles $\mathbf{p}_i = \mu_i \mathbf{u}$ are positioned along the unit vector $\mathbf{u} = (\mathbf{r}_1 - \mathbf{r}_2)/|\mathbf{r}_1 - \mathbf{r}_2|$, which points along the CO_2 molecular axis from the O-atom at $\mathbf{r}_2$ to the C-atom at $\mathbf{r}_1$. The orientations and values for the point dipoles and point charges (2 dipole 3 point charge model) reproduce the experimental value of quadrupole moment and estimated value of the hexadecapole moment. A three point charge model reproduces the quadrupole moment and would have been computationally advantageous to use, but such a model cannot reproduce the higher order moments. This situation has been encountered in work on the HBr/LiF(001) system where such a model does not yield an adsorbate orientation consistent with the infrared (IR) experimental results[18,22]. Instead, the two point dipole - three point charge model described above has been used. For this model the electrostatic interaction energy of a single CO_2 molecule on NaCl(001) surface is written as below:

$$V(\boldsymbol{r}_1,\boldsymbol{r}_2) = \sum_{i=1}^{2} \boldsymbol{p}_i \cdot \boldsymbol{E}(\boldsymbol{r}_i) + \sum_{i=1}^{3} q_i \phi(\boldsymbol{r}_i) = \sum_{i=1}^{2} \mu_i \boldsymbol{u} \cdot \boldsymbol{E}(\boldsymbol{r}_i) + \sum_{i=1}^{3} q_i \phi(\boldsymbol{r}_i) \tag{2.3}$$

where the μ_i are point dipoles and the q_i are point charges (the calculations of these values are presented later on).

The repulsion and dispersion interactions, between the NaCl crystal and an adsorbed CO_2 molecule are quantum mechanical in origin. They are treated as being pairwise additive, and the potential is written in terms of two body interactions between each constituent atom of the adsorbed molecule and the individual ions of the substrate. For an atom and an ion separated by a distance **r** the repulsion (Pauli exclusion) and dispersion (van der Waals) interactions potential is assumed to be described by the Tang-Tonnies potential[23],

$$V(r) = A \exp(-\alpha r) - \sum_{n=3}^{\infty} \left[f_{2n}(r) \frac{C_{2n}}{r^{2n}} \right] \tag{2.4}$$

where the Born-Mayer parameters α (decay constant) and A characterize the range and strength of the potential respectively, and

$$f_{2n}(r) = 1 - \sum_{k=0}^{2n} \left[\frac{(\alpha r)^k}{k!} \right] \exp(-\alpha r) \tag{2.5}$$

is a phenomenological damping function which is characterized by the decay constant of the repulsion term. The C_{2n} coefficients define the dispersion series of which the first three terms were retained in the surface potential and only the first term in the molecule-molecule (CO_2-CO_2) potential.

The total potential due to the repulsion and dispersion interactions is obtained by summing all distinct pairs of adsorbate and substrate sites. By adding coulombic interactions to equation (2.4), the following equation (2.6) was obtained and subsequently used in our calculations,

$$V_{ij}(r)=A_{ij}\exp(-\alpha_{ij} r_{ij}) - f_6(r_{ij})\frac{C_6^{ij}}{r_{ij}^6} - f_8(r_{ij})\frac{C_8^{ij}}{r_{ij}^8} - f_{10}(r_{ij})\frac{C_{10}^{ij}}{r_{ij}^{10}}+\frac{q_i q_j}{r_{ij}} \tag{2.6}$$

where $+\frac{q_i q_j}{r_{ij}}$ is the coulombic part, q_i is the partial charge of atom (i), q_j is the partial charge of atom (j) or the charge of ion (j), and r_{ij} is the distance of atom (i) to atom/ion (j). The coefficients C_6^{ij}, C_8^{ij} and C_{10}^{ij} are dispersion constants denoting the strength of the mutually induced dipole-dipole, dipole-quadrupole and quadrupole-quadrupole plus dipole-octopole interactions respectively.

An alternative formulation of the repulsion term is:

$$V_{ij}(r) = (B_i+B_j)\exp[(A_i+A_j - r_{ij}) / (B_i+B_j)] \tag{2.7}$$

where A_i , A_j are repulsion radii, and B_i , B_j are softness parameters. If A_i , A_j , B_i and B_j are in angstroms, then the energy is in units of kcal/mol. The repulsion term of formula (2.6) and formula (2.7) are connected via the equations below:

$$\alpha_{ij} = \frac{1}{B_i + B_j} \tag{2.8}$$

$$A_{ij} = (B_i+B_j)\exp[(A_i+A_j) / (B_i+B_j)] \tag{2.9}$$

In other words, if the A_i , A_j , B_i and B_j are known for the C-C and O-O interactions, then the values of the Born-Mayer parameters, α_{ij} and A_{ij}, may be calculated.

To calculate the values of the Born-Mayer parameters α_{ij} and A_{ij} for two interacting nonidentical atoms, Gilbert[24,25] and Smith[26] proposed a set of combining rules. These combining rules, which can be used to calculate the repulsion parameters for the interaction of the various atom-ion pairs (C-Na^+, C-Cl^-, O-Na^+ and O-Cl^-) required for the CO_2-NaCl surface potential, are shown below:

$$\alpha_{ij} = \frac{2\alpha_{ii}\alpha_{jj}}{\alpha_{ii} + \alpha_{jj}} \tag{2.10}$$

$$A_{ij} = [(\alpha_{ii} + \alpha_{jj}) / (2\alpha_{ii}\alpha_{jj})](A_{ii}\alpha_{ii})^c(A_{jj}\alpha_{jj})^d \tag{2.11}$$

with

$$c = \alpha_{jj} /(\alpha_{ii} + \alpha_{jj}) \tag{2.12}$$

$$d = \alpha_{ii} /(\alpha_{ii} + \alpha_{jj}) \tag{2.13}$$

where α_{ii} and A_{ii} are the parameters for the like atom (C-C, O-O) interactions, while α_{jj} and A_{jj} are the parameters for the like ion (Na^+-Na^+, Cl^--Cl^-) interactions.

The values for the ion-ion repulsion parameters are available in the literature but suitable parameters for the atom-atom (C-C and O-O) repulsion parameters were not available. In order to obtain these latter parameters it was necessary to employ the computer program WMIN (A computer program to model molecules and crystals in terms of potential energy functions)[27]. WMIN is capable of manipulating static and dynamic models of crystals or isolated molecules and able to calculate their energies using interatomic potential functions of the type shown in equation (2.6). This program can be used for a wide variety of materials ranging from ionic crystals to large organic molecules. In our case the energy of a crystal of CO_2 was minimized through the variation of the repulsion parameters (radii and softness parameters) and the partitioning of the dispersion interactions; the values of the A_i and B_i which minimize the energy are the values subsequently used in our calculations of the repulsion parameters. Of course in order to evaluate the potential energy the parameters for the electrostatic and dispersion interactions needed to be specified.

2.1. Electrostatic model of CO_2

Carbon dioxide, which has two symmetric polar bonds, does not have a permanent dipole moment or octopole moment but does have permanent quadrupole and hexadecapole moments. A 3 charge model of the molecule will have partial charges on the C atom (2q) and each of the O atoms (-q). The partial charges for the 3 charge model were calculated using the value of the molecular quadrupole moment and the following equation:

$$\Theta = -2qr_0^2 \qquad (2.14)$$

where Θ is the quadrupole moment which has an experimental value of -4.3 D·Å[28] and r_0 is the length of the C=O bond which has the value of 1.163 Å[29] in the gas phase. Using equation 2.14, the partial charge on the O was calculated to be q_O = -1.590 D·Å^{-1} = -0.3310 e$^-$ (electron charge) so that the charge on the C atom was q_C=+3.180 D·Å^{-1} =+0.6620 e$^-$ (electron charge) (see Figure 2.1).

An alternative model of the charge distribution of the CO_2 molecule is to assign partial charges to the three atomic sites as well as point dipoles μ to each of the O atoms (3 charge-2 dipole model). The dipoles represent the polarity of the C=O bonds. In this model the quadrupole and hexadecapole moments can be expressed in terms of the partial charges and point dipoles through the following equations.

$$\Theta = \sum_{i=1}^{3} q_i r_i^2 + 2\sum_{i=1}^{2} \mu_i r_i = -2qr_0^2 + 4\mu r_0 \qquad (2.15)$$

$$\Lambda = \sum_{i=1}^{3} r_i^4 + 4\sum_{i=1}^{2} \mu_i r_i^3 = -2qr_0^4 + 8\mu r_0^3 = \Theta r_0^2 + 4\mu r_0^3 \qquad (2.16)$$

where Λ is the molecular hexadecapole moment, which has a value of -1.6795 D·Å^3 as calculated by Murthy, O'Shea and McDonald[30] from a wave function due to Stone and Alderton[31].

Using the values of the molecular quadrupole and hexadecapole moments mentioned above the values of the partial charges and point dipoles were calculated. Solving equations (2.15) and (2.16) for μ and q for the 3 charge-2 dipole model yields μ=0.7645 D =0.1592 electron Å, q_O = -2.7201 D·Å^{-1} =-0.5663 electron charge and q_C=+5.4402 D·Å^{-1} =+1.1326 electron charge. In order to use the program WMIN the electrostatic model must be expressed in terms of point charges only. To mimic the point dipole moments each dipole was replaced by a pair of point charges thus yielding a "7 charge model". Specifically, charges of -1.5920 electrons were placed between the C atom and each of the O atoms at distance ±1.113 Å from the C atom and balancing charges of +1.5920 electrons were placed on the other side of each of the O atoms at distances of ±1.213 Å from the C atom (using equation 2.17 it was arranged that these positive and negative charges be separated by l=0.1 Å as shown in Figure 2.1). This 7 charge model was subsequently used in WMIN to calculate repulsion and softness parameters,

as well as the ratio of the van der Waals coefficient PL_6C/PL_6O ($C_6 = PL_6 \times PL_6$) for the 3 charge-2 dipole model.

$$\mu = q \times l \tag{2.17}$$

After testing the parameters of each model, it was found that the parameters of the 3 charge-2 dipole electrostatic model gave better results than those of the 3 charge model.

A-THREE - CHARGE MODEL

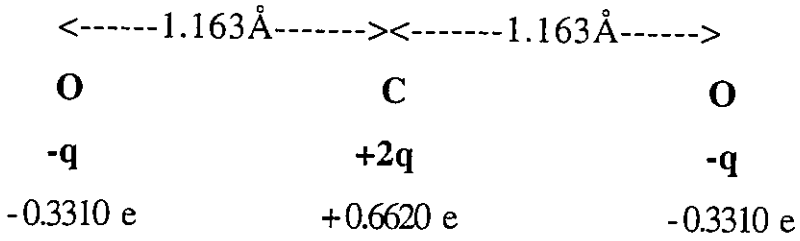

B- SEVEN - CHARGE MODEL

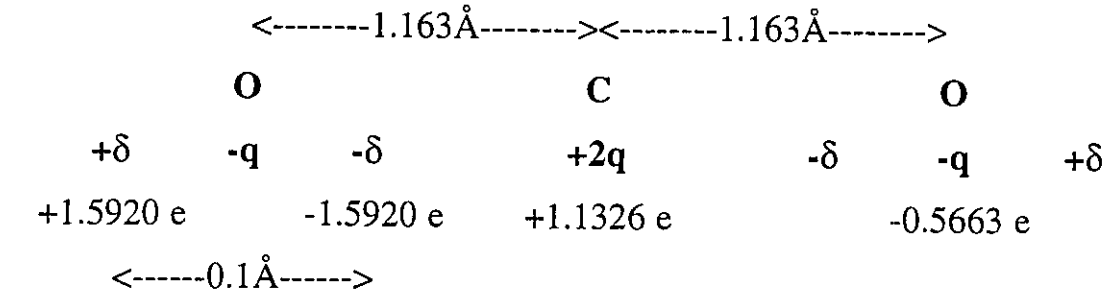

FIGURE 2.1: POINT CHARGE MODELS

2.2. Repulsion parameters

In equation (2.6), the van der Waals and Coulomb terms are known. Using these terms, repulsion parameters (repulsion radii A_i , A_j and softness parameters B_i , B_j) and the distribution of the dispersion interactions between the carbon and oxygen sites have been calculated by WMIN (a more complete discussion of the dispersion interactions is found in section 2.3 that follows). For the 3 charge-2 dipole electrostatic model two parameter sets were calculated. In both cases repulsion and softness parameters were allowed to vary, but in the first case the crystal binding energy was allowed to vary (set I) while in the second case this energy was fixed (set II). The results are shown in Table 2.1.

Repulsion parameters for the CO_2 - NaCl surface potentials were subsequently calculated using the combining rules mentioned previously. Both parameter sets I and II were used in the steepest descent method to further refine the CO_2 - NaCl surface potentials. The resulting Born-Mayer repulsion parameters are summarized in Table 2.2. It should be noted that the parameters A (C-Na^+, *etc.*) were subsequently multiplied by a factor which brought the heat of adsorption into closer agreement with the experimental value. In the Metropolis Monte Carlo simulations parameter set I was used for the surface potential while parameter set II was developed as an alternative set.

TABLE 2.1: REPULSION PARAMETERS FOR CO_2-CO_2 INTERACTION (CALCULATED FROM WMIN).

Parameter	nonfixed lattice energy (final E=-5.582 kcal/mol) set I	fixed lattice energy (E=-6.836 kcal/mol) set II
ArC(radius)Å	1.612	1.618
ArO(radius)Å	1.550	1.553
BrC(softness)Å	0.1429	0.1014
BrO(softness)Å	0.1240	0.0956
PL_6C *	21.77	20.95
PL_6O *	15.01	15.83

*) $(2PL_6O + PL_6C)^2 = C_6 (CO_2)$

TABLE 2.2: REPULSION PARAMETERS FOR CO_2-NaCl SURFACE POTENTIAL.

Parameters	set I	set II
$\alpha(C\text{-}Na^+)$ Å	4.381	5.355
$\alpha(C\text{-}Cl^-)$ Å	2.910	3.310
$\alpha(O\text{-}Na^+)$ Å	4.775	5.524
$\alpha(O\text{-}Cl^-)$ Å	3.079	3.374
$A(C\text{-}Na^+)$ kcal/mol *	6.817×10^4	9.522×10^5
$A(C\text{-}Cl^-)$ kcal/mol *	2.053×10^4	8.350×10^4
$A(O\text{-}Na^+)$ kcal/mol *	14.43×10^4	10.45×10^5
$A(O\text{-}Cl^-)$ kcal/mol *	3.030×10^4	8.366×10^4

* These parameters must be multiplied by a correction factors to obtain heats of adsorption consistent with experiment. For set I the factor is 1.22 while for set II the factor is 1.19.

2.3. Dispersion parameters

The dispersion coefficients C_6^{ij}, C_8^{ij} and C_{10}^{ij} for unlike atoms/ions may be estimated in a number of ways. The most common way to calculate the dispersion coefficient C_6^{ij} is through the use of the London[32] formula as derived by Tang and Toennies[33]. In this work the C_6^{ij} were calculated using equation (2.18), the C_8^{ij} were estimated in the same manner as Tang and Toennies, and equation (2.19) was used to estimate the C_{10}^{ij}.

$$C_6^{ij} = \frac{3}{2} \times \left[\frac{\beta_1^i \beta_1^j \eta_1^i \eta_1^j}{\eta_1^i + \eta_1^j} \right] \qquad (2.18)$$

$$C_{10}^{ij} \approx \frac{49}{40} \times \left[\frac{C_8^2}{C_6} \right] \qquad (2.19)$$

In the above formulas the β_1^i and β_1^j are dipole polarizabilities, while the η_1^i and η_1^j are the ionization energies (as interpreted by London[32]) of atom (i) and atom (j). The polarizabilities have been calculated by Stone[34] using the CADPAC program[35]. This program can carry out Coupled Perturbed Hartree-Fock calculations for any perturbation whose matrix elements can be provided.

On the other hand, C_6, and the ratios of C_8/C_6 and C_{10}/C_6 for like molecules (CO_2-CO_2) have been calculated by Mulder, Thomas and Meath[36]. The parameter η_1 have been calculated using equation 2.20

which is obtained from 2.18 when i=j (*i.e.* for like atoms) as below[33]. The calculated values of η_1 are listed in Table 2.3.

$$\eta_1 = \frac{4}{3} \times \frac{C_6}{\beta_1^2} \qquad (2.20)$$

From these sets of parameters dispersion constants C_6, C_8, and C_{10}, as well as the C_8/C_6 and C_{10}/C_6 ratios were estimated for the (CO_2-Na^+) and (CO_2-Cl^-) surface potentials using equations 2.18, 2.19 and 2.20. The results are listed in Table 2.4. Although the C_8/C_6 (CO_2-Cl^-) ratio seems to be over estimated when compared with the ratio for like pairs *i.e.* one would expect the ratio of the CO_2-Cl^- (44.28 a.u.) pair to be between the values of the like pairs CO_2-CO_2 (40.9 a.u.) and Cl^--Cl^- (33.88 a.u.), the results are generally acceptable.

An alternative scheme was also used to calculate the ratios of the dispersion constants and subsequently the values of the constants themselves. In this scheme the ratios of the unlike species were calculated as the average of the two like pairs of atoms/ions. The results are listed in table 2.5.

TABLE 2.3: PARAMETERS USED TO CALCULATE $C_6(CO_2$-$Na^+,Cl^-)$.

parameters	β_1 (a.u.)	C_6(a.u.)	η_1 (a.u.)	C_8/C_6(a.u.)
CO_2-CO_2	17.56[a]	192[a]	0.8302	40.9[a]
Na^+- Na^+	1.002[c]	1.588[c]	2.109	8.14[b]
Cl^-- Cl^-	21.153[c]	180.3[c]	0.5373	33.88[b]

[a]Reference [36].

[b]Calculated from reference [37].

[c]Reference [38].

TABLE 2.4: ESTIMATED VALUES OF C_6, C_8, C_{10} AND THEIR RATIOS FOR (CO_2-Na^+, Cl^-) INTERACTIONS.

parameters	C_6 (a.u.)	C_8 (a.u.)	C_{10} (a.u.)	C_8/C_6 (a.u.)	C_{10}/C_6(a.u.)
CO_2-Na^+	15.72	423.6	11410.0	26.94	725.9
CO_2-Cl^-	181.7	8048.0	376000.0	44.28	1961.0

TABLE 2.5: CALCULATED PARAMETERS OF C_6, C_8, C_{10} AND THEIR RATIOS FOR (CO_2-Na^+, Cl^-) INTERACTIONS USING AVERAGE OF LIKE PAIRS.

parameters	C_6 (a.u.)	C_8 (a.u.)	C_{10} (a.u.)	C_8/C_6 (a.u.)	C_{10}/C_6(a.u.)
CO_2-Na^+	15.72	385.5	11590.0	24.52	736.5
CO_2-Cl^-	181.7	6799.0	311600.0	37.41	1714.0

At this stage the dispersion interactions are expressed in terms of molecule-ion pairs. However, the potential requires that parameters for atom-ion interactions be specified. The atom-ion dispersion parameters are obtained from the molecule-ion dispersion parameters through scaling arguments based on atomic polarizabilities. How to breakdown a molecular polarizability into constituent atomic polarizabilities is not an exact procedure. Estimates of the atom-ion polarizabilities can be made through the examination of the van der Waals coefficients PL_6C, PL_6O and PL_6CO_2 which are formally proportional to the atomic and molecular polarizabilities *viz.* $PL_6C \propto \beta_C$, $PL_6O \propto \beta_O$ and $PL_6CO_2 \propto \beta_{CO_2}$. It is worth noting that:

$$C_6^{CO_2-CO_2} = \left(PL_6CO_2\right)^2 = \left(PL_6C + 2PL_6O\right)^2$$

As a result, PL_6C and PL_6O can vary while maintaining a constant value for the dispersion coefficient $C_6^{CO_2-CO_2}$ within the WMIN program. In other words, the polarizabilites of C and O are allowed to vary, but the total polarizability of CO_2 does not vary. The ratios of $\frac{\beta_C}{\beta_{CO_2}}$ and $\frac{\beta_O}{\beta_{CO_2}}$ are listed in Table 2.6. By using the obtained PL_6C and PL_6O from WMIN and the equations below, the dispersion constant C_6 for C-Na^+, C-Cl^-, O-Na^+ and O-Cl^- pairs were calculated for parameter sets I and II.

$$\frac{\beta_C}{\beta_{CO_2}} = \frac{PL_6C}{PL_6C + 2\,PL_6O} \qquad (2.21)$$

$$\frac{\beta_O}{\beta_{CO_2}} = \frac{PL_6O}{PL_6C + 2\,PL_6O} \tag{2.22}$$

$$C_6^{C\text{-}Na^+} = C_6^{CO_2\text{-}Na^+} \times \frac{\beta_C}{\beta_{CO_2}} \tag{2.23}$$

$$C_6^{C\text{-}Cl^-} = C_6^{CO_2\text{-}Cl^-} \times \frac{\beta_C}{\beta_{CO_2}} \tag{2.24}$$

$$C_6^{O\text{-}Na^+} = C_6^{CO_2\text{-}Na^+} \times \frac{\beta_O}{\beta_{CO_2}} \tag{2.25}$$

$$C_6^{O\text{-}Cl^-} = C_6^{CO_2\text{-}Cl^-} \times \frac{\beta_O}{\beta_{CO_2}} \tag{2.26}$$

The dispersion constants C_8 and C_{10} for the C-Na^+, C-Cl^-, O-Na^+ and O-Cl^- pairs were derived for parameter sets I and II. It was assumed that the C_8/C_6 and C_{10}/C_6 ratios for each of the atom-ion pairs is the same as the corresponding ratio for the molecule-ion pairs, *e.g.* C_8/C_6(C-Na^+) ≈ C_8/C_6(O-Na^+) ≈ C_8/C_6(CO_2-Na^+) as listed in tables 2.4-5. By multiplying the values of C_6 for the individual atom-ion pairs (table 2.6) by the appropriate ratio (C_8/C_6 or C_{10}/C_6) from tables 2.4-5 the values of the dispersion constants C_8 and C_{10} were obtained. The obtained dispersion constants C_6, C_8 and C_{10} are presented in table 2.7.

TABLE 2.6: RATIOS OF ATOMIC POLARIZABILITY OF CO_2 MOLECULE.

Ratio	Set I	Set II
$\frac{\beta_C}{\beta_{CO_2}}$	0.4202	0.3981
$\frac{\beta_O}{\beta_{CO_2}}$	0.2899	0.3009

TABLE 2.7: CALCULATED DISPERSION CONSTANTS FOR ATOM-ION INTERACTIONS.

Parameters	set I	set II
C_6(C-Na^+) $Å^6$ · kcal/mol	0.9103×10^2	0.8624×10^2
C_6(C-Cl^-) $Å^6$ · kcal/mol	10.52×10^2	9.968×10^2
C_6(O-Na^+) $Å^6$ · kcal/mol	0.6279×10^2	0.6518×10^2
C_6(O-Cl^-) $Å^6$ · kcal/mol	7.259×10^2	7.535×10^2
C_8(C-Na^+) $Å^8$ · kcal/mol	6.868×10^2	5.922×10^2
C_8(C-Cl^-) $Å^8$ · kcal/mol	13.05×10^3	10.44×10^3
C_8(O-Na^+) $Å^8$ · kcal/mol	4.737×10^2	4.475×10^2
C_8(O-Cl^-) $Å^8$ · kcal/mol	8.000×10^3	7.893×10^3
C_{10}(C-Na^+) $Å^{10}$ · kcal/mol	5.180×10^3	4.980×10^3
C_{10}(C-Cl^-) $Å^{10}$ · kcal/mol	16.18×10^4	13.40×10^4
C_{10}(O-Na^+) $Å^{10}$ · kcal/mol	3.573×10^3	3.764×10^3
C_{10}(O-Cl^-) $Å^{10}$ · kcal/mol	11.16×10^4	10.13×10^4

3. COMPUTATIONAL SIMULATION STUDY

Simulations of mono and multilayers of CO_2/NaCl(001) were performed using Metropolis Monte Carlo method. These simulations require realistic interaction potentials (both CO_2-CO_2 and CO_2-NaCl) whose characteristic parameters have been optimized. The CO_2-NaCl surface potentials as characterized by parameter set I and set II, were examined and optimized using the steepest descent method for energy minimization. Equation (2.6) was used in both methods. The temperature dependent total energy U(T) of CO_2 on NaCl(001) can be written as below.

$$U(T) = U_p(T) + U_k(T) \tag{3.1}$$

where $U_p(T)$ is the potential energy and $U_k(T)$ is the kinetic energy of CO_2 on NaCl(001) at temperature T.

The steepest descent method calculates the potential energy E_0 at zero degree Kelvin for a single molecule. This method was used to calculate the absolute potential minimum and saddle point of a single CO_2 molecule on NaCl(001) surface as well as the position and orientation of the CO_2 molecule at both sites. This method was also used to investigate whether there are any other local minimum in the system.

The Metropolis Monte Carlo method calculates $U_p(T) = V_0 + 5k_B\Delta T/2$ for N molecules, where V_0 is the potential energy at zero degree Kelvin for N molecules. If N=1 then $V_0=E_0$. This method was used to calculate the position and orientation of monolayers and multilayers CO_2 molecules on the NaCl(001) surface. Calculations were done at finite temperature at (1 K - 90 K) for monolayer, bilayer and three-layer systems. Also, some preliminary calculations were done for four and five layer systems, but were stopped because the results showed that these systems are not stable.

In the simulations, the potential energy, φ the angle between projection of molecular axis of CO_2 and x direction (<110> direction of NaCl unit cell is x direction in our model), and θ the angle between molecular axis of CO_2 and surface normal were calculated see Figure 3.1.

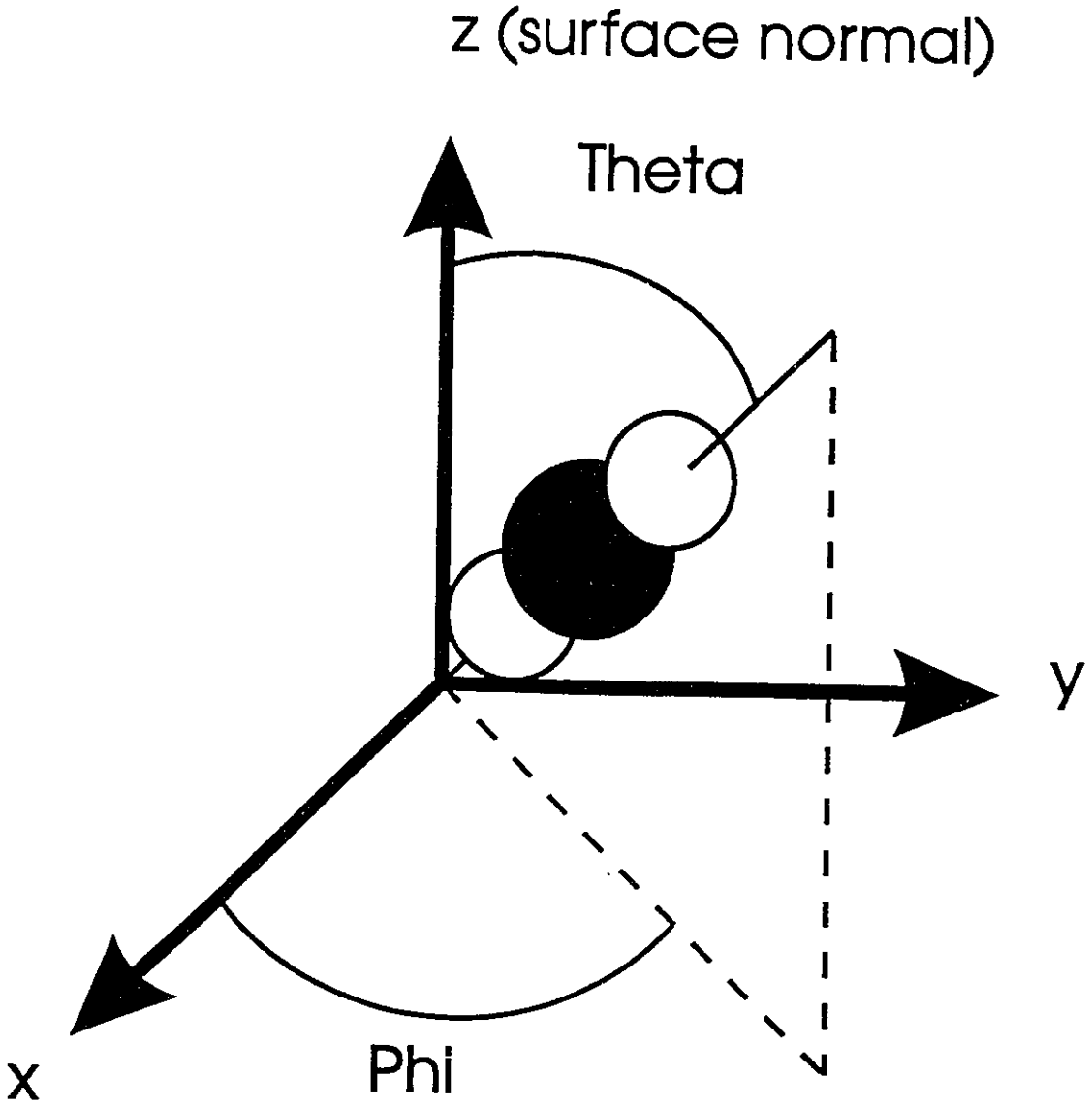

FIGURE 3.1. DEFINITION OF ORIENTATION ANGLE.

3.1. STEEPEST DESCENT (ENERGY MINIMIZATION OF A SINGLE CO_2/NaCl(001))

In this method the position of every atom in the molecule is calculated at zero degree temperature (T = 0 K). This is done by calculating the energy and forces f_x, f_y and f_z on each atom in the x, y and z directions. If f_x, f_y and f_z are equal to zero or are close to zero the program stops and the positions are kept. If one or all of these forces are not equal to zero then the forces in each direction are multiplied by an adjustable constant α and then added to the old position to obtain the new positions (new coordinates of each atom). Once again the energy and forces are calculated on each atom. This process is continued until the forces on each atom in the x, y and z directions become zero or close to zero. The process is shown in Figure 3.1.1.

The two groups of parameters mentioned in Table 2.1 were examined in this way. In the case of parameter set I, the repulsion parameters (A_{rep}) of the atom-ion pairs were multiplied with a factor 1.22 in order to match the experimental value of the isosteric heat of adsorption of the 2D-gas at 90 K (32.4 ± 1.1 kJ/mol= 7.74 ± 0.26 kcal/mol)[7]. Surface potential calculations were done and are plotted in Figures 3.1.2-3.1.10. In the case of parameters set II, the experimental value of the isosteric heat of adsorption of 2D-gas at 0 K, was estimated by adding the thermal factor $3k_BT/2$ to the isosteric heat of adsorption at 90 K (32.4 + 1.12 kJ/mol = 8.01 kcal/mol) in keeping with equation (2.6). This correction gives better estimate of the energy because the steepest descent

method calculates only at 0 K and does not include temperature dependent potential and kinetic energy contributions. To fit the calculated value to the estimated experimental value of the isosteric heat of adsorption, the repulsion parameters of the atom-ion pairs were multiplied by a factor 1.19. The resulting surface potentials are shown in Figures 3.1.11-3.1.19. In all cases, the constant α was kept at 0.00001 and the forces on the carbon in the x and y directions were set to zero; *i.e.* the lateral position of the carbon atom was fixed. All forces on the oxygen atoms were kept. The carbon dioxide molecule was moved along the x axis from Na^+ to adjacent Na^+ (along the <110> direction of a NaCl unit cell) and the resulting potential energy, angle and height of the molecule were determined. For both parameter sets the results show that a carbon dioxide molecule above the Na^+ ion sits perpendicular to the surface, and when moved along the x axis the angle decreases from 90° with respect to the surface. When the molecule sits overtop of the center of the connection line of two adjacent Na^+ ions, it lies parallel to the surface (absolute potential minimum). From this point the angle decreases to negative values until the CO_2 molecule sits perpendicular to the surface once again over the next Na^+ site; *i.e.* from one Na^+ to the next Na^+ the CO_2 molecule flips over. In another study, the carbon dioxide molecule was moved from Na^+ to Cl^- along the <100> direction of the NaCl unit cell. The results show that at the potential energy minimum along this direction (saddle point), the molecule sits over the connection line between Na^+ and Cl^- with tilted angle 35° from surface (55° from the surface normal) for parameter set I and 32° from surface (58° from the surface normal) for parameter set II.

Also molecule was moved from saddle point to absolute potential minimum, the results show no other local minimum exist (Figures 3.1.8 to 3.1.10) and (Figures 3.1.17 to 3.1.19). The results show that the parameter set II have slightly higher accuracy than parameter set I.

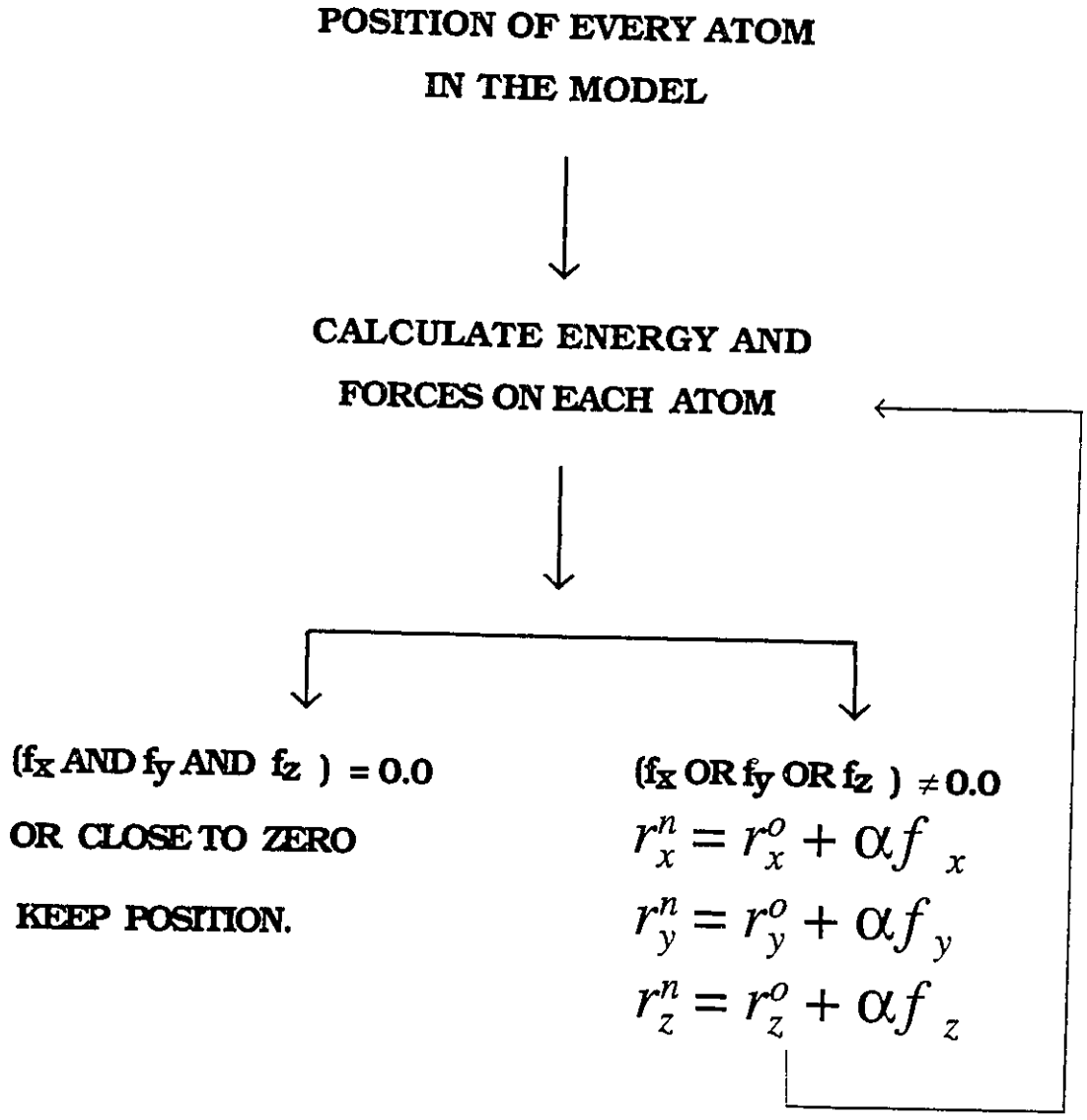

FIGURE 3.1.1. FLOW CHART OF THE STEEPEST DESCENT METHOD.

3.1.1. RESULTS AND DISCUSSION OF ENERGY MINIMIZATION.

The potential energy surfaces of a single CO_2 molecule for parameter sets I and II were examined using the steepest descent method. The absolute potential minimum of parameter sets I and II was determined, and in both cases it was found that the CO_2 molecule sits parallel to the surface above the center of the connection line of two adjacent Na^+ ions (the <110> direction as shown in Figure 3.1.2) *i.e.* the lateral distance of the C atom is 1.994 Å from each of the Na^+ ions. The results of these calculations are listed in Table 3.1.1 and are discussed below.

Parameter set I yielded a binding energy, E_{min} = -7.643 kcal/mol, which agreed with the 90 K isosteric heat of adsorption (32.4 ± 1.1 kJ/mol= 7.74±0.26 kcal/mol) as shown in Figure 3.1.2. The potential minimum occurs when the molecule lies flat (see Figure 3.1.3) and the C atom sits at a height of z= 2.5 Å above the surface (see Figure 3.1.4). A saddle point in the potential energy surface E_{sad} = -5.723 kcal/mol (see Figure 3.1.5) was found above connection line between the Na^+ and Cl^- ions (the <100> direction). While in this position as shown in Figure 3.1.6 the molecular axis is tilted by 35° from surface (55° from the surface normal) and the C atom sits at a lateral distance of 0.92 Å from the Na^+ and at a height of z=2.95 Å (see Figure 3.1.7). The difference in energy between the minimum and saddle point energies is E_{diff} = 1.918 kcal/mol and provides an estimate of the surface diffusion barrier.

The region of the potential energy surface around the saddle point was explored using a restricted version of the energy minimization program (the lateral coordinates were fixed while the height z and the orientation of the molecule were allowed to vary). The results of these studies are shown in Figs. 3.1.8 -3.1.10 and confirm the hyperbolic nature of the potential energy surface in the saddle point region. This finding is in contrast to Heidberg's theoretical work[9] in which they found that a stable local minimum exists in this region. It should also be noted that Heidberg's calculated 2D-gas heat of adsorption is almost half of the experimental value whereas the calculation presented here almost matches the experimental value.

The orientation of the CO_2 molecule at the absolute potential minimum is in agreement with the 2D-gas phase while the orientation at the saddle point (Theta=35° from surface) is very similar to that observed in the monolayer structure (Theta=34°±5° from surface)[7]. The coordinates for these points are very similar to those calculated by Heidberg *et al.*[9]. The heat of adsorption of the absolute potential minimum is in good agreement with the experimental value of Heidberg[7], although the diffusion barrier energy calculated in this work is higher, by a factor 2.2, than the estimated experimental value of Heidberg[9].

For parameter set II there are only minor changes compared with the set I. The absolute potential minimum was again found along the <1$\bar{1}$0> axis midway between two neighbouring sodium ions and at a height of z=2.5 Å above the surface. The binding energy at this site was found to

be E_{min} = -8.000 kcal/mol which matches the 0 K isosteric heat of adsorption (32.4 + 1.12 kJ/mol = 8.01 kcal/mol). Once again the saddle point was found to be along the <100> direction, *i.e.* the C atom sat at height z = 3 Å above the connection line of Na^+ and Cl^- and at a lateral distance of 0.94 Å from the Na^+ with the molecule tilted by 32° from surface (58° from the surface normal) (Figures 3.1.11-3.1.19). The potential energy at this site was E_{sad} = -5.924 kcal/mol, yielding a diffusion barrier energy of E_{diff} = 2.075 kcal/mol. The only significant change is the 5% increase in the depth of the surface potential at the absolute potential minimum.

The results for both parameter sets are in good agreement with the experimental results, and thus provide good descriptions for the admolecule-surface interactions for the CO_2/NaCl(001) system. These parameters were subsequently used in the Monte Carlo simulations of monolayer and multilayer films of CO_2/NaCl(001) reported in the next section.

TABLE 3.1.1: ENERGY, HEIGHT AND ANGLE OF CO_2 AT SURFACE POTENTIAL MINIMUM AND SADDLE POINT.

parameters	Set I		Set II	
Position of CO_2	absolute potential min.	saddle point site	absolute potential min.	saddle point site
Energy (kcal/mol)	-7.643	-5.723	-8.000	-5.924
Height from surface (Å)	2.50	2.95	2.50	3.00
Angle from surface (Deg.)	0.0	35.0	0.0	32.0
Angle from surface normal (Deg.)	90.0	55.0	90.0	58.0

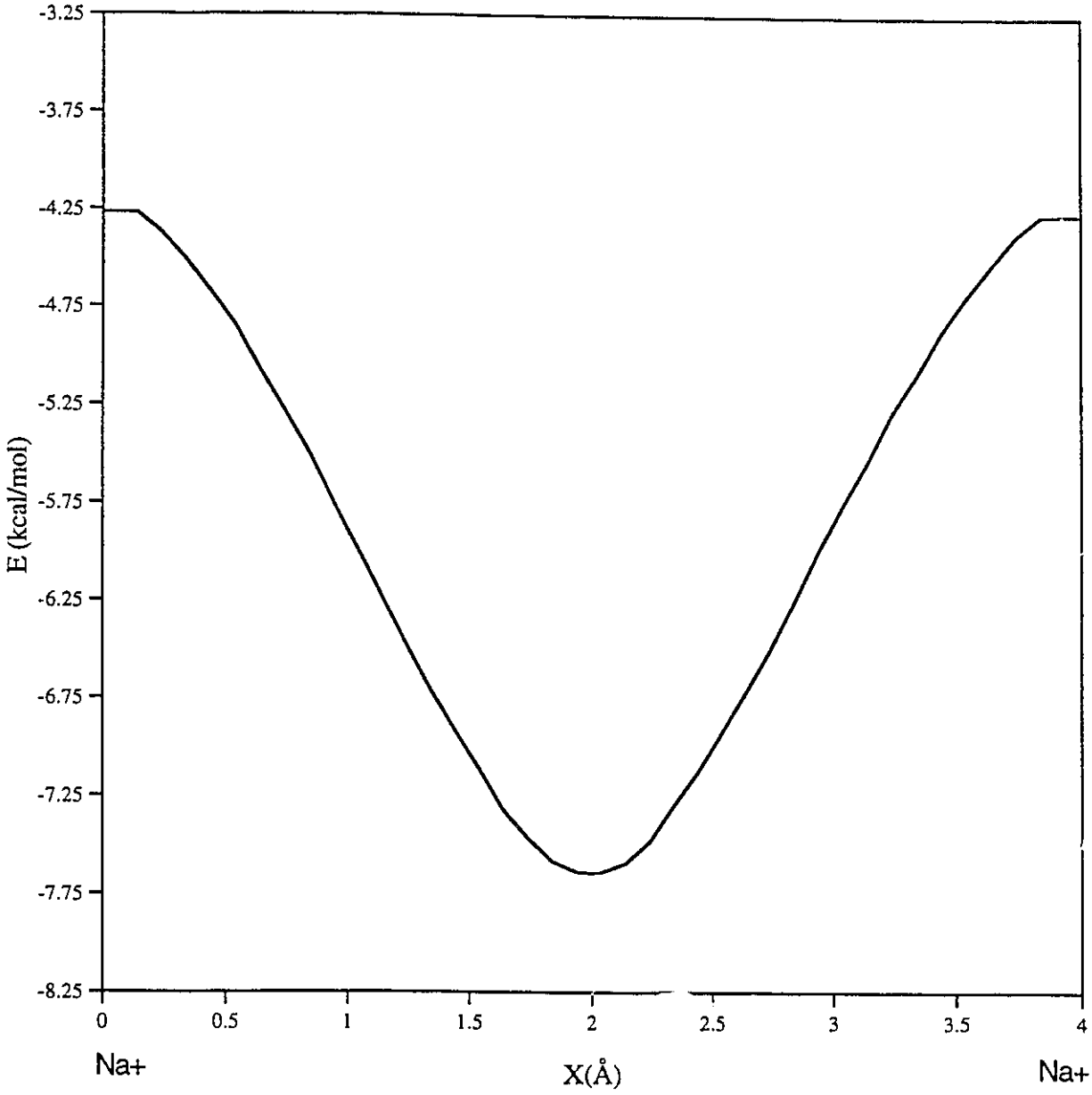

FIGURE 3.1.2: SURFACE POTENTIAL OF CO2/NaCl(001) ALONG THE <110> DIRECTION (PARAMETER SET I).

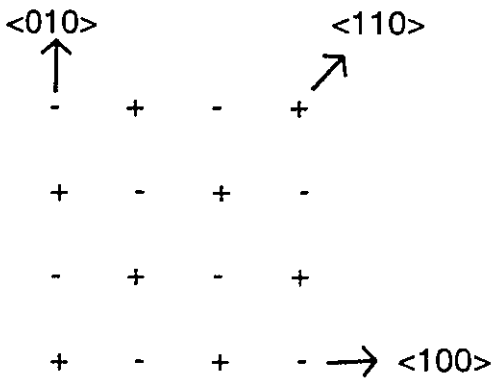

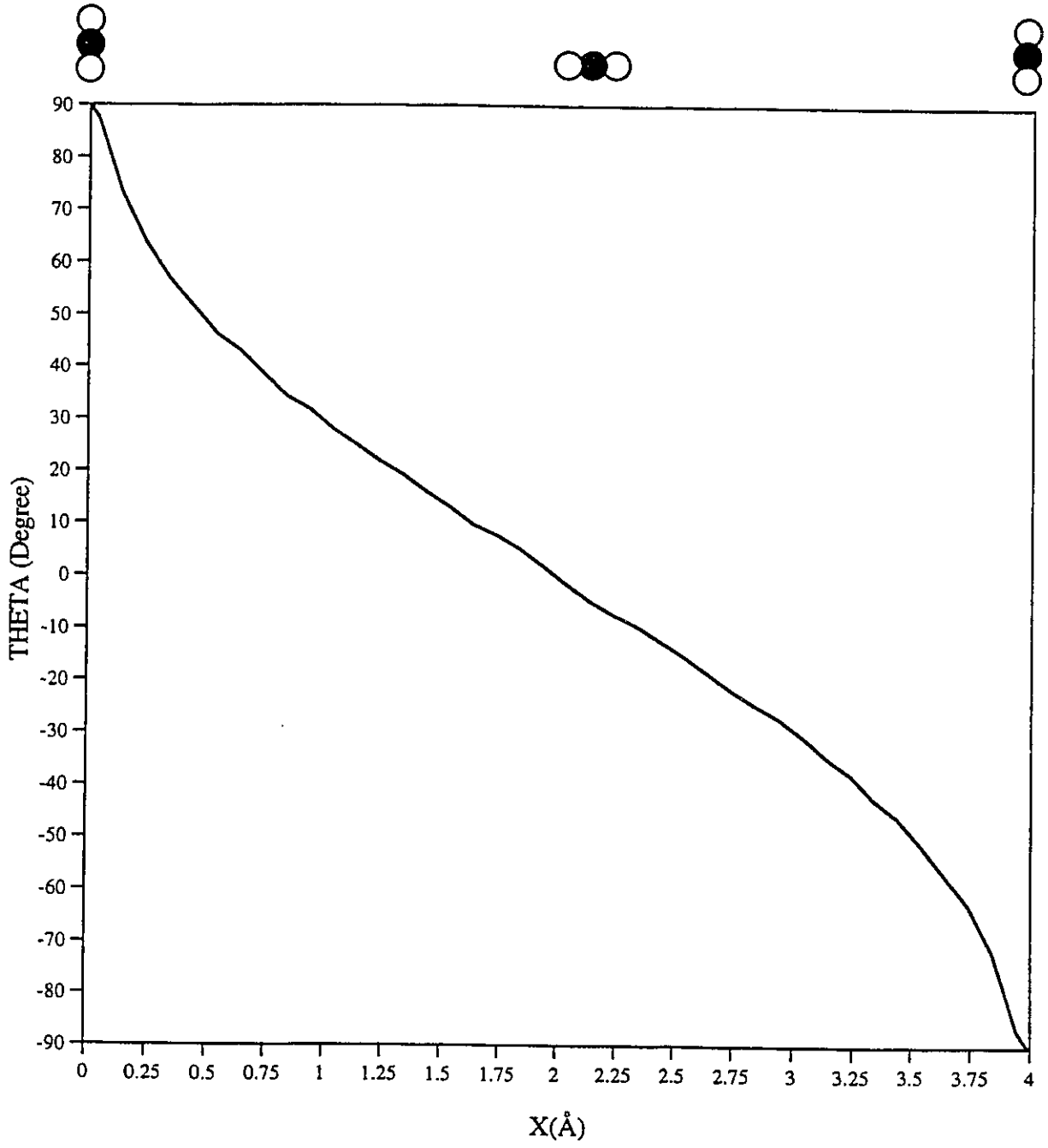

FIGURE 3.1.3: THETA VS. POSITION OF CO2 ALONG THE <110> DIRECTION (PARAMETER SET I).

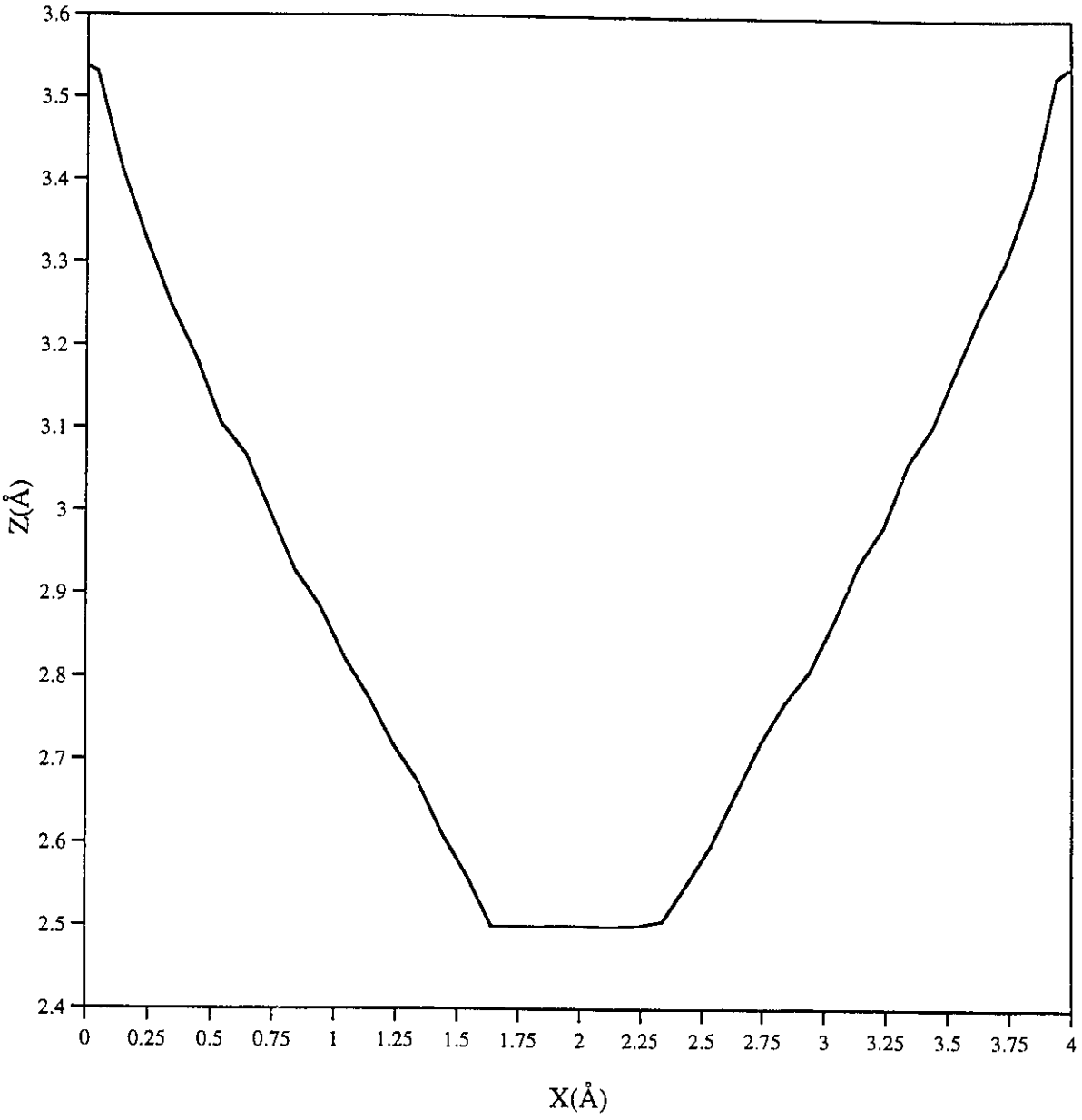

FIGURE 3.1.4: HEIGHT (Z) VS. POSITION OF CO2 ALONG THE <110> DIRECTION (PARAMETER SET I).

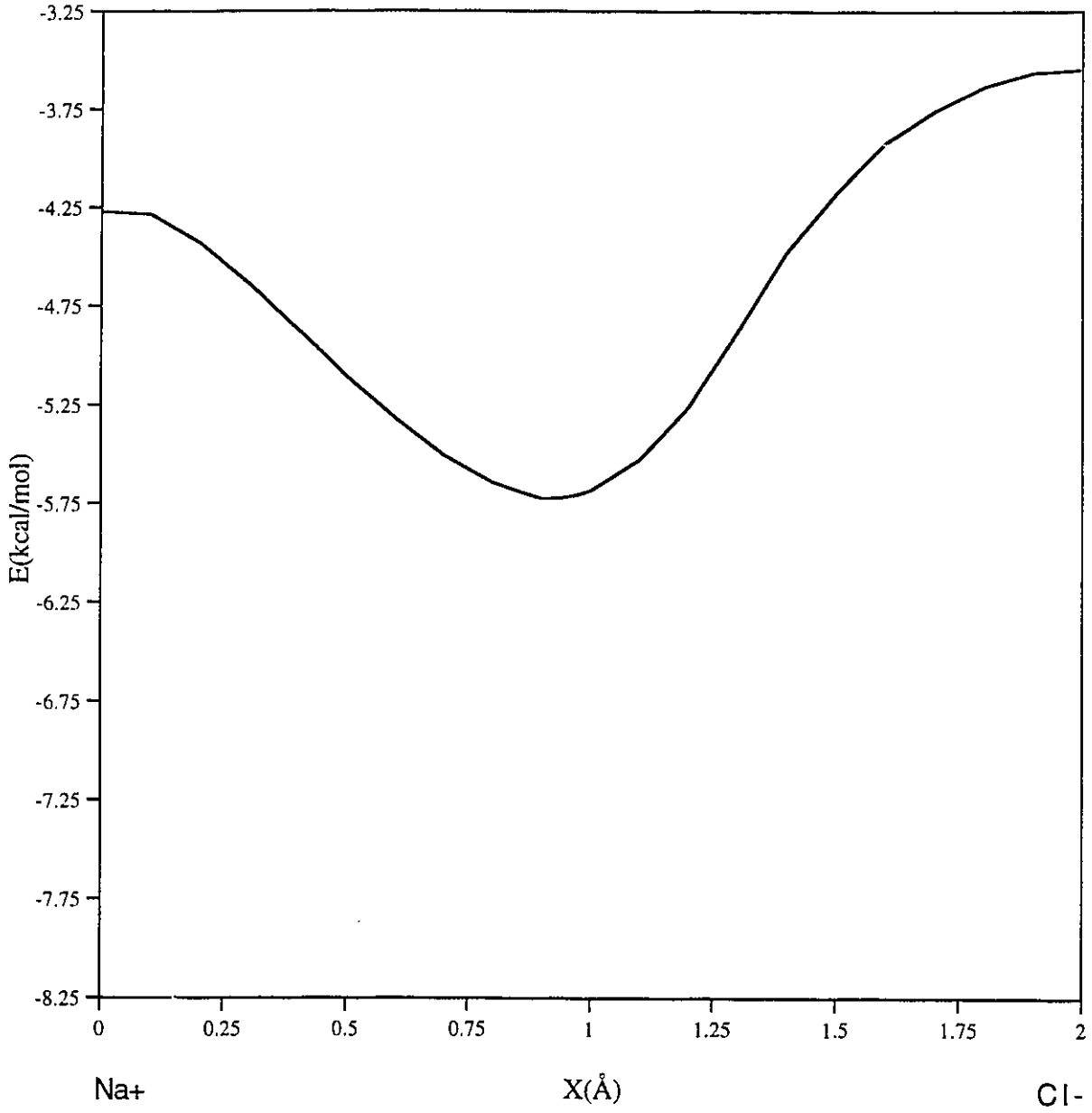

FIGURE 3.1.5: SURFACE POTENTIAL OF CO2/NaCl(001) ALONG THE <100> DIRECTION (PARAMETER SET I).

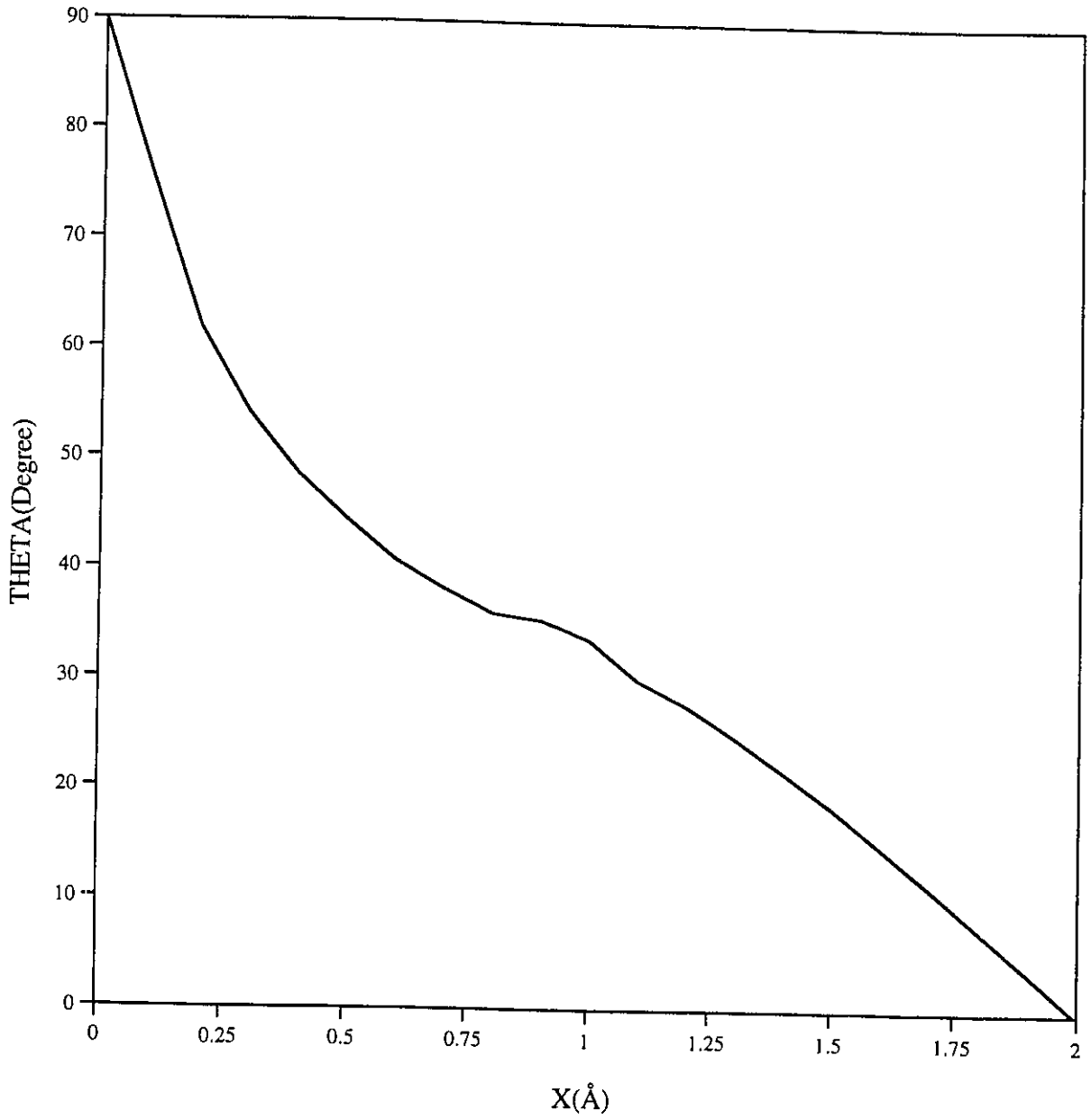

FIGURE 3.1.6: THETA VS. POSITION OF CO2 ALONG THE <100> DIRECTION (PARAMETER SET I).

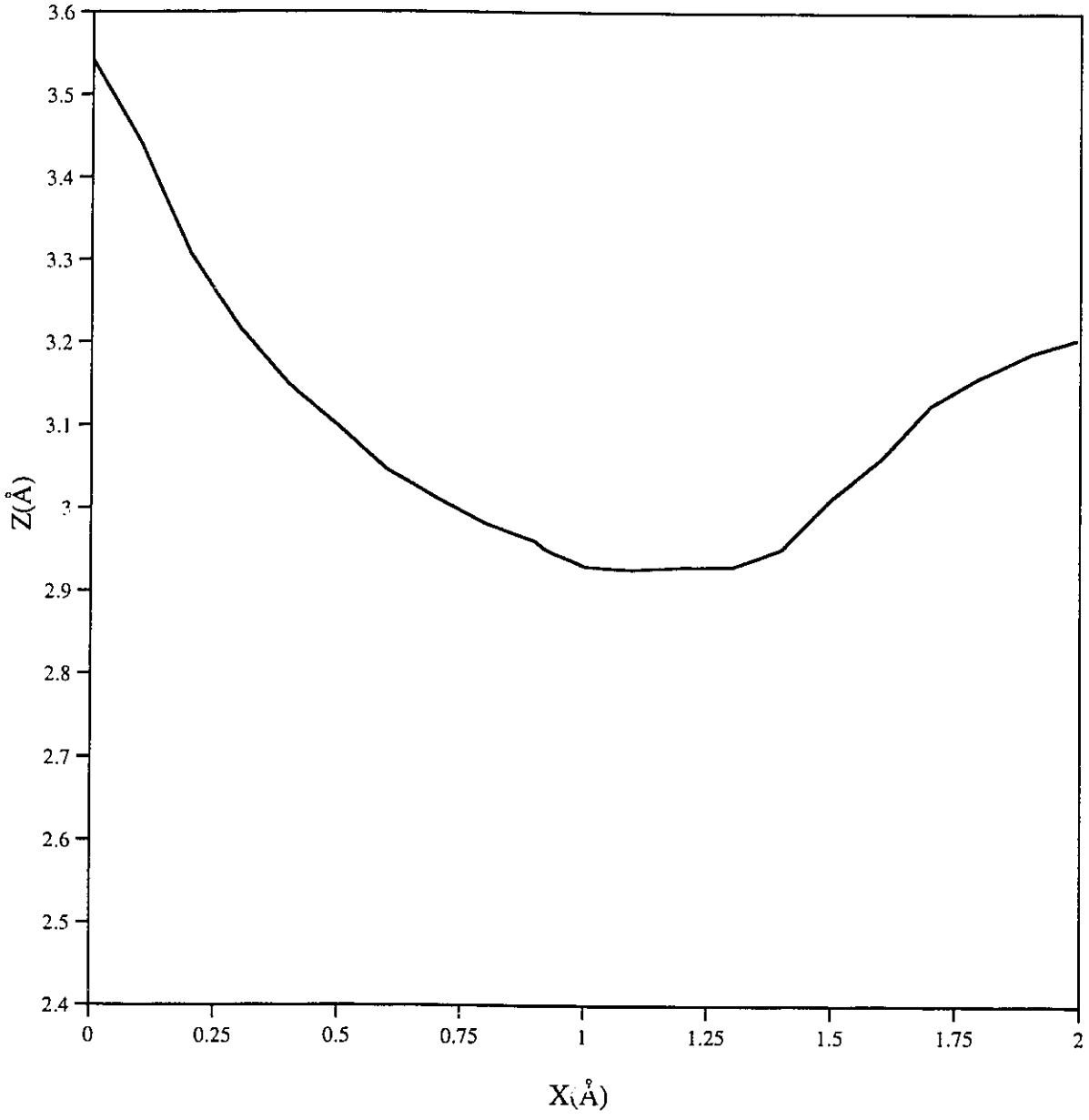

FIGURE 3.1.7: HEIGHT (Z) VS. POSITION OF CO2 ALONG THE <100> DIRECTION (PARAMETER SET I).

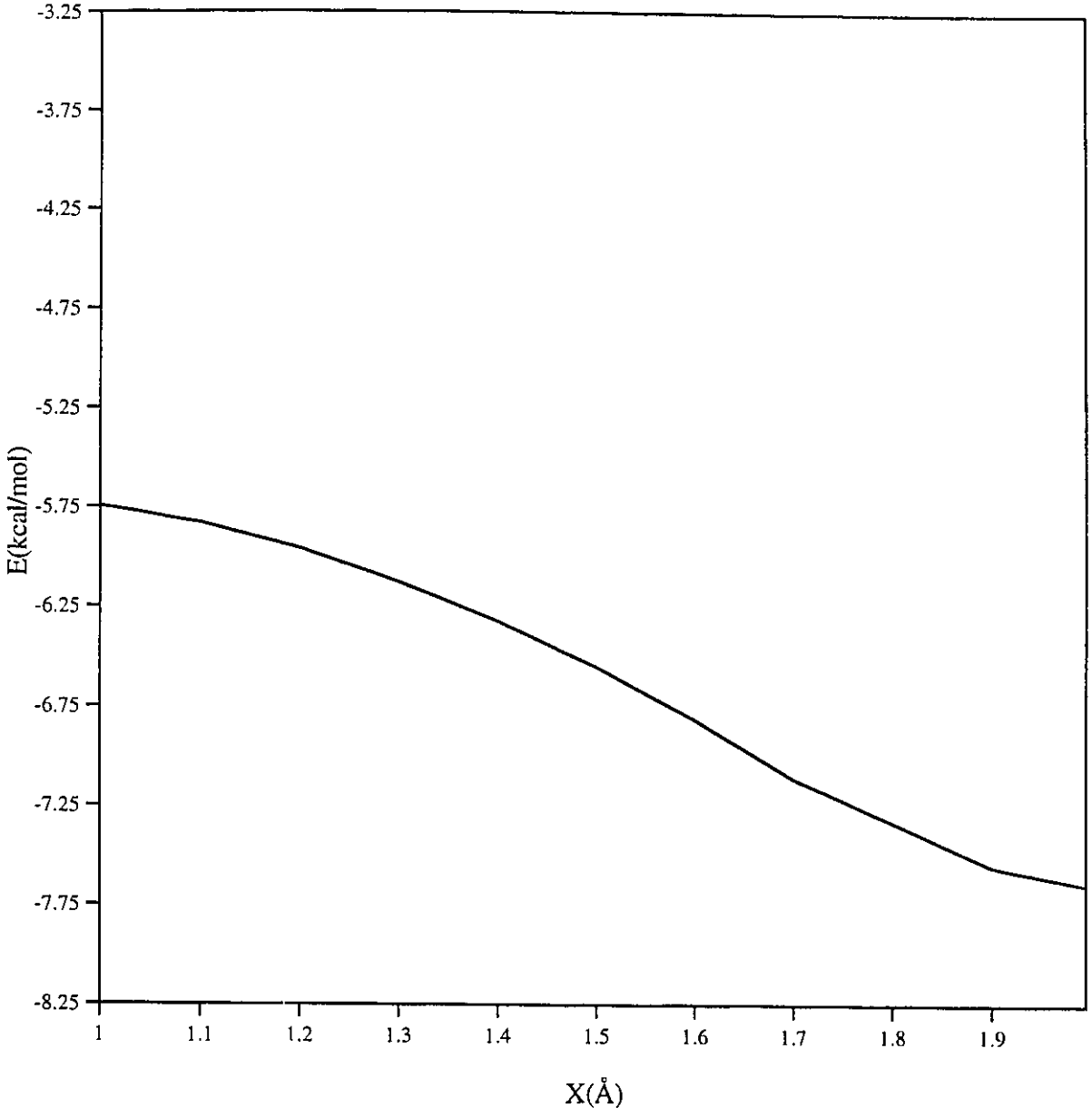

FIGURE 3.1.8: SURFACE POTENTIAL OF CO2/NaCl(001) FROM SADDLE POINT TO ABSOLUTE POTENTIAL MINIMUM (PARAMETER SET I).

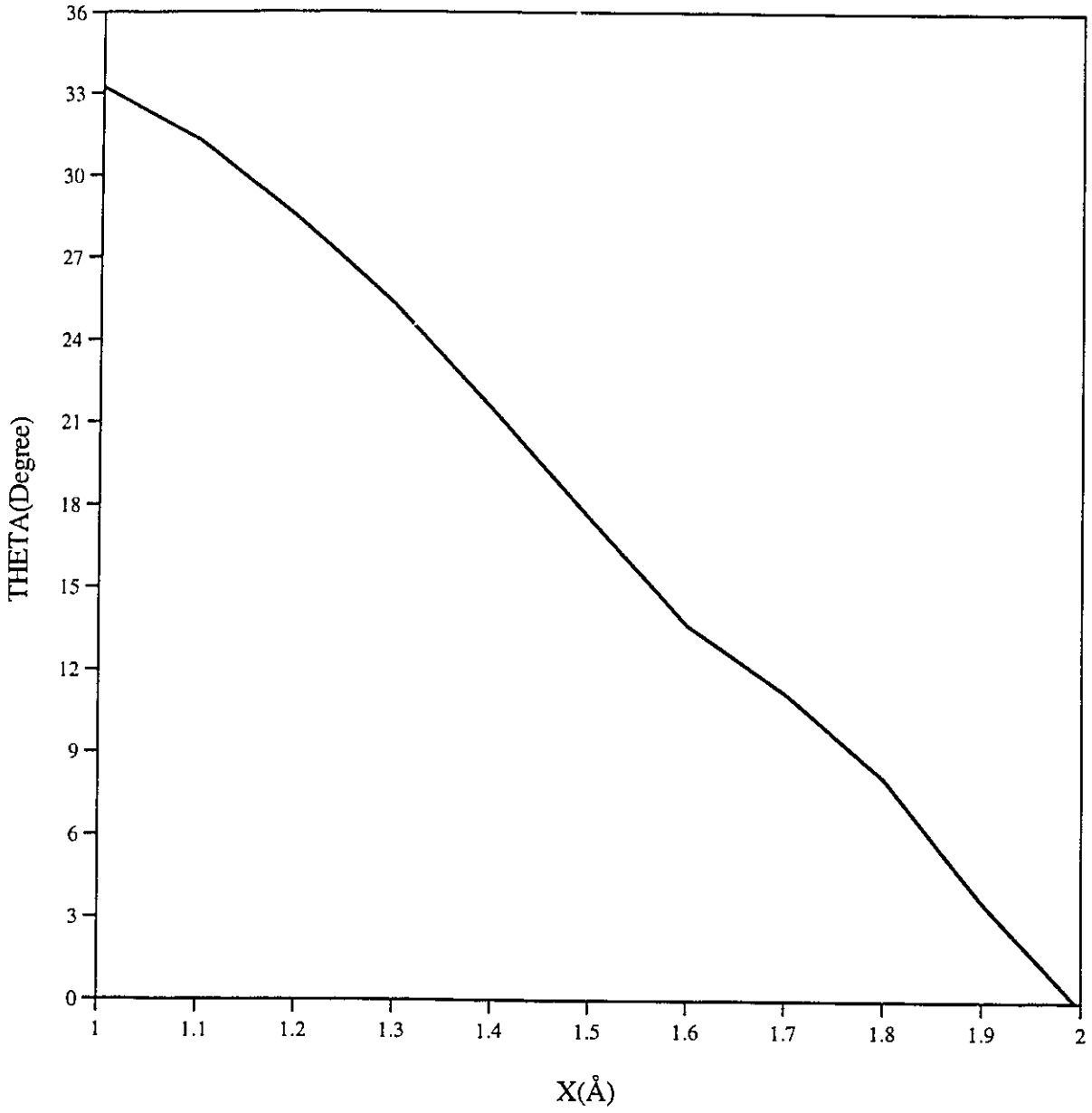

FIGURE 3.1.9: THETA VS. POSITION OF CO2 FROM SADDLE POINT TO ABSOLUTE POTENTIAL MINIMUM (PARAMETER SET I).

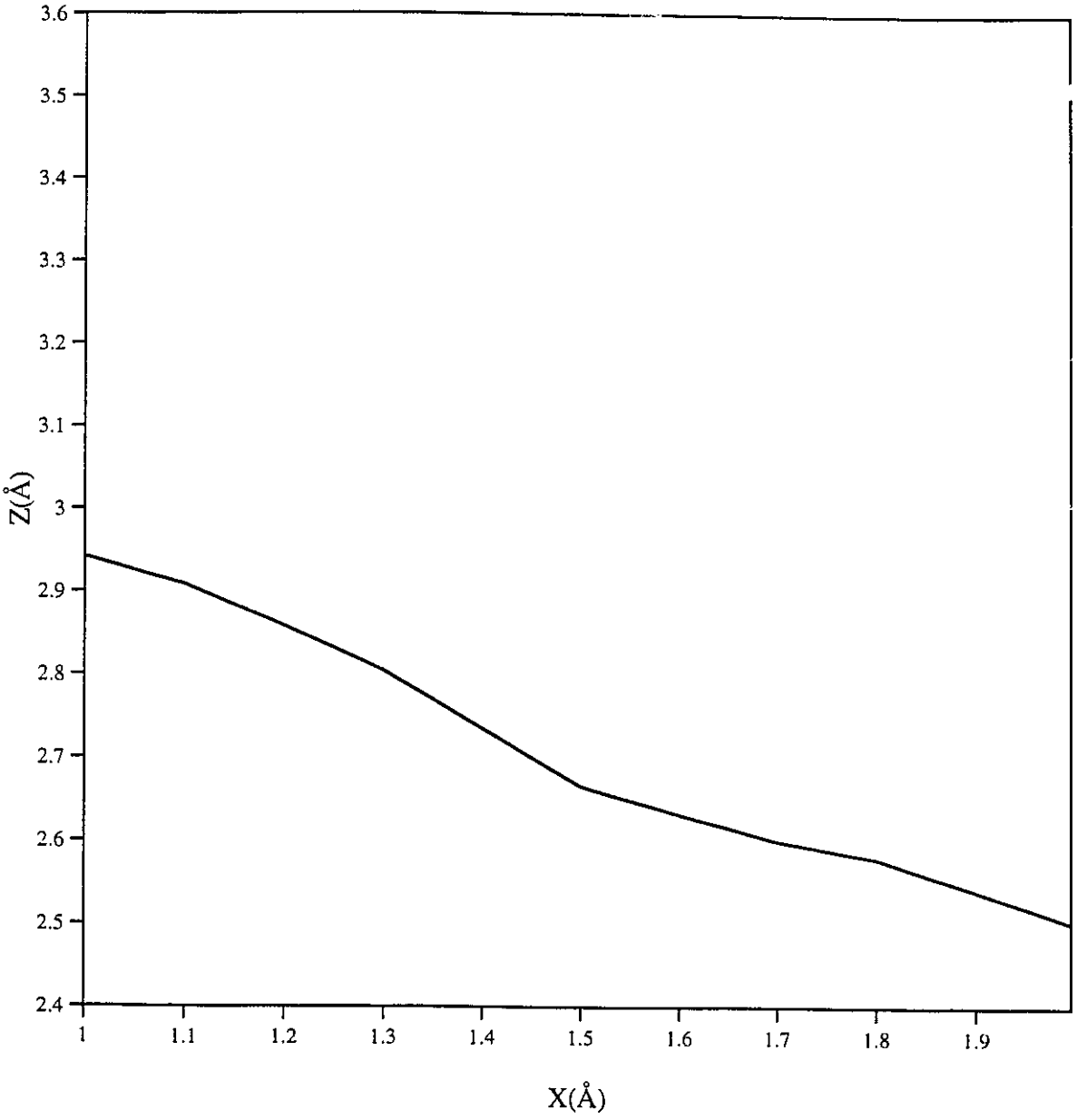

FIGURE 3.1.10: HEIGHT (Z) VS. POSITION OF CO2 FROM SADDLE POINT TO ABSOLUTE POTENTIAL MINIMUM (PARAMETER SET I).

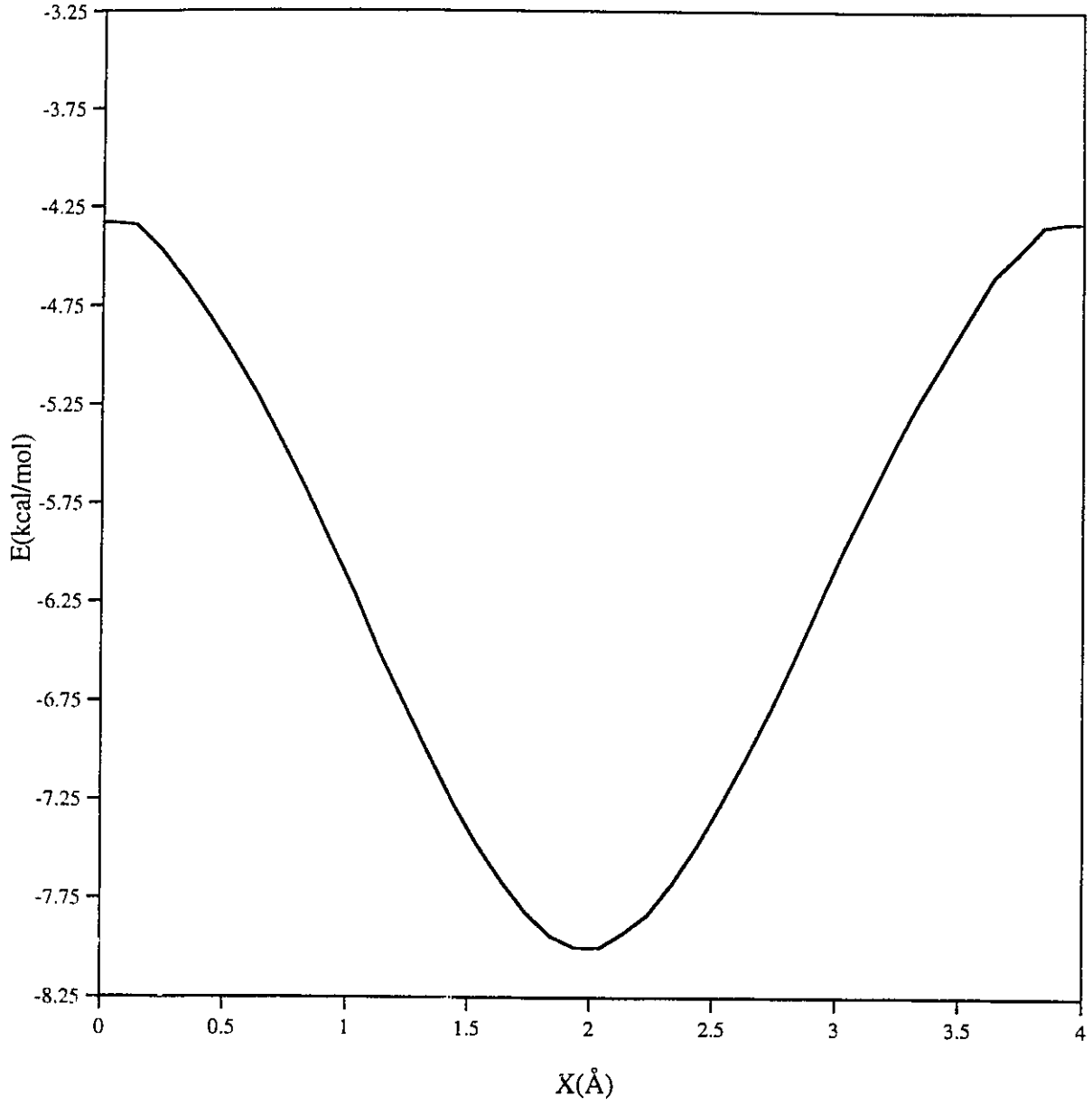

FIGURE 3.1.11: SURFACE POTENTIAL OF CO2/NaCl(001) ALONG THE <110> DIRECTION (PARAMETER SET II).

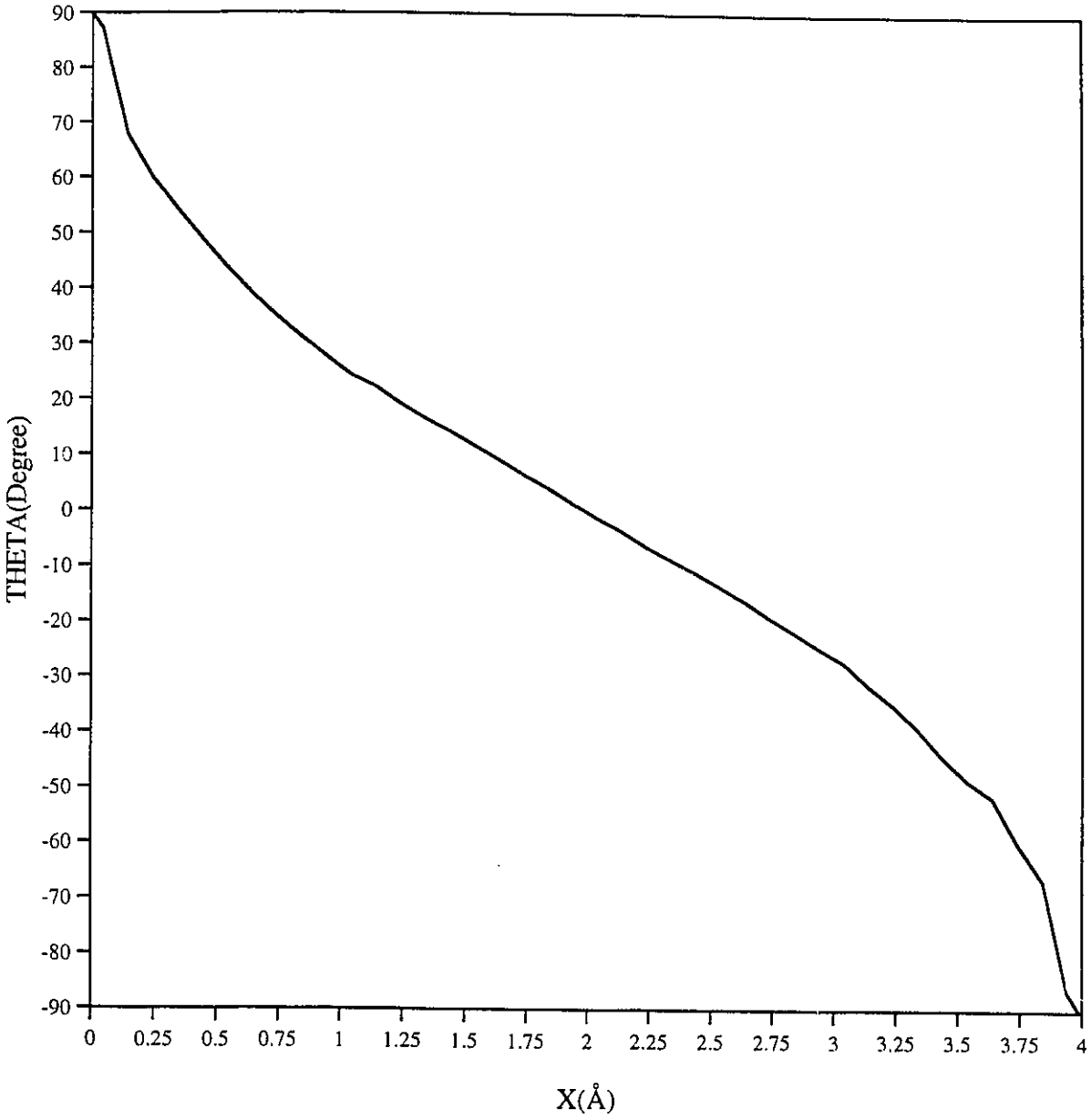

FIGURE 3.1.12: THETA VS. POSITION OF CO2 ALONG THE <110> DIRECTION (PARAMETER SET II).

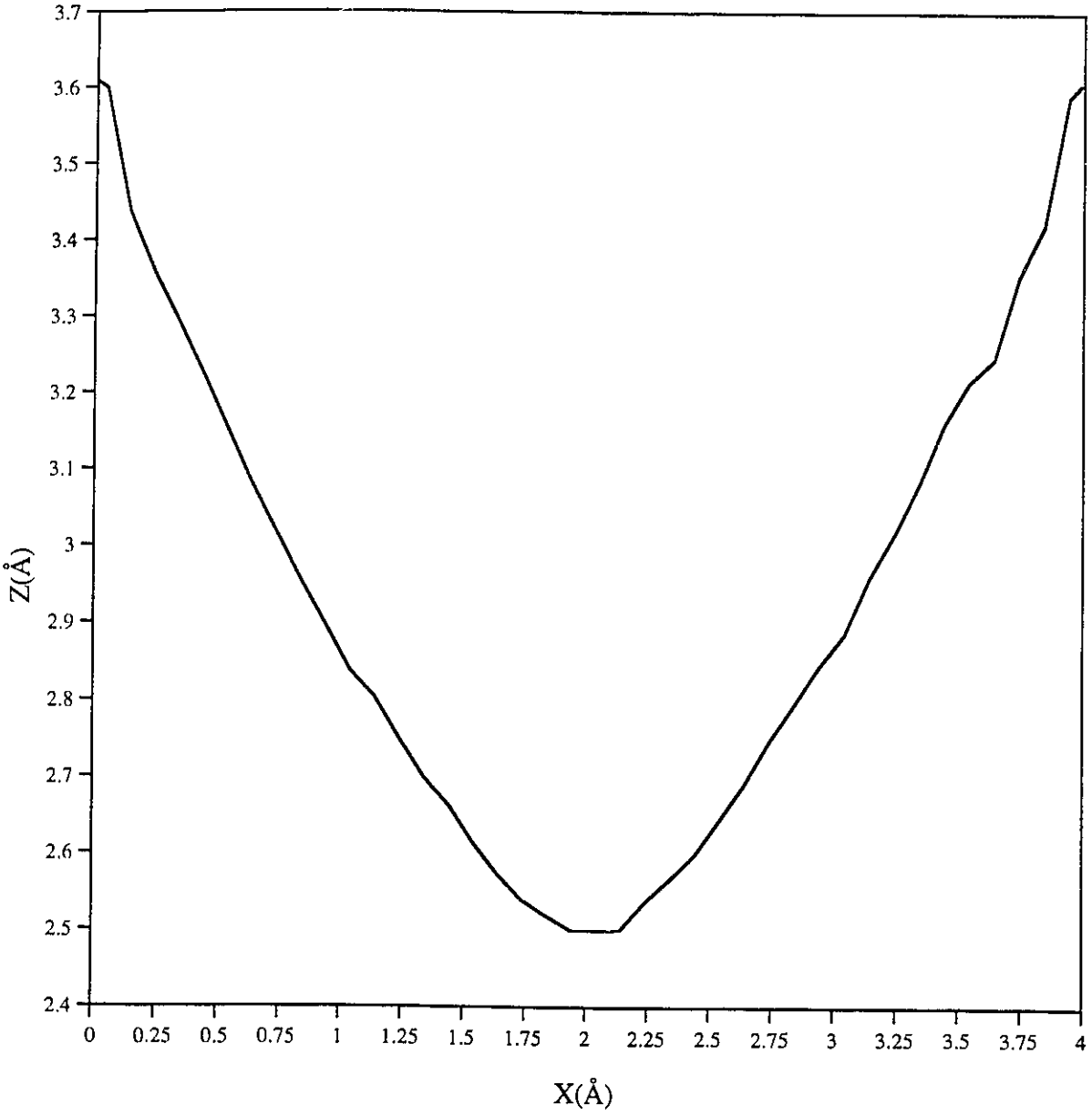

FIGURE 3.1.13: HEIGHT (Z) VS. POSITION OF CO2 ALONG THE <110> DIRECTION (PARAMETER SET II).

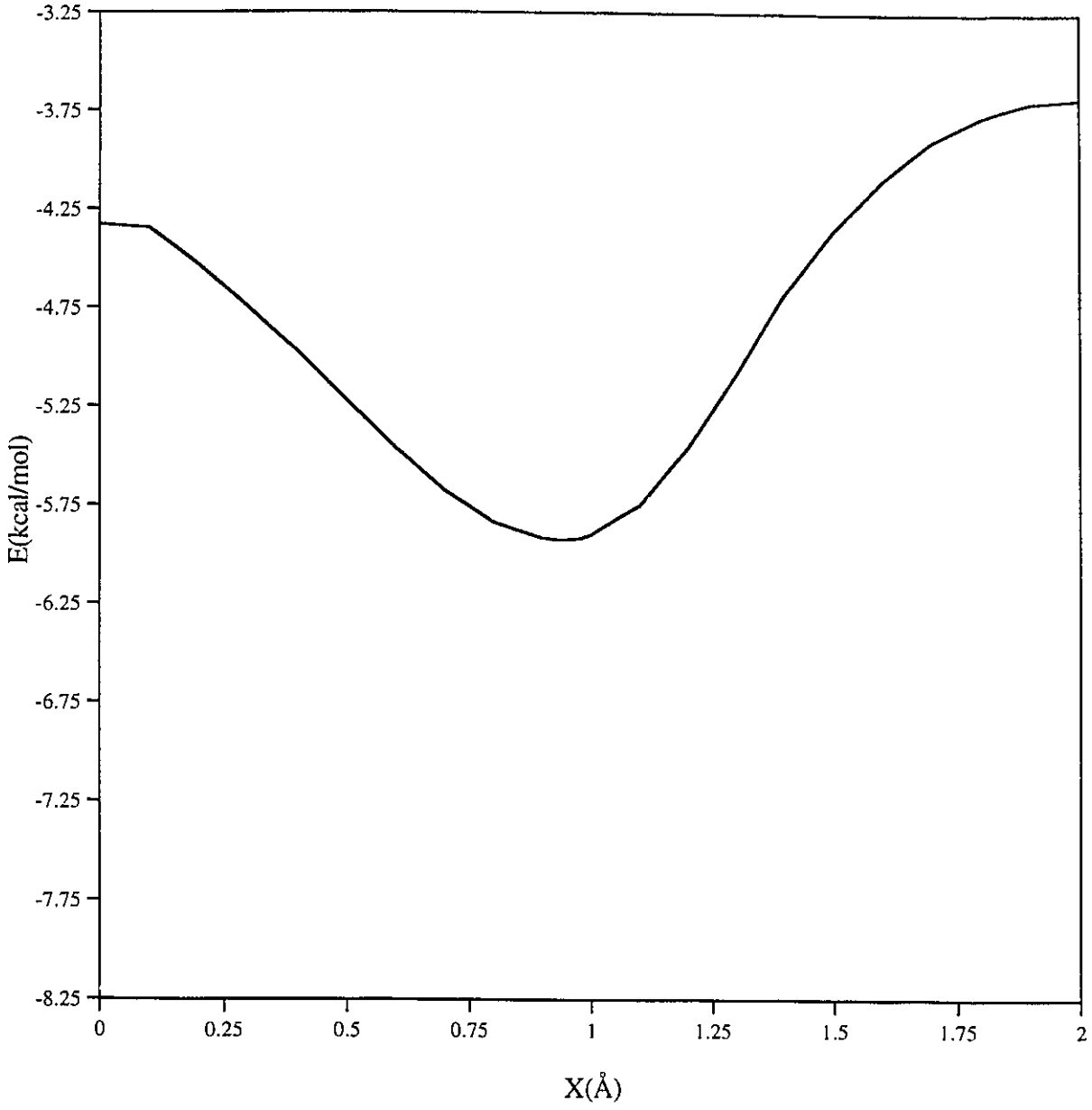

FIGURE 3.1.14: SURFACE POTENTIAL OF CO2/NaCl(001) ALONG THE <100> DIRECTION (PARAMETER SET II).

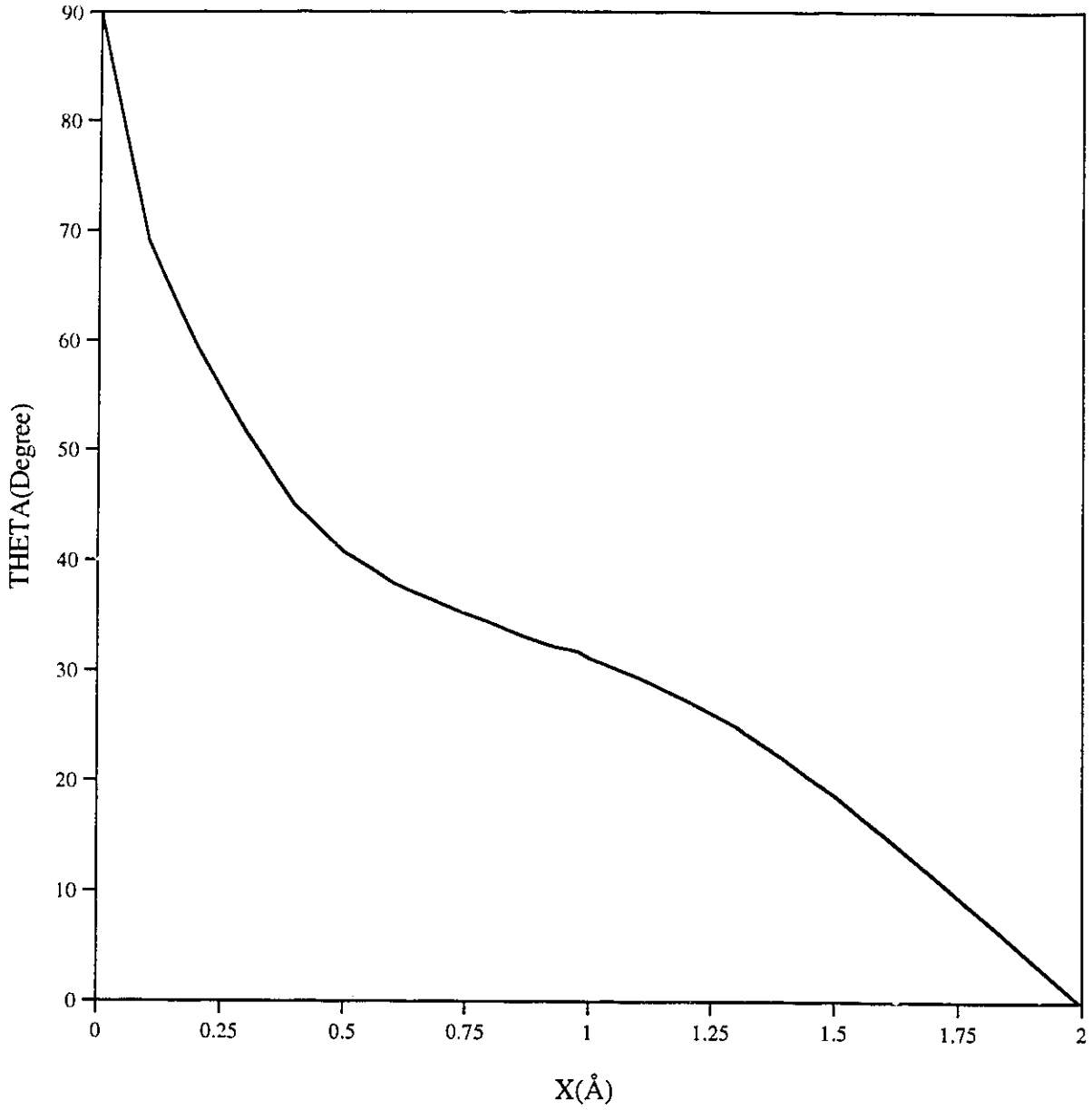

FIGURE 3.1.15: THETA VS. POSITION CO2 ALONG THE <100> DIRECTION (PARAMETER SET II).

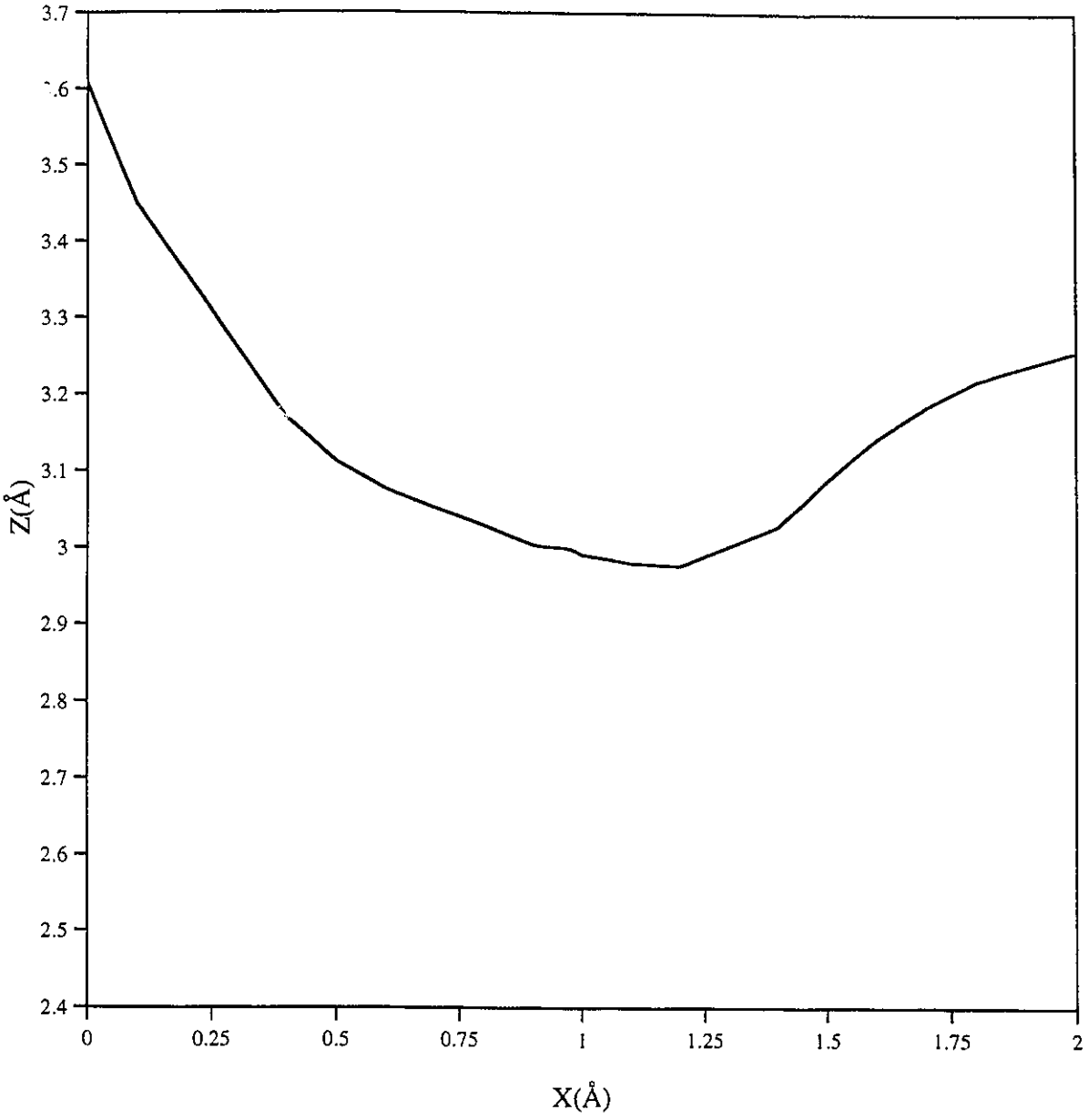

FIGURE 3.1.16: HEIGHT (Z) VS. POSITION OF CO2 ALONG THE <100> DIRECTION (PARAMETER SET II).

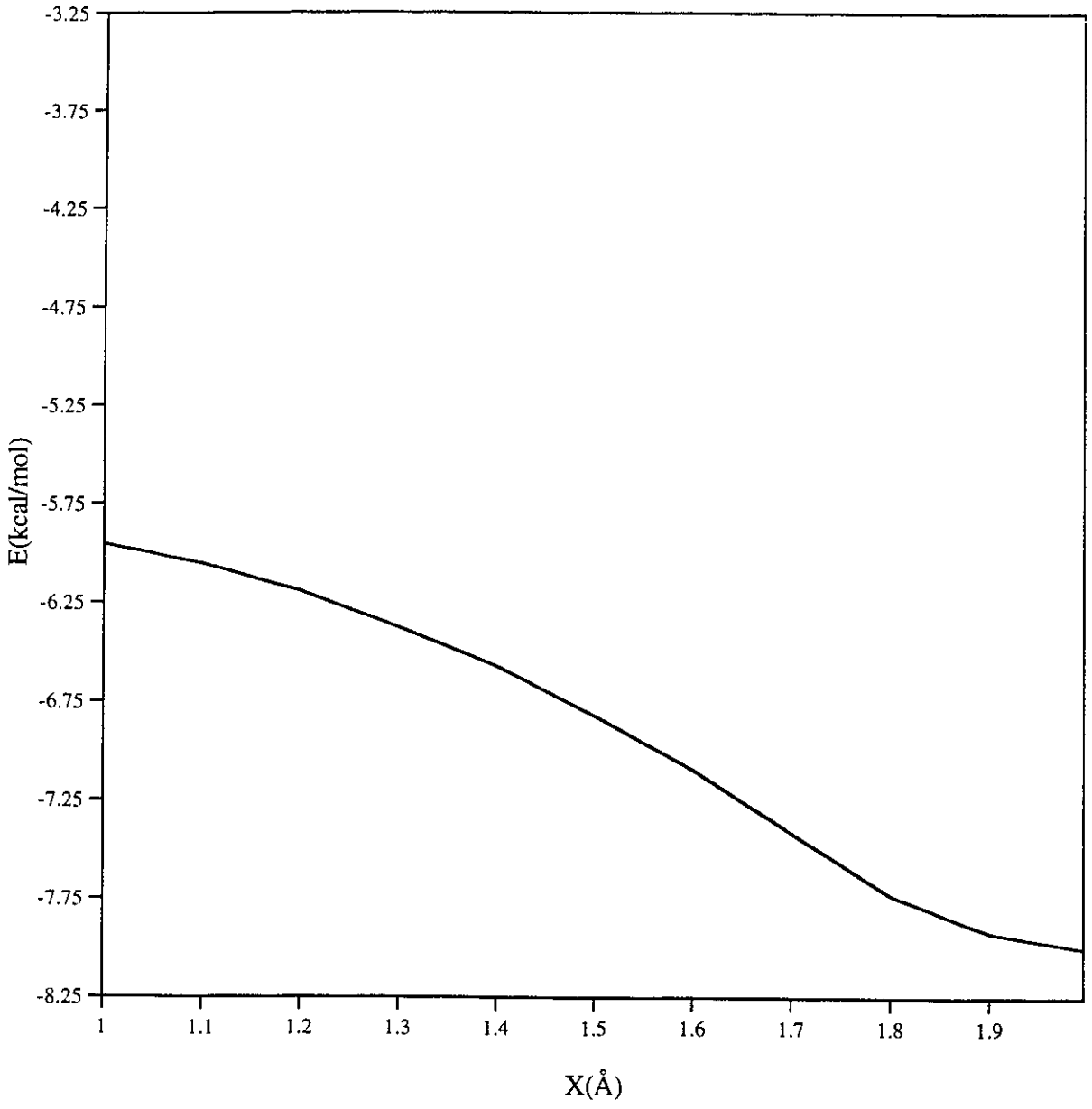

FIGURE 3.1.17: SURFACE POTENTIAL OF CO2/NaCl(001) FROM SADDLE POINT TO ABSOLUTE POTENTIAL MINIMUM (PARAMETER SET II).

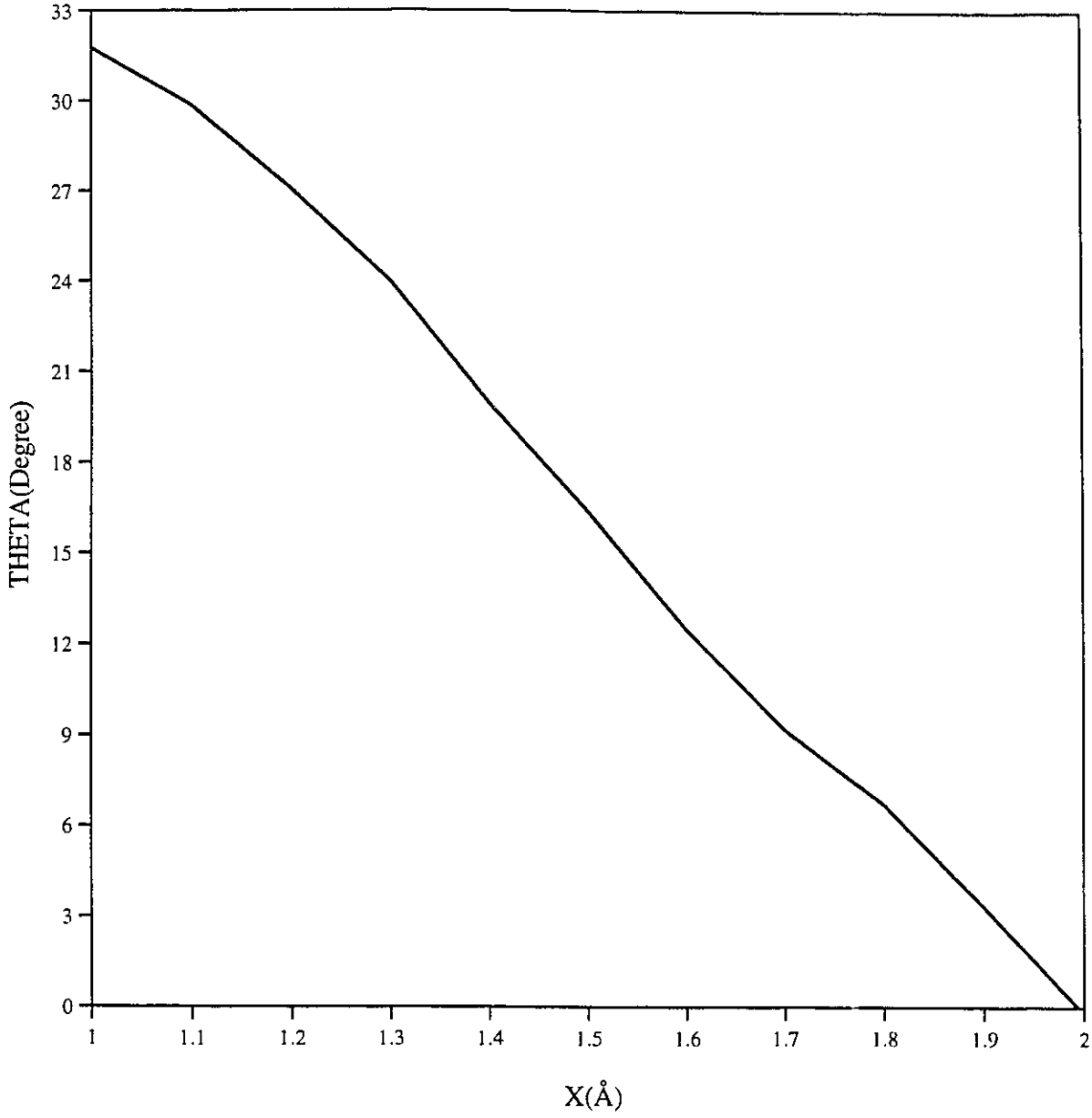

FIGURE 3.1.18: THETA VS. POSITION OF CO2 FROM SADDLE POINT TO ABSOLUTE POTENTIAL MINIMUM (PARAMETER SET II).

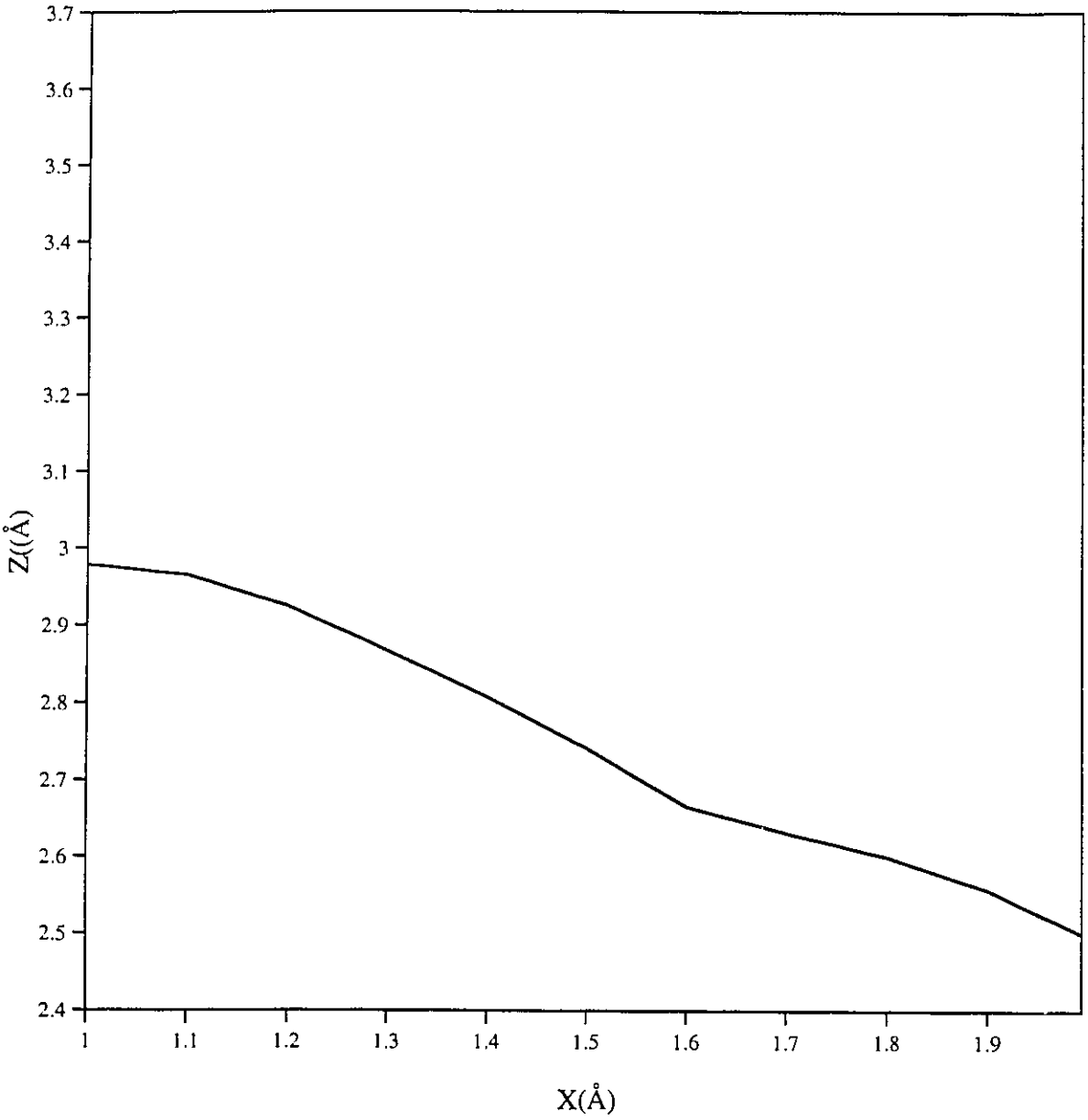

FIGURE 3.1.19: HEIGHT (Z) VS. POSITION OF CO2 FROM SADDLE POINT TO ABSOLUTE POTENTIAL MINIMUM (PARAMETER SET II).

3.2. METROPOLIS MONTE CARLO SIMULATION

Why has the Metropolis Monte Carlo method been used instead of the Molecular Dynamics method in these simulation? Molecular Dynamics is a deterministic method used to solve the classical equations of motion for a system of N molecules interacting via an intermolecular potential. The key idea in Molecular Dynamics is motion which describes how position, velocities and orientations change with time. In general, the molecular position, velocities, and other dynamical information are given at time t and then calculated, to a sufficient degree of accuracy, at a later time $t + \delta t$. In effect, "Molecular Dynamics constitutes a motion picture that follows molecules as they dart to and fro, twisting, turning, colliding with one another, and perhaps colliding with their container"[39,40]. It is best at describing detailed motion and dynamically correlated quantities and structures. The temperature is difficult to control in Molecular Dynamics because the kinetic energy involved fluctuates. The simulation must be propagated through a large number of time steps in order to obtain good results.

In contrast, Monte Carlo is a statistical method and collects statistics for quantities such as (φ, θ). It is easy to control the temperature in Monte Carlo and obtain results quickly. Monte Carlo uses a random number in its calculations, works with a large number of particles and generates many more different configurations than can be generated from the Molecular Dynamics method.

In this method, the position and orientation of the CO_2 molecules on the surface of NaCl(001) were varied while the number of molecules, as well as the volume and temperature of the system were kept constant (canonical ensemble Q(N,V,T)). In Monte Carlo simulations, the general idea is as follows. The old energy is calculated, then a randomly chosen molecule temporarily moves to a new position by choosing a random rotation (changing φ or θ) or translation (changing x, y or z). The new energy (E_{new}) and the energy difference $\Delta E = E_{new} - E_{old}$ is calculated. If ΔE is zero or negative the move is accepted. If ΔE is positive, then the ΔE dependent acceptance probability $P(\Delta E) = \exp\left(\frac{-\Delta E}{k_B T}\right)$ (where: k_B is Boltzman constant and T is the absolute temperature) is calculated and compared with a random number ξ which is generated by the computer. If ξ is smaller or equal to $P(\Delta E)$ then the move is accepted. If ξ is larger than $P(\Delta E)$ then the move is rejected (see Figures 3.2.1 and 3.2.2). After all of the molecules are chosen one cycle is finished.

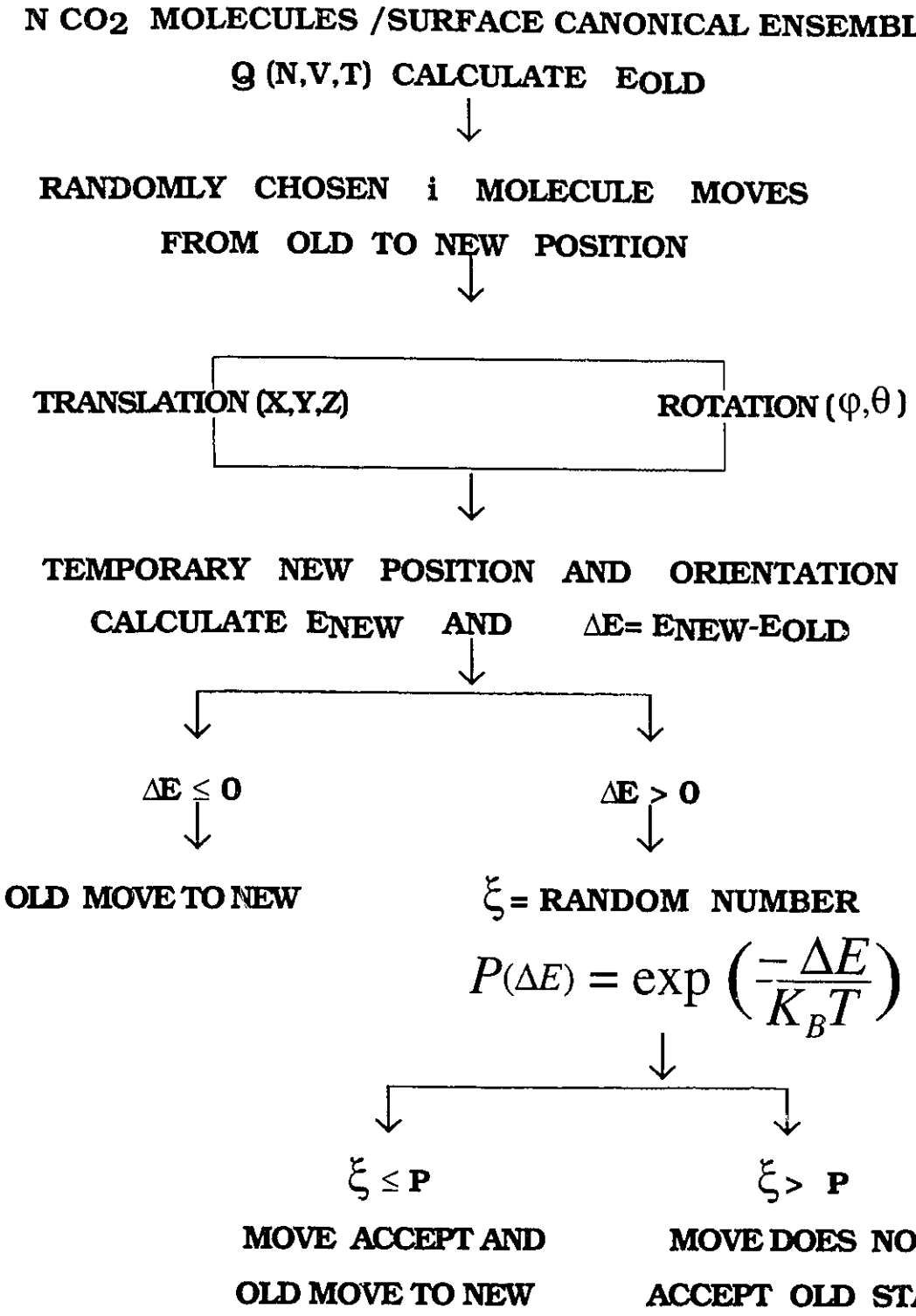

FIGURE 3.2.1. FLOW CHART AND SUMMARY OF MONTE CARLO SIMULATION.

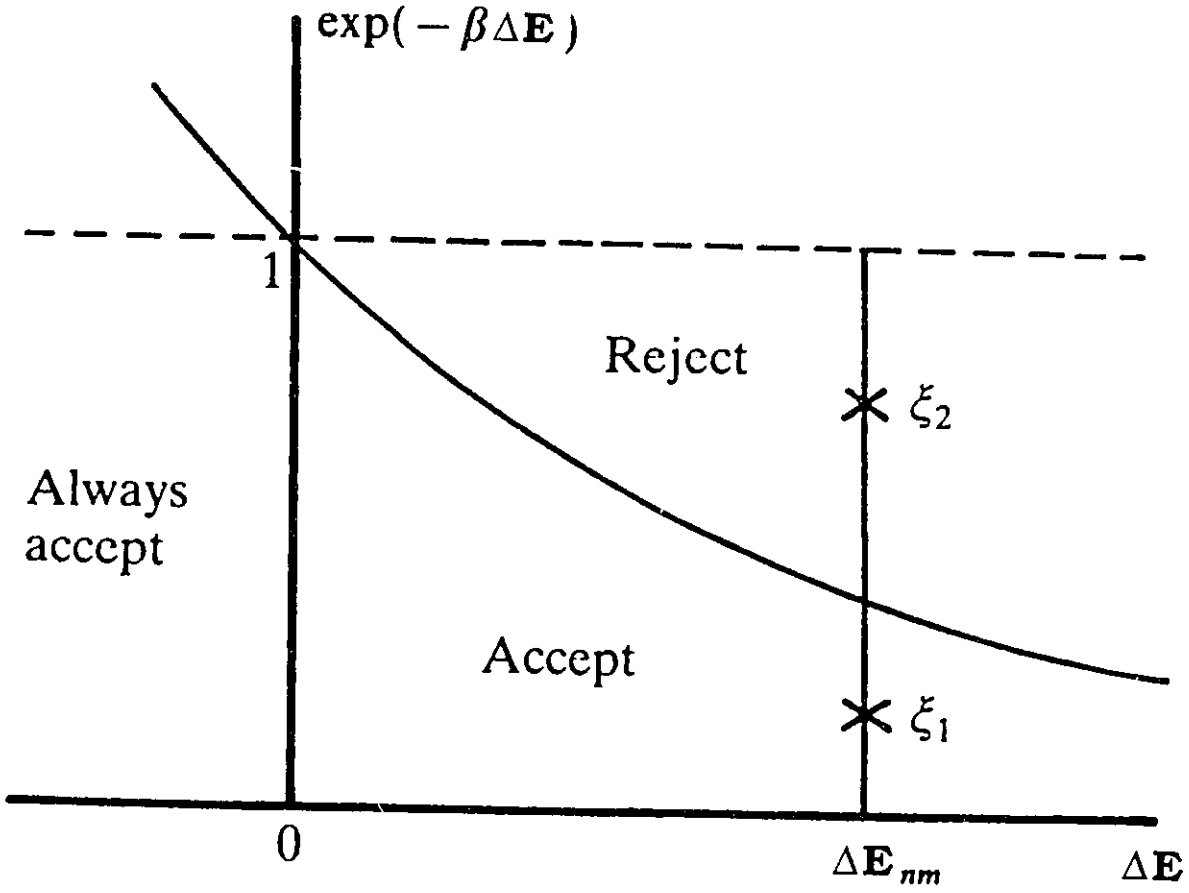

FIGURE 3.2.2: ACCEPTANCE CRITERIA FOR "UPHILL" MOVES IN A MONTE CARLO SIMULATION (From ref. [39]).

3.2.1. RESULTS AND DISCUSSION OF MONTE CARLO SIMULATION

The Metropolis Monte Carlo method (canonical ensemble) was used to examine the structure and cohesive energy of monolayer and multilayer films of CO_2/NaCl(001). This investigation was also concerned with the stability of the overlayer structures as well as the temperature dependence of the adlayer energies and molecular orientations. The computationally accessible quantities examined were the potential energy and individual molecular orientations with respect to the surface.

The monolayer, bilayer and trilayer systems of CO_2/NaCl(001) were examined at the following temperatures 1 K, 5 K, 55 K and 90 K. The lowest temperatures (1 K and 5 K) were examined to obtain information on ideal structures. The higher temperatures correspond to the experimental conditions under which this system was examined by various research groups. For monolayer and multilayer systems the Monte Carlo simulations showed that the CO_2 molecules sit above the connection line between Na^+ and Cl^- (along the <100> and <010> directions) and form a herringbone-like pattern. Specifically, the CO_2 adlayers have a $p(2\times1)$ structure with two CO_2 molecules in each unit cell related via a glide plane.

3.2.1.1. Monolayer system

For the monolayer system the temperature dependent average potential energy per CO_2 molecule was computed and found to almost match the values calculated from the equation $E_{1K}+5k_B\Delta T/2$ (Table 3.2.1), where E_{1K} is the potential energy at 1 K. As may be seen in the high temperature limit of equation 1.2.2 there is a thermal correction factor of $k_BT/2$ to the potential energy for each harmonic oscillator degree of freedom of the molecule at the surface. For the case of a rigid linear triatomic molecule localized at an adsorption site there are five degrees of freedom: three frustrated translations (vibrations) and two frustrated rotations (librations). Hence the potential energy is given by $E_{1K}+5k_B\Delta T/2$. The computed value of the potential energy at 1 K was found to be -8.46 kcal/mol which is in good agreement with the 0 K isosteric heat of adsorption (-8.77± 0.31 kcal/mol) estimated from the 90 K experimental value (-8.51± 0.31 kcal/mol) of Heidberg[7] using equation 1.2.6.

The Monte Carlo simulations were started from a $p(2\times1)$ monolayer structure (N=100) and were run for at least 50,000 cycles. Although the molecules acquired a thermal distribution for their positions and orientations there was no change in the overall structure, indicating that the $p(2\times1)$ monolayer structure is stable. Snapshots of the final configuration of the monolayer at various temperatures are shown in Figures 3.2.3-3.2.5. At 1 K the monolayer structure (Figure. 3.2.3) is

very ordered (the structure of 5 K is almost the same and hence is not shown) with thermal disorder increasing with temperature (Figures. 3.2.4, 3.2.5) as one would expect.

The "crystallographic" structure of the CO_2 monolayer is shown diagrammatically in Figure 3.2.3. The $p(1\times1)$ structure is that of the real space surface lattice of NaCl(001) where each of the vertices of the square sits overtop of a sodium ion site. This defines the surface mesh which all other adlayer structures are referred to. The $(\sqrt{2}\times\sqrt{2})$ structure shown corresponds to the (001) face of the standard unit cell of bulk NaCl. It should be noted that by virtue of the almost identical lattice constants of solid NaCl (5.65Å) and CO_2 (5.57Å) this pattern coincides with the (001) face of a bulk crystal of CO_2. However, the orientation of the CO_2 molecules in the bulk phase is <u>not</u> the same as in the monolayer (see Figure 3.2.21). Instead, the appropriate unit cell for the monolayer is the $p(2\times1)$ structure as shown. This is the simplest unit cell consistent with the experimental results[7, 12]. It is interesting to note that the monolayer can also be described by the $(2\sqrt{2}\times2\sqrt{2})$ structure shown, however, it has a larger unit cell and contains no new information. Scoles *et al.*[10] have reported the observation of a true $(2\sqrt{2}\times2\sqrt{2})\mathbf{R}45°$ structure using Low Energy Helium Atom Diffraction, although Toennies *et al.*[12] claim that this observation is instead a simple superposition of the monolayer and multilayer patterns, *i.e.* the $p(2\times1)$ and $c(2\times2)$ patterns respectively.

The orientation of the molecules on the surface can be best discussed in terms of their azimuthal angle φ and polar angle θ. The temperature dependence of these angular distributions is shown in Figures 3.2.6 and 3.2.7 respectively. The maxima of the φ distribution were found at -43° and 43° for all temperatures, and hence the angle between the projected molecular axes of two neighbouring molecules is 86° which is in good agreement with experimental value of 80°± 5°. At low temperatures the peak of the φ probability is sharp and broadens with increasing temperature (Figure 3.2.6). The maximum in the θ probability was found to be 60° (with respect to the surface normal) for all temperatures, again in good agreement with the experimental value of 56°± 5°. The peak of the θ distribution is also sharp at low temperatures and broadens as the temperature increases (Figure 3.2.7). Higher temperatures (150K) were also examined but no significant shift in the distribution maxima were seen.

TABLE 3.2.1: ENERGY OF THE $p(2\times1)$ STRUCTURE OF A MONOLAYER OF CO_2 ON NaCl(001).

<E>/CO_2 kcal/mol	1 K	5 K	55 K	90 K
CO_2-CO_2(V)*	-1.745	-1.742	-1.678	-1.639
CO_2-CO_2(el)**	-0.908	-0.9077	-0.8803	-0.8588
CO_2-NaCl(V)*	-1.377	-1.385	-1.393	-1.396
CO_2-NaCl(el)**	-4.426	-4.405	-4.241	-4.127
Total Energy	-8.457	-8.440	-8.193	-8.021
$E_{1K}+5k_B\Delta T/2$	-8.457	-8.437	-8.189	-8.015

*) Repulsion and dispersion

**)Electrostatic

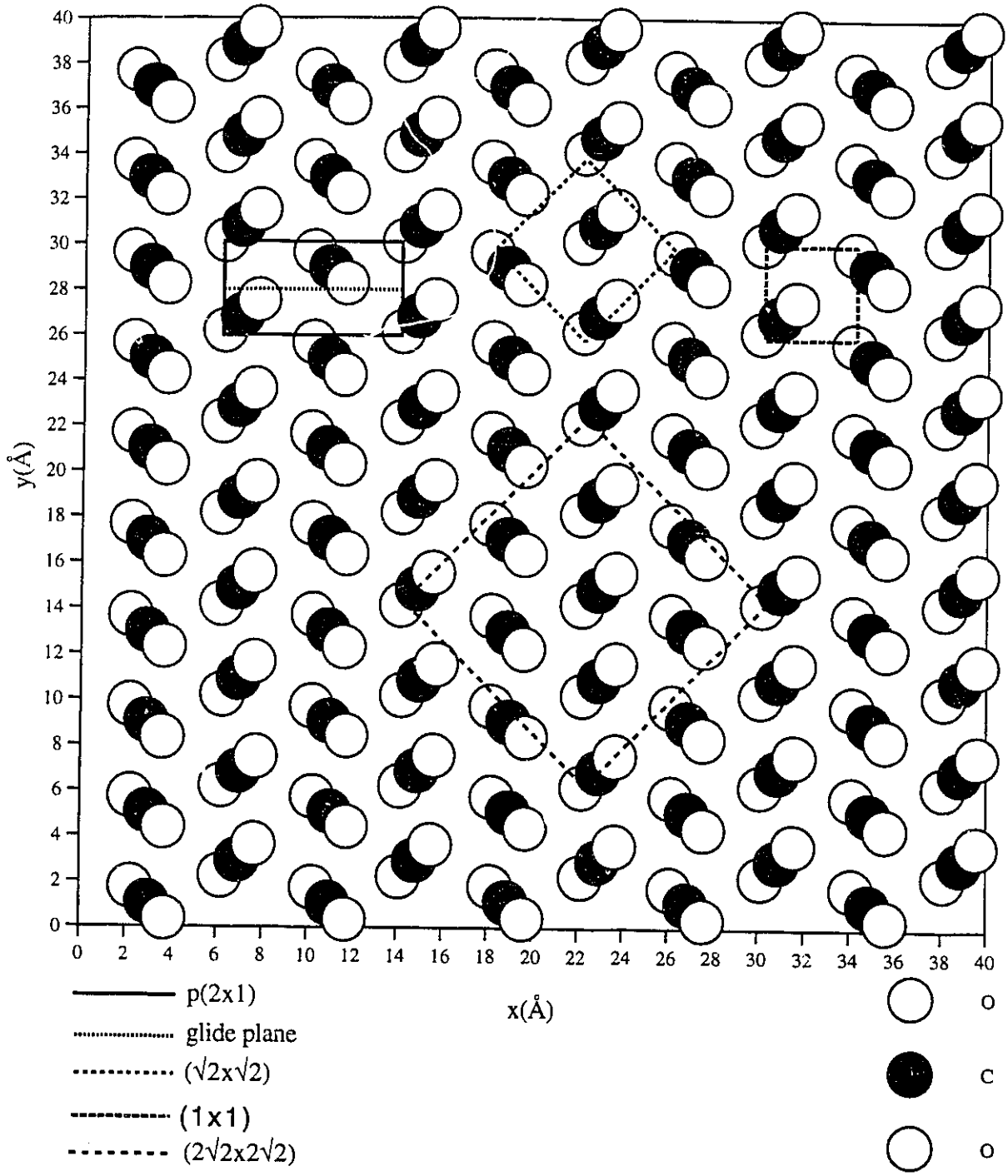

FIGURE 3.2.3: THE p(2x1) STRUCTURE OF MONOLAYER CO2/NaCl(001) AT T=1K.

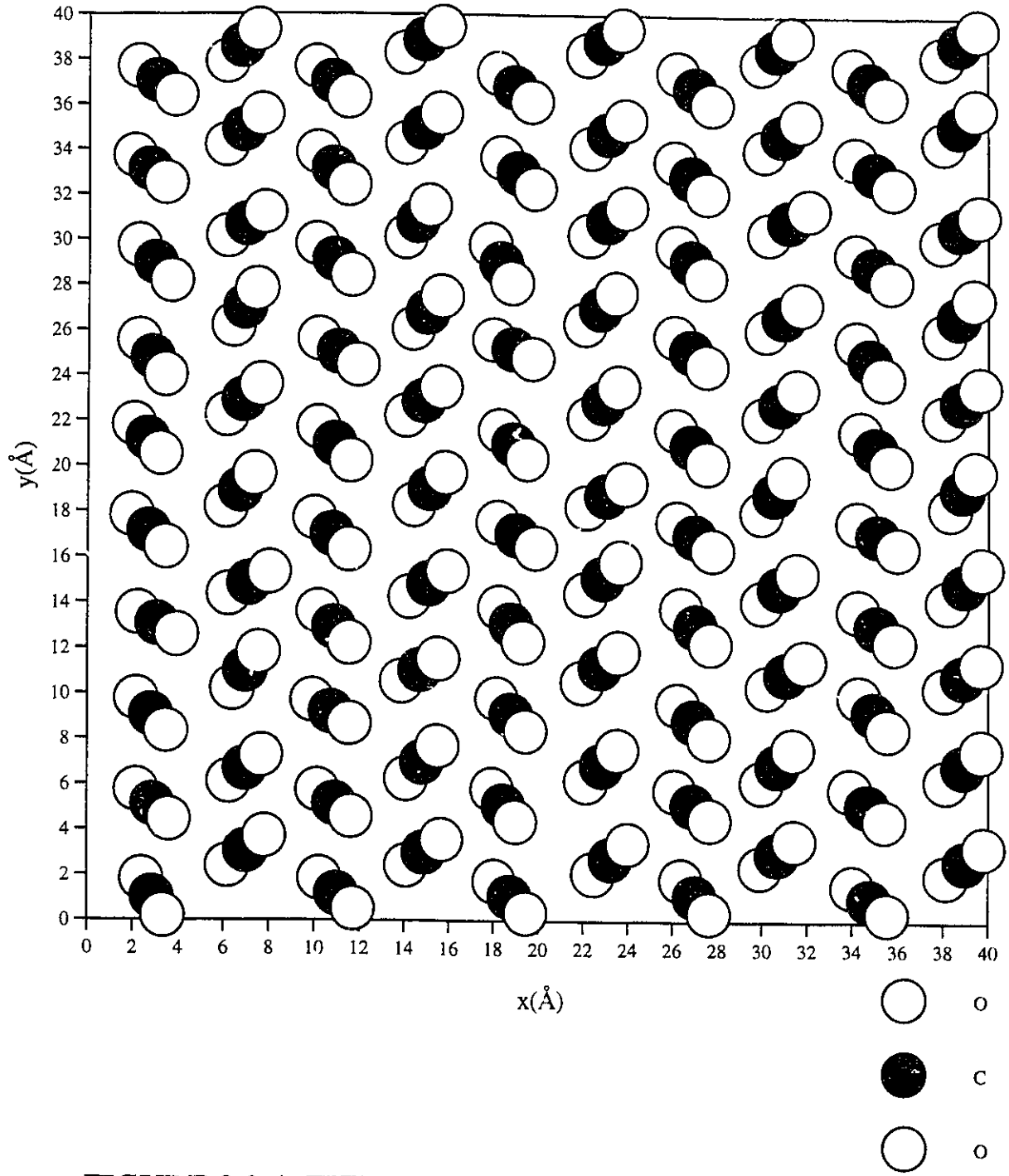

FIGURE 3.2.4: THE p(2x1) STRUCTURE OF MONOLAYER CO2/NaCl(001) AT T=55K.

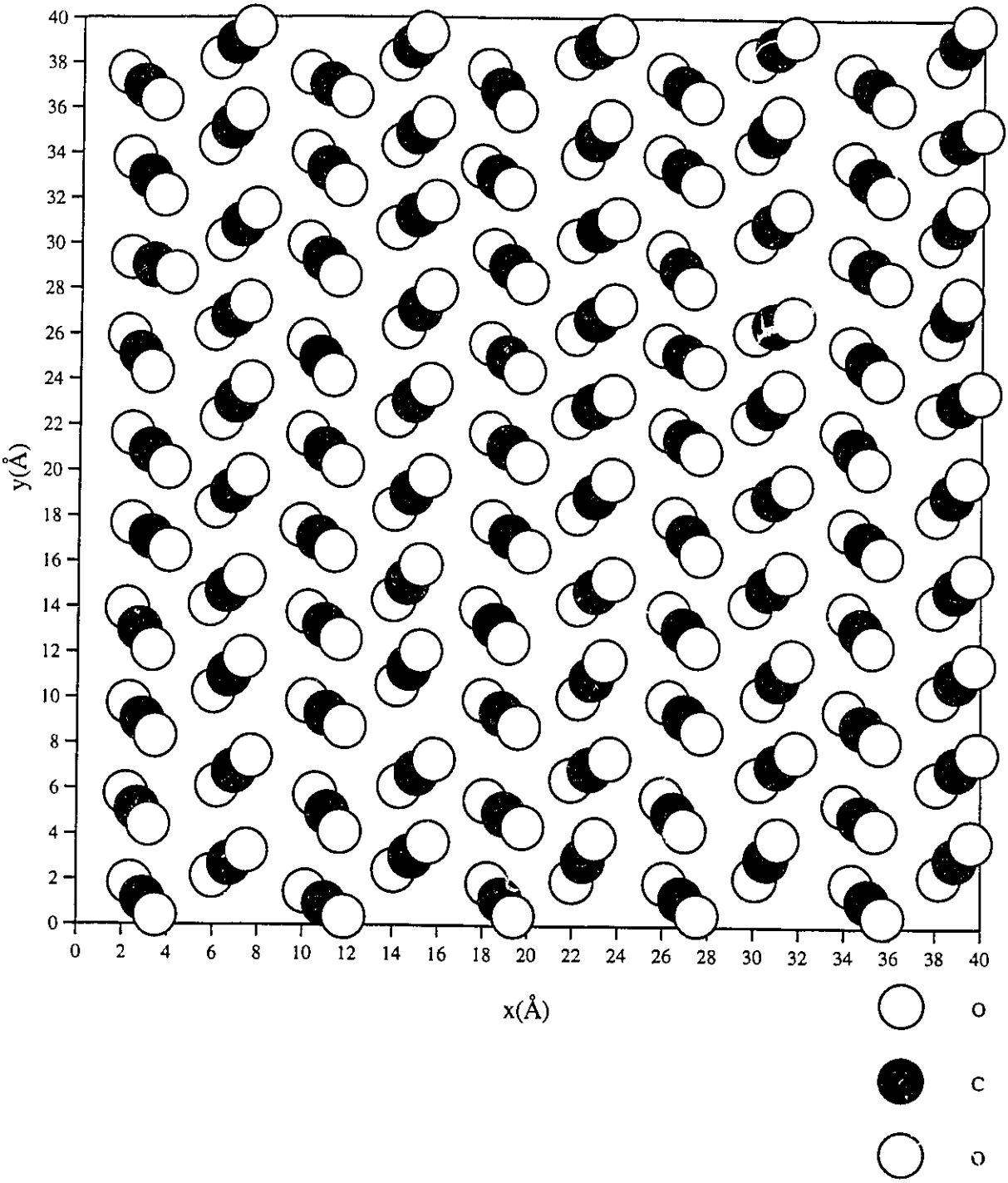

FIGURE 3.2.5: THE p(2x1) STRUCTURE OF MONOLAYER CO2/NaCl(001) AT T=90K.

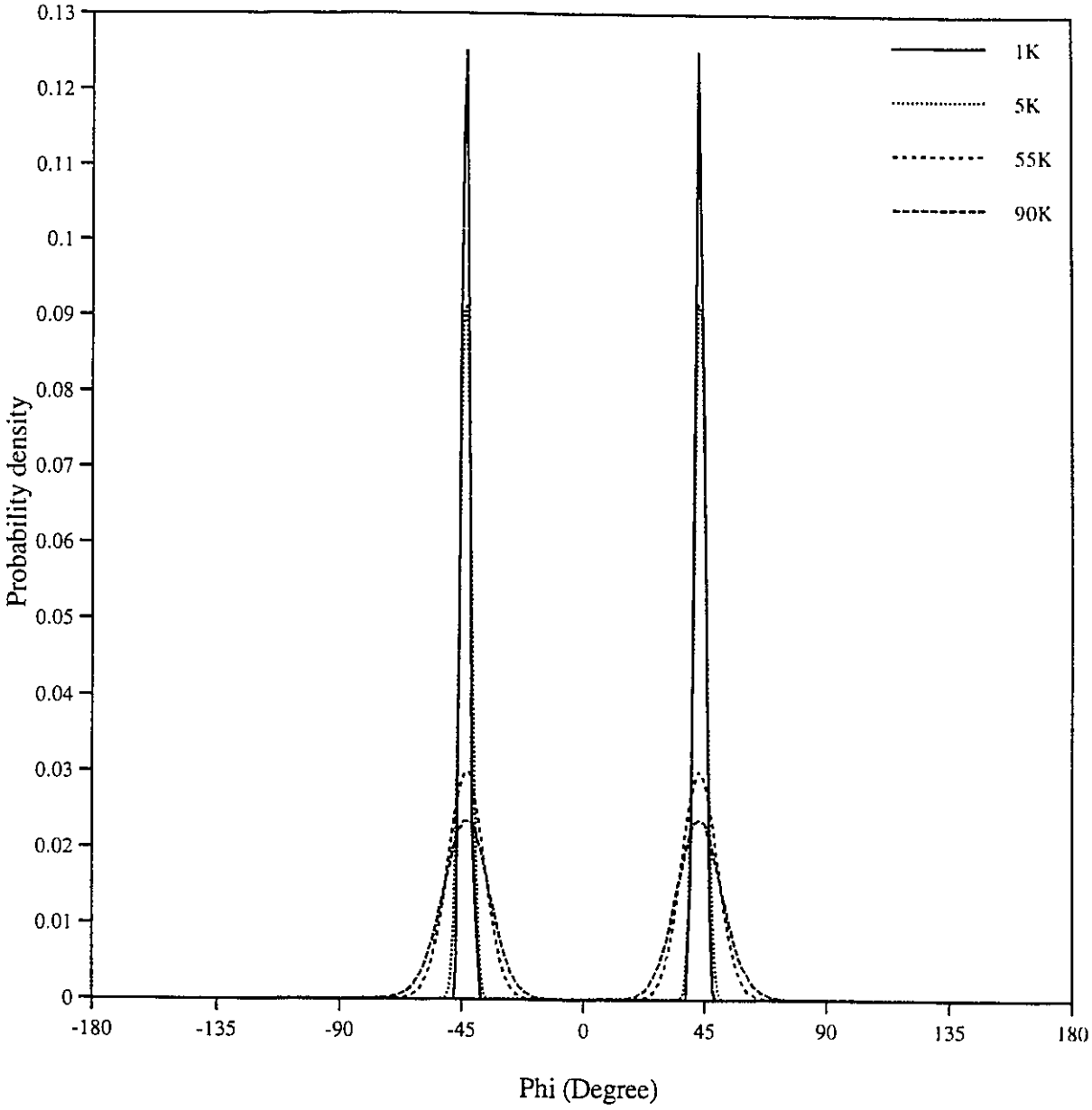

FIGURE 3.2.6: PHI PROBABILITY OF A p(2x1) MONOLAYER SYSTEM (T=1 K, 5 K, 55 K, 90 K).

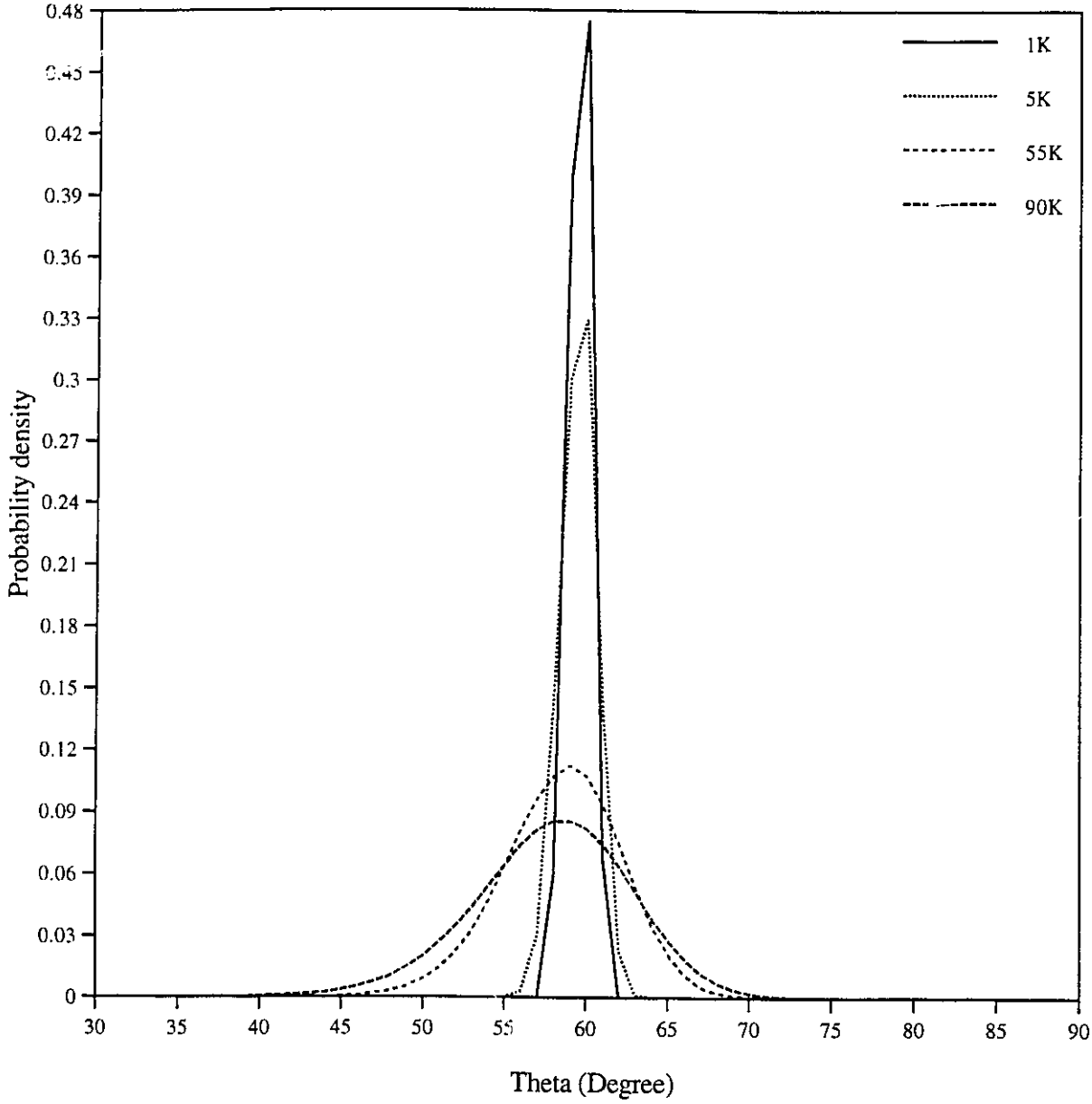

FIGURE 3.2.7: THETA PROBABILITY OF A p(2x1) MONOLAYER SYSTEM (T=1 K, 5 K, 55 K, 90 K).

3.2.1.2. Bilayer system

A Monte Carlo simulation of a bilayer system was also run. An assembly of 200 CO_2 molecules was started from a $p(2\times1)$ bilayer structure and were run for at least 50,000 cycles. The temperature dependent average potential energy per CO_2 molecule was computed and again almost matched the potential energies calculated from the equation $E_{1K}+5k_B\Delta T/2$ as may be seen in Table 3.2.2. Although the molecules acquired a thermal distribution for their positions and orientations, there was no change in the overall structure indicating that the $p(2\times1)$ bilayer structure is stable. Snapshots of the final configuration of the bilayer at various temperatures are shown in Figures 3.2.8 - 3.2.13.

The orientation of the molecules was also determined. For the first layer the maxima of the φ probability was found at about -44° and 44° (Figure 3.2.14) and the maximum of the θ probability was found at about 60° (Figure 3.2.15). For the second layer the maxima of the φ probability switched directions and was found at about -138° and 138° (Figure 3.2.16) while the maximum of the θ probability remained at 60° (Figure 3.2.17). The maxima of the angular probability distributions showed no temperature dependence, although the peak widths broaden as the temperature increased. The CO_2-CO_2 interaction energy for the bilayer is -4.049 kcal/mol which is less than 2/3 of the cohesive energy of a bulk CO_2 crystal (-6.8356 kcal/mol); a lesser value is expected because the bilayer structure differs from the $c(2\times2)$ structure of bulk CO_2.

TABLE 3.2.2: ENERGY OF THE $p(2\times1)$ STRUCTURE OF A BILAYER OF CO_2 ON NaCl(001).

<E>/CO_2 kcal/mol	1 K	5 K	55 K	90 K
CO_2-CO_2(V)*	-2.865	-2.854	-2.734	-2.657
CO_2-CO_2 (el)**	-1.184	-1.183	-1.137	-1.094
CO_2-NaCl(V)*	-0.8162	-0.8163	-0.8146	-0.8126
CO_2-NaCl(el)**	-2.251	-2.241	-2.163	-2.109
Total Energy	-7.116	-7.095	-6.850	-6.673
$E_{1K}+5k_B\Delta T/2$	-7.116	-7.097	-6.848	-6.674

*) Repulsion and dispersion

**)Electrostatic

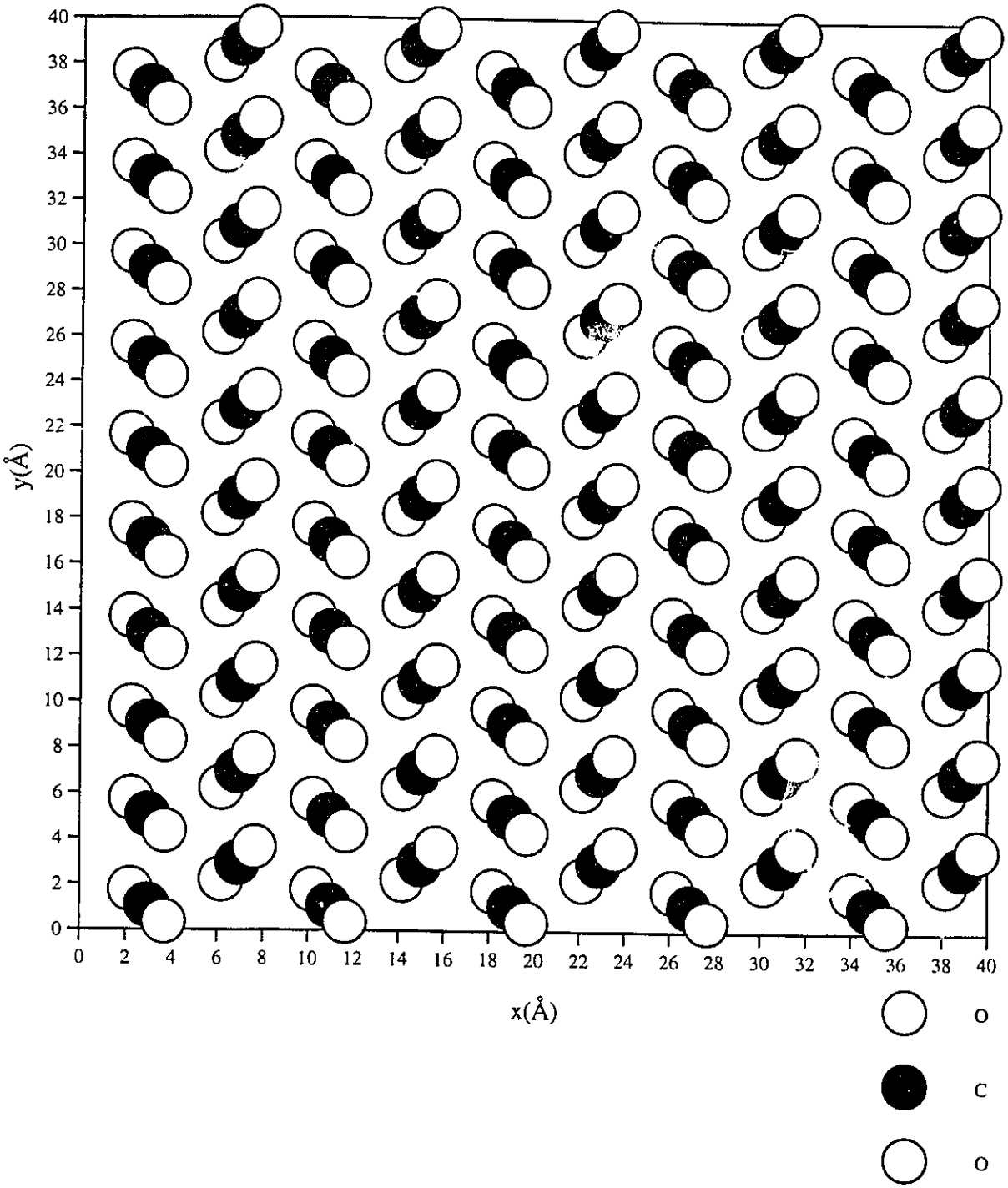

FIGURE 3.2.8: THE p(2x1) STRUCTURE OF THE FIRST LAYER OF A BILAYER SYSTEM OF CO2/NaCl(001) AT T= 1K.

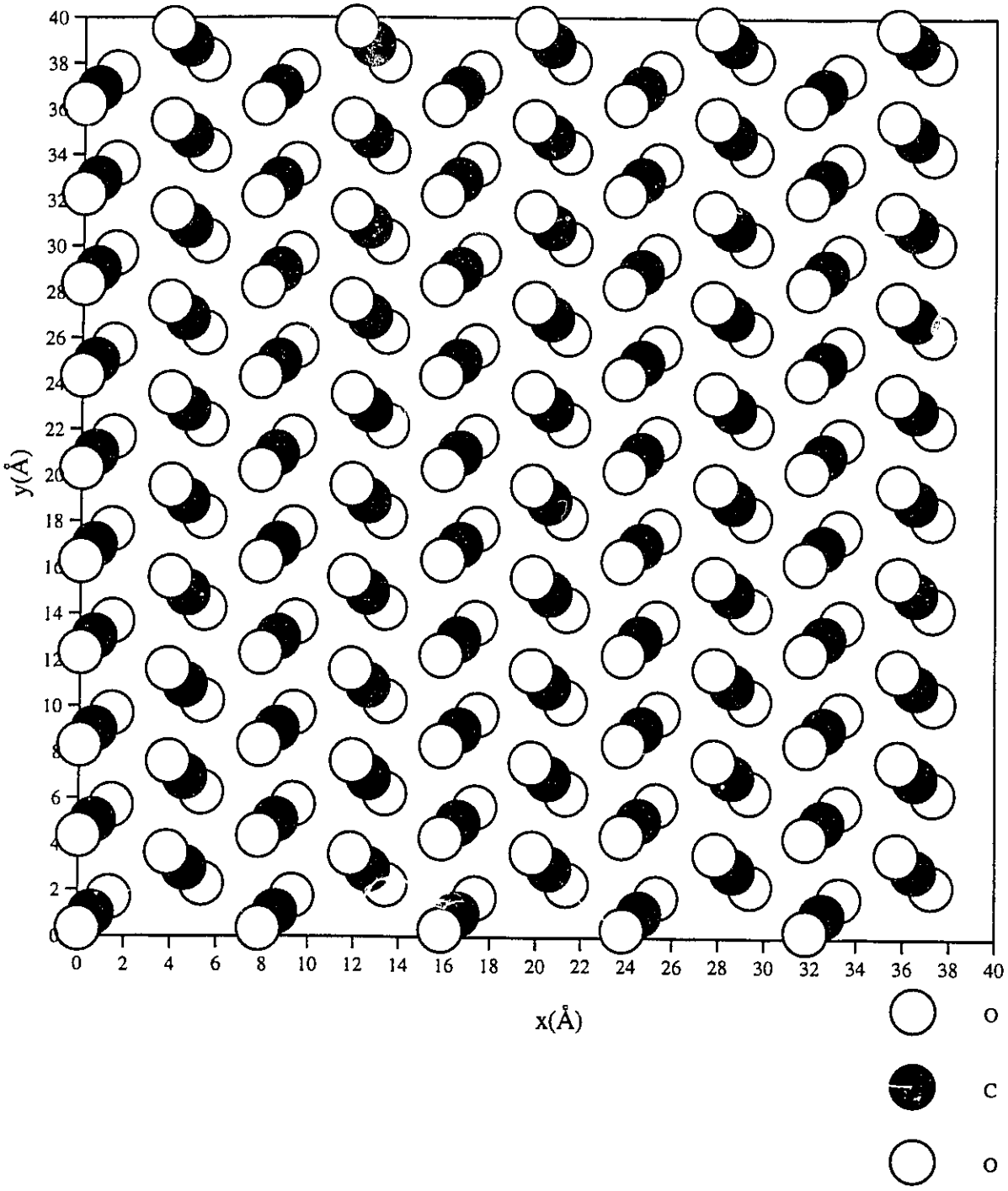

FIGURE 3.2.9: THE p(2x1) STRUCTURE OF THE SECOND LAYER OF A BILAYER SYSTEM OF CO2/NaCl(001) AT T= 1K.

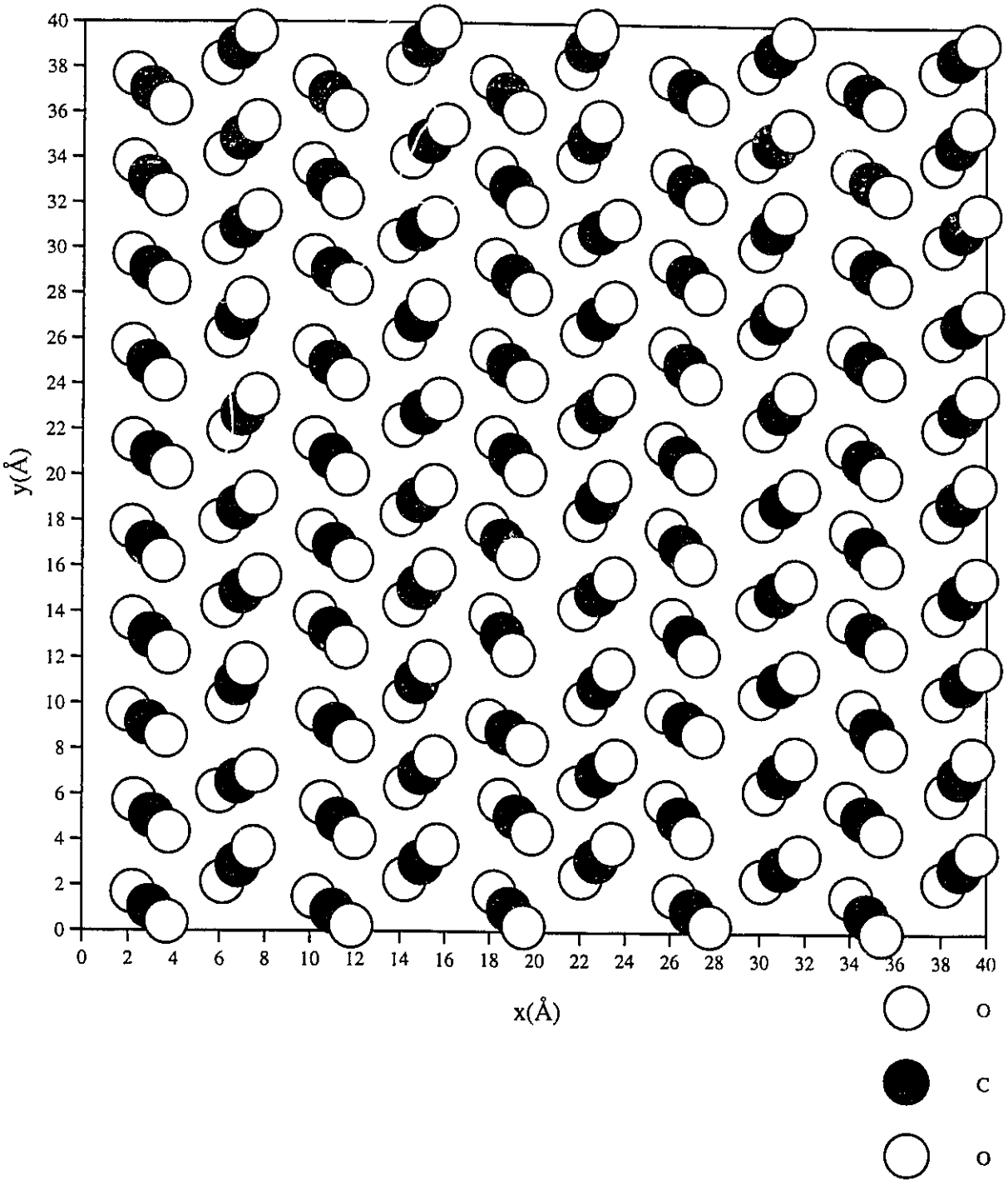

FIGURE 3.2.10: THE p(2x1) STRUCTURE OF THE FIRST LAYER OF A BILAYER SYSTEM OF CO2/NaCl(001) AT T= 55K.

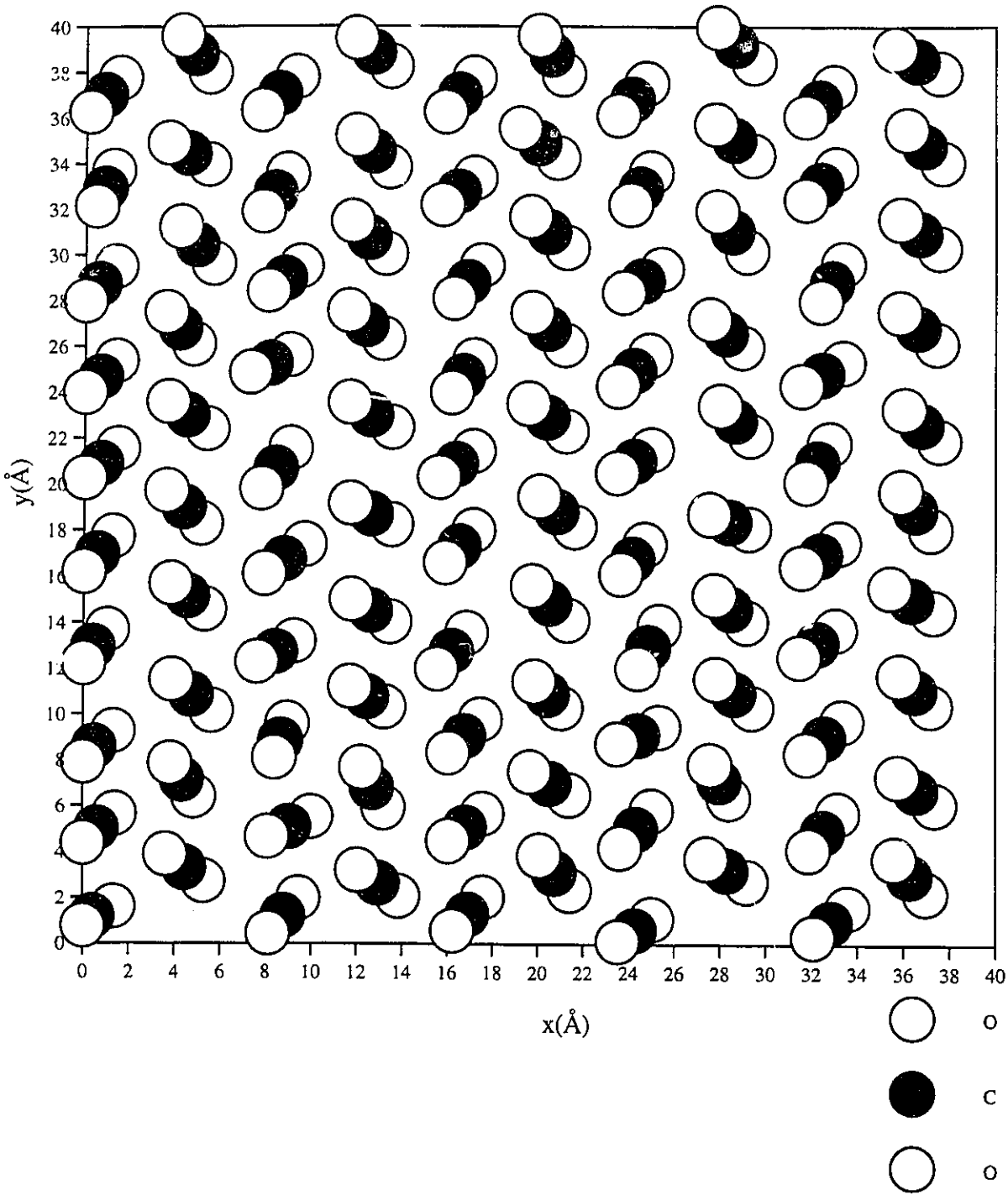

FIGURE 3.2.11: THE p(2x1) STRUCTURE OF THE SECOND LAYER OF A BILAYER SYSTEM OF CO2/NaCl(001) AT T=55K.

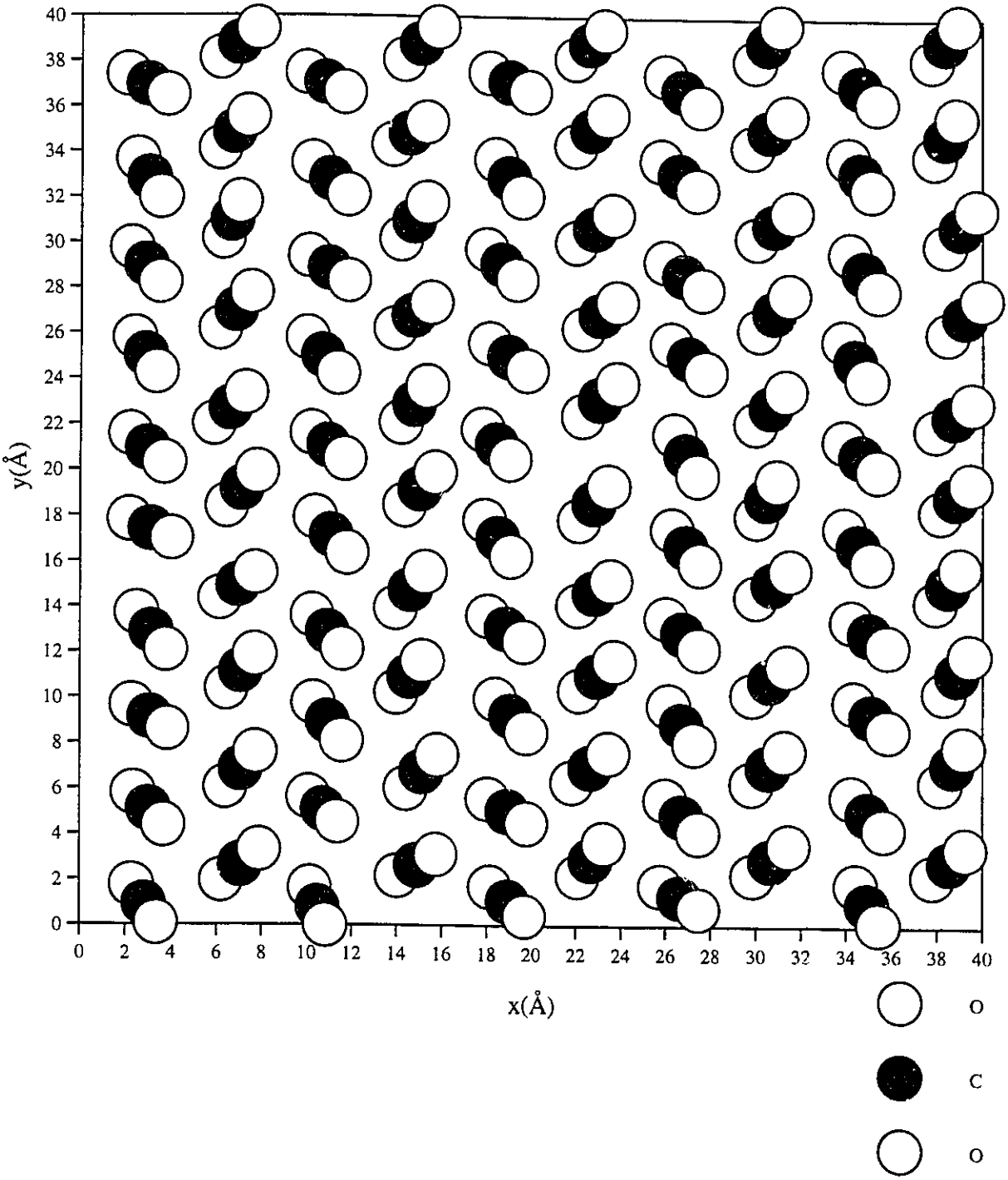

FIGURE 3.2.12: THE p(2x1) STRUCTURE OF THE FIRST LAYER OF A BILAYER SYSTEM OF CO2/NaCl(001) AT T= 90K.

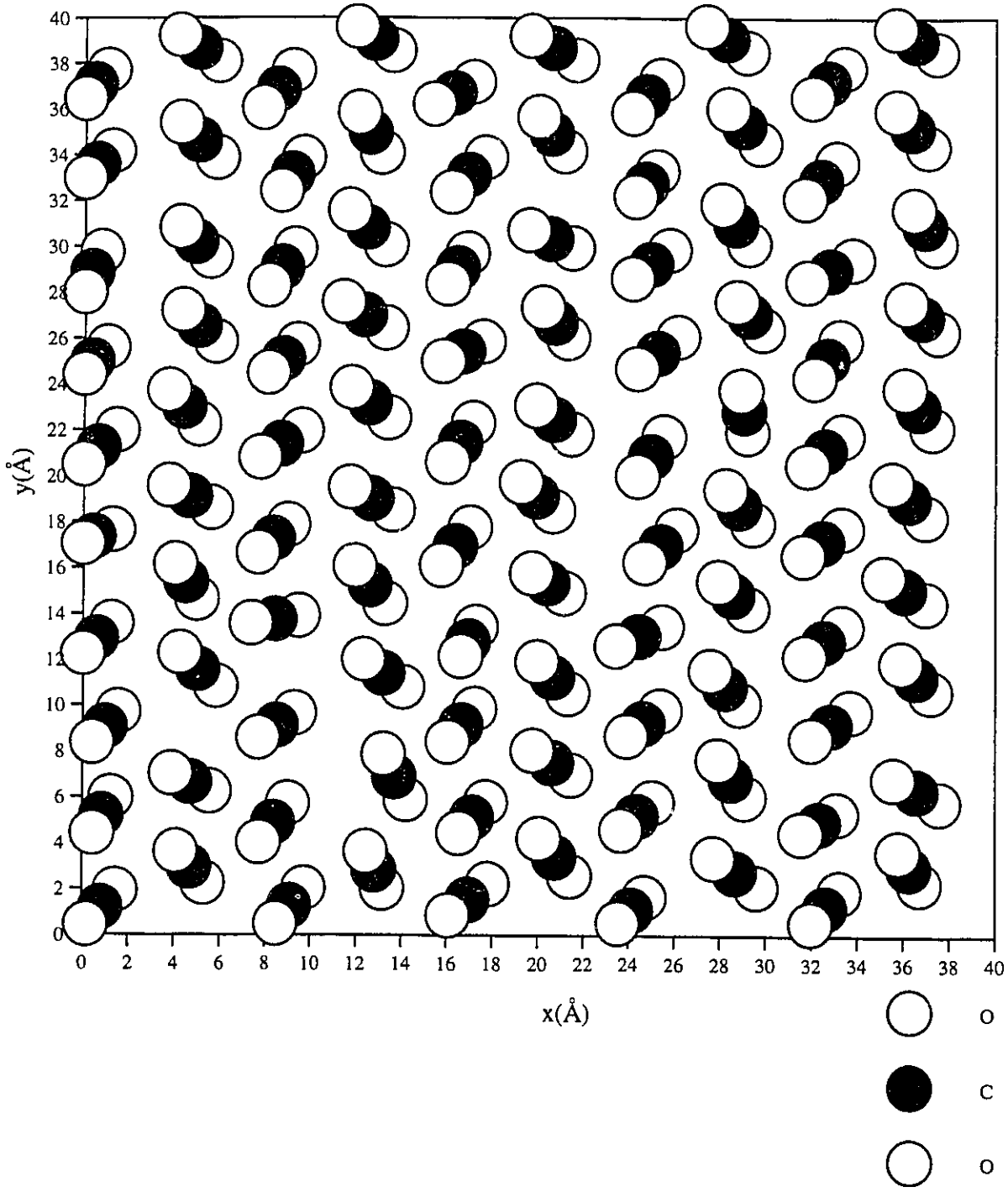

FIGURE 3.2.13: THE p(2x1) STRUCTURE OF THE SECOND LAYER OF A BILAYER SYSTEM OF CO2/NaCl(001) AT T=90K.

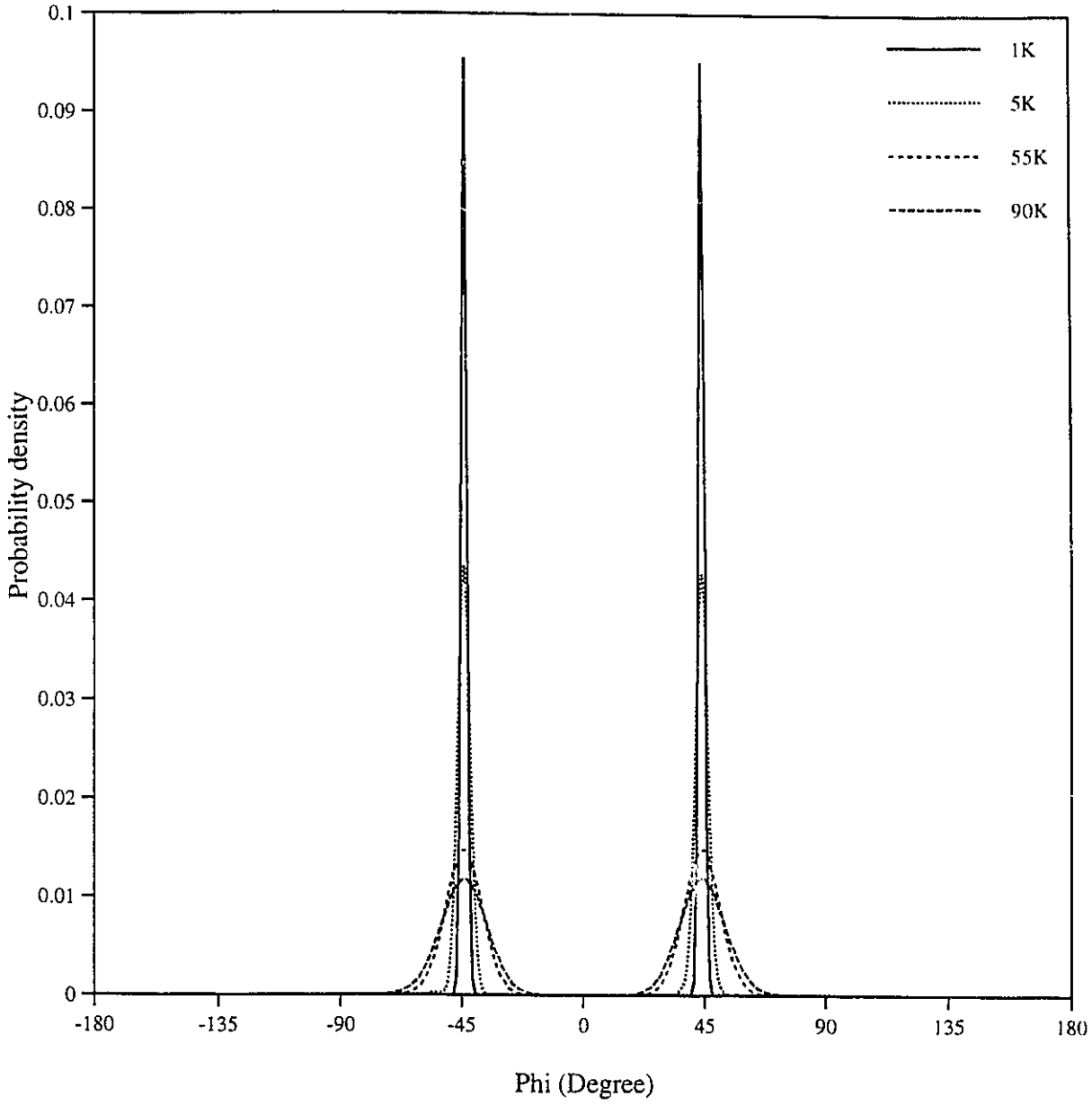

FIGURE 3.2.14: PHI PROBABILITY OF THE FIRST LAYER OF A p(2x1) BILAYER SYSTEM (T=1K,5K, 55K, 90K).

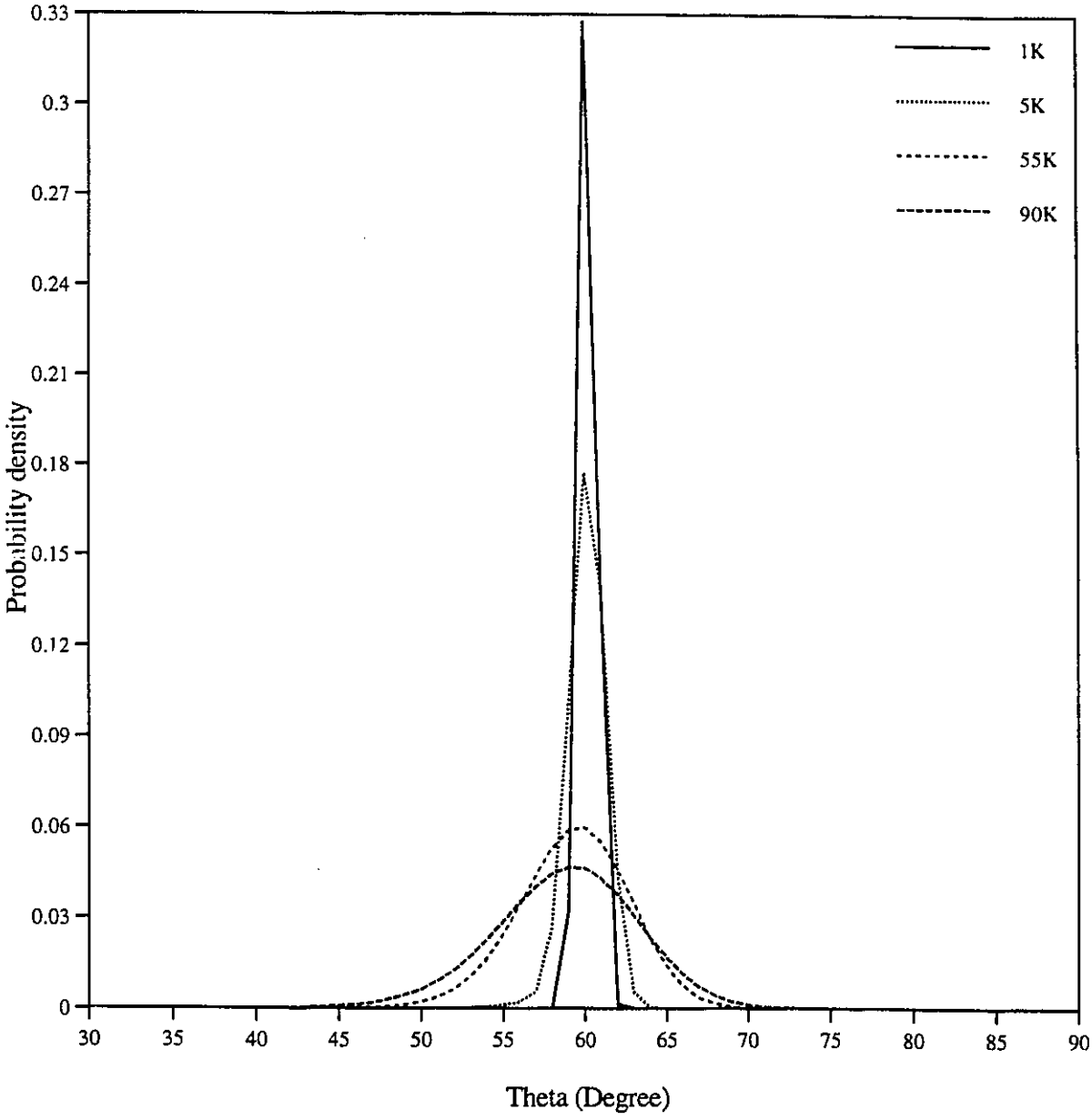

FIGURE 3.2.15: THETA PROBABILITY OF THE FIRST LAYER OF A p(2x1) BILAYER SYSTEM (T=1K,5K, 55K, 90K).

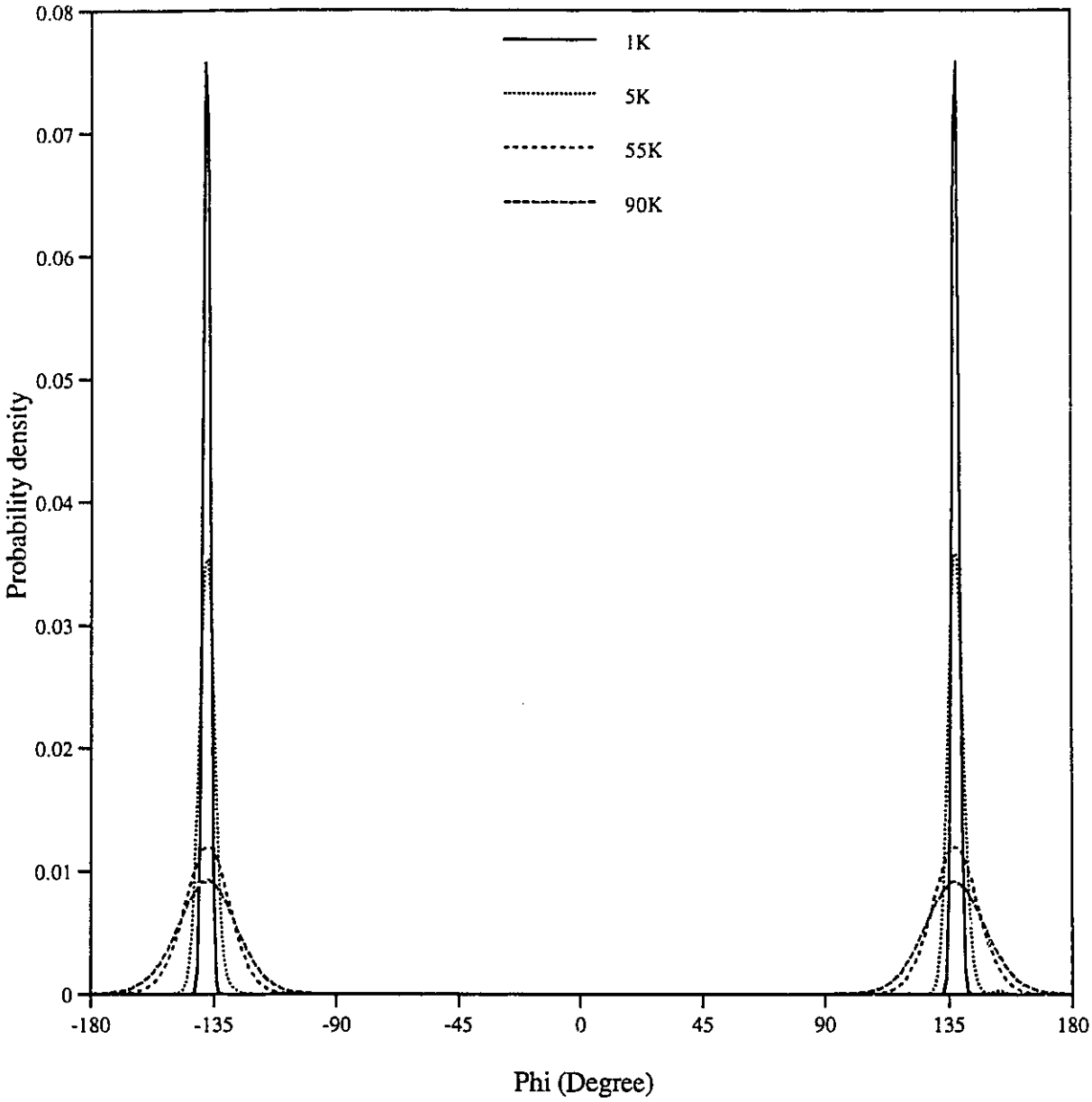

FIGURE 3.2.16: PHI PROBABILITY OF THE SECOND LAYER OF A p(2x1) BILAYER SYSTEM (T=1K,5K, 55K, 90K).

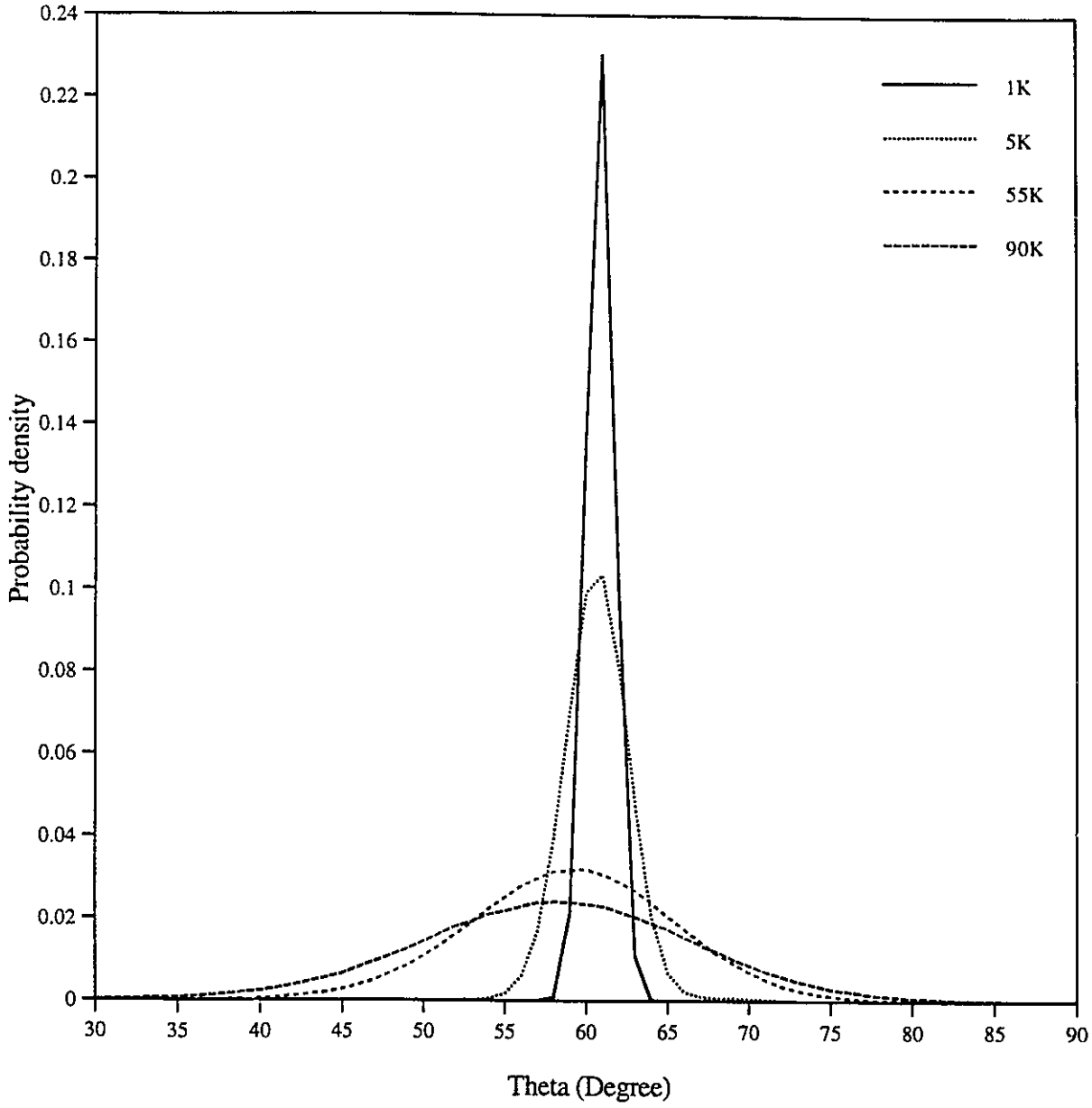

FIGURE 3.2.17: THETA PROBABILITY OF THE SECOND LAYER OF A p(2x1) BILAYER SYSTEM (T=1K,5K, 55K, 90K).

3.2.1.2. Trilayer system

The trilayer system was also examined using the same methods. Again the simulations (300 molecules) were started from a $p(2\times1)$ trilayer structure and were run at least 50,000 cycles. The results show that trilayer system is not stable and that CO_2 molecules in the second and third layers become disordered (Figure 3.2.18-3.2.20). In particular, at 55 K some molecules from the third layer collapse into the second layer as may be seen in Figure 3.2.18. The total number of CO_2 molecules in the second layer is 106 rather than 100 with the number of molecules in the third layer (Figure 3.2.19) decreasing to 94. The additional molecules in the second layer do not sit at the same height as other molecules but rather have partially penetrated into that layer; they primarily occupy the interstitial space between the second and third layers. At 90 K the layers do not collapse but the molecules begin to reorient into a different phase within the layers. A snapshot of the final configuration of the top layer of the trilayer system at 90 K is shown in Figure 3.2.20. The encircled region shows evidence of reordering into a $c(2\times2)$ structure. It seems that the addition of a third layer destabilizes the bilayer system causing it to try and adopt the more condensed $c(2\times2)$ structure similar to that of the bulk solid phase (Figure 3.2.21).

TABLE 3.2.3: ENERGY OF THE $p(2\times1)$ STRUCTURE OF A TRILAYER OF CO_2 ON NaCl(001).

<E>/CO_2 kcal/mol	1 K	5 K	55 K	90 K
CO_2-CO_2(V)*	-3.307	-3.306	-3.151	-3.053
CO_2-CO_2 (el)**	-1.333	-1.331	-1.234	-1.181
CO_2-NaCl(V)*	-0.5452	-0.5473	-0.5445	-0.5430
CO_2-NaCl(el)**	-1.485	-1.477	-1.440	-1.407
Total Energy	-6.671	-6.663	-6.370	-6.184
$E_{1K}+5k_B\Delta T/2$	-6.671	-6.651	-6.403	-6.229

*) Repulsion and dispersion

**)Electrostatic

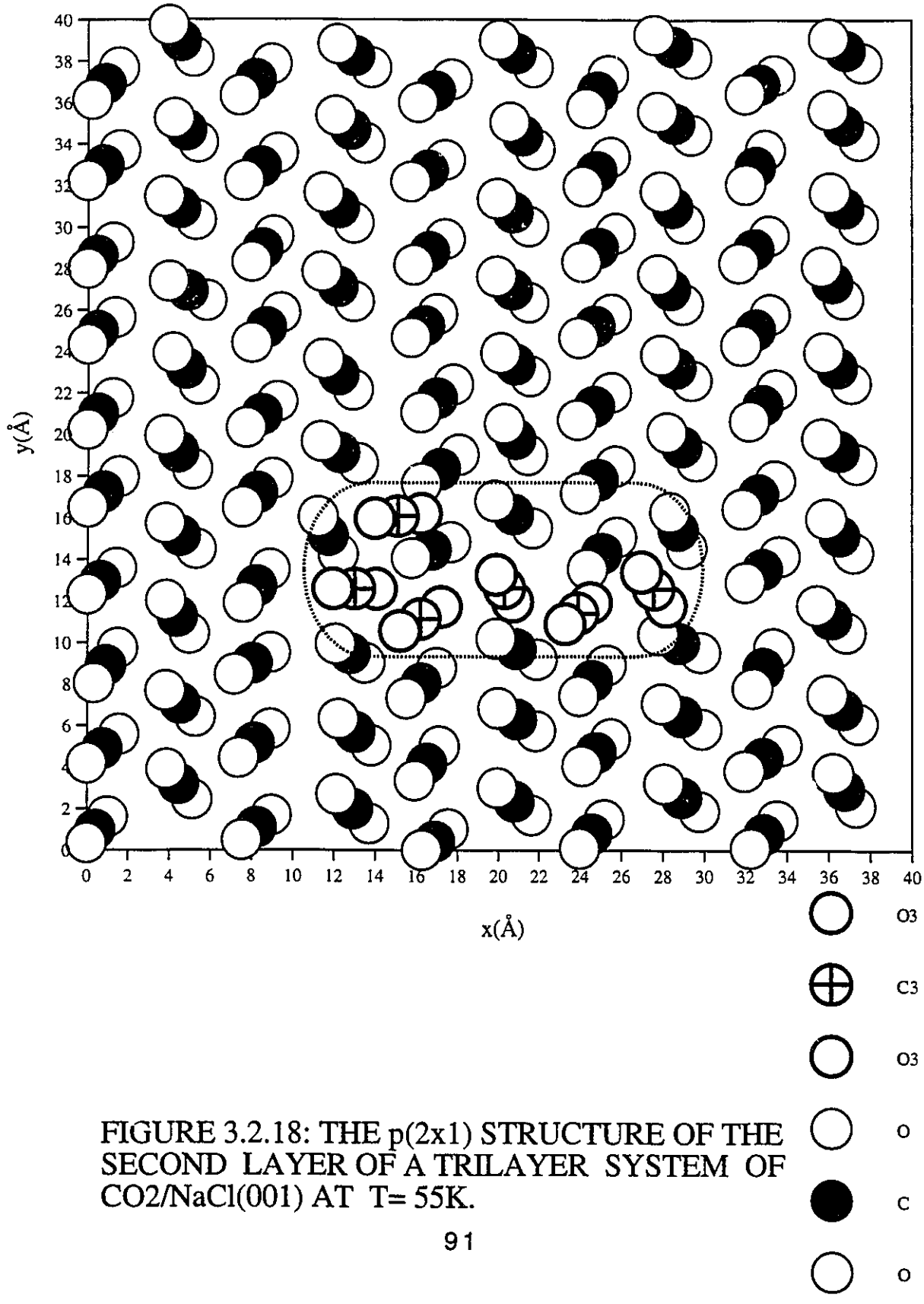

FIGURE 3.2.18: THE p(2x1) STRUCTURE OF THE SECOND LAYER OF A TRILAYER SYSTEM OF CO2/NaCl(001) AT T= 55K.

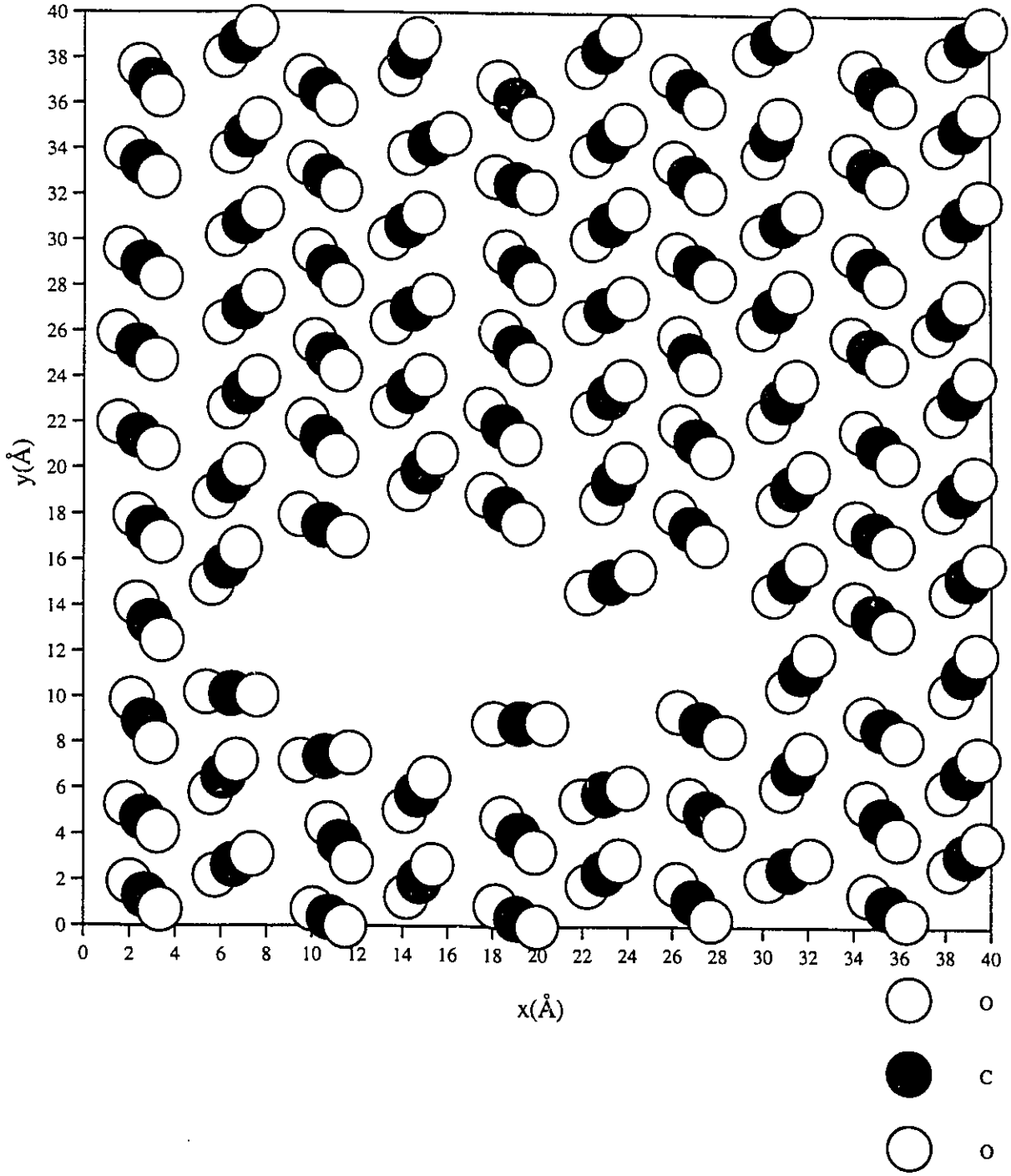

FIGURE 3.2.19: THE p(2x1) STRUCTURE OF THE THIRD LAYER OF A TRILAYER SYSTEM OF CO2/NaCl(001) AT T= 55K.

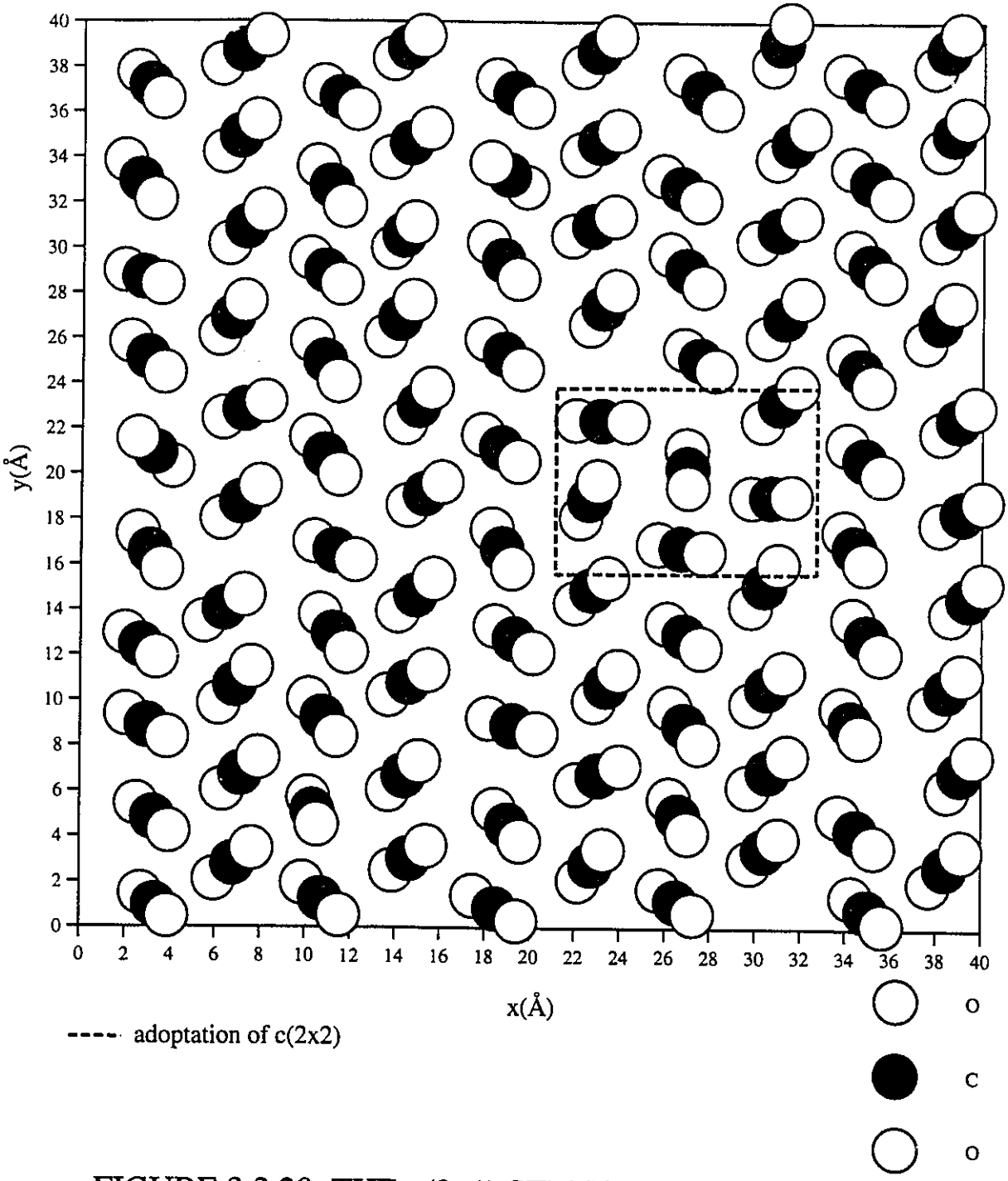

FIGURE 3.2.20: THE p(2x1) STRUCTURE OF THE THIRD LAYER OF A TRILAYER SYSTEM OF CO2/NaCl(001) AT T= 90K.

A)

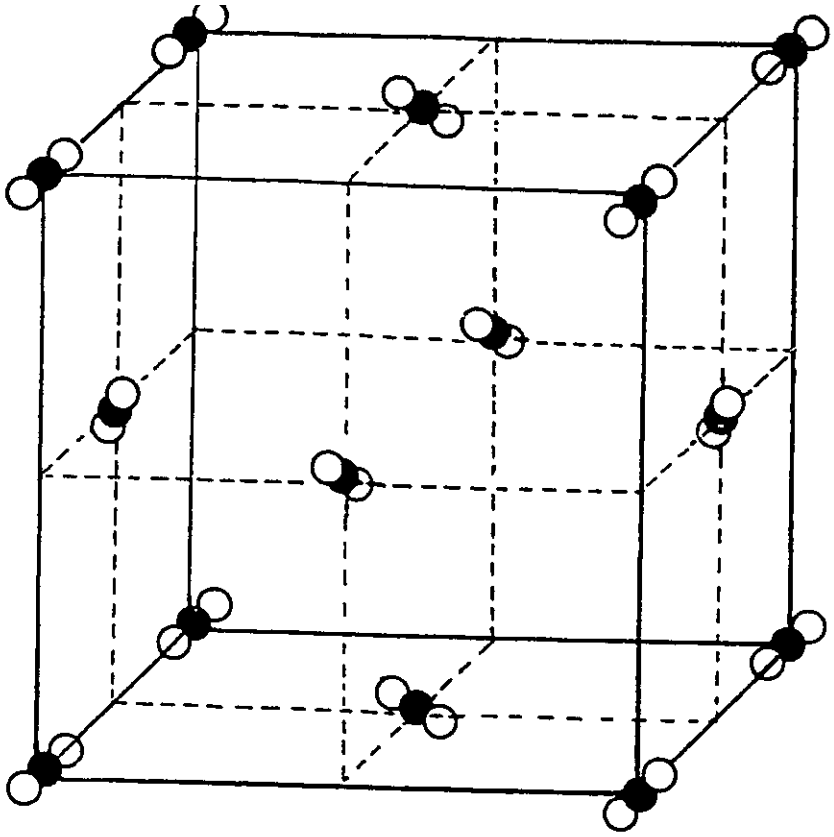

B)

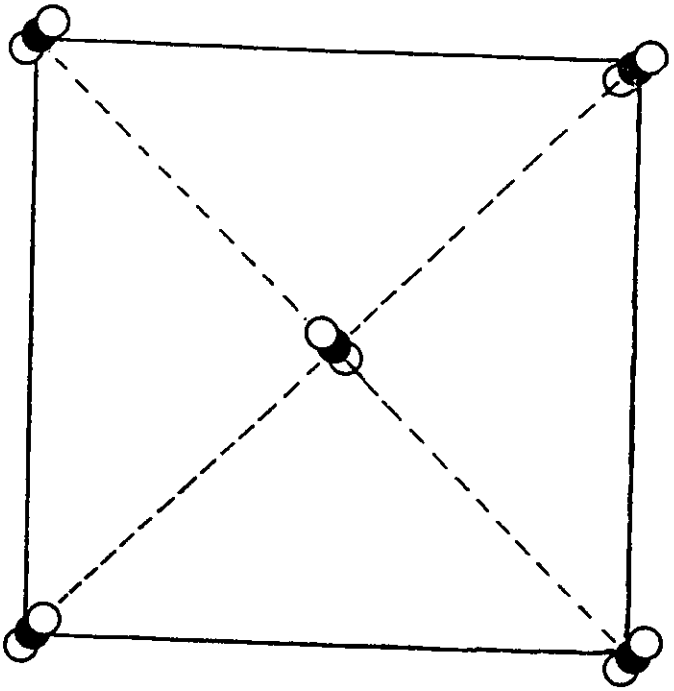

FIGURE 3.2.21: A) THE UNIT CELL OF CO_2 AND B) TOP VIEW OF UNIT CELL.

4. SUMMARY AND CONCLUSION

The Steepest Descent method for energy minimization and Metropolis Monte Carlo method were employed in our simulations. The Steepest Descent method was used to calculate the potential energy surface for a single CO_2 molecule on NaCl(001) surface and the angle between molecular axis and surface. Adjustments to the parameters which characterize the surface potential were made in order to obtain agreement with the experimental heats of adsorption. Two sets of parameters (I and II) were developed and reflected different estimates of the van der Waals interaction (CO_2-CO_2) and the heat of adsorption of the CO_2/NaCl system. For a single CO_2 molecule on NaCl(001) surface we investigated the energy minima on the surface by calculating the potential energy using parameters set I and II. The parameter set I was eventually used to construct the surface potential which was used in the Monte Carlo simulations.

The following can be concluded from these studies.

i) The absolute potential minimum was found above the center of connection line between two adjacent Na^+ at <110> direction with the molecule sitting parallel to the surface. For parameter sets I and II the minimum value of the energy was found to be E_{min}= -7.643 kcal/mol and E_{min}= -8.000 kcal/mol respectively.

ii) Saddle points in the potential energy surfaces were found above the

connection line between Na^+ and Cl^- along the <100> direction. For parameter set I it was found that the molecule tilted by 55° from the surface normal and had a binding energy of E_{sad} = -5.723 kcal/mol. Parameter set II yielded similar results; the molecule tilted by 58° from surface normal and had a binding energy of E_{sad} = -5.924 kcal/mol. Although the location of the saddle point is similar to that of the second minimum obtained by Heidberg's group[9], our calculated diffusion barrier energy is higher than the estimated experimental value.

On the whole, this method works well and gives results which match experiment. This method provides detailed calculations of the various contributions to the interaction energy between an adsorbed molecule and an alkali halide surface and thus provides a means for developing and refining the parameters which characterize the gas-solid interaction. This holds out the possibility that an even better set of parameters might be found, tested, and used in the future; indeed, this program could be used to develop a parameter set which yields a diffusion barrier in better agreement with the experimental estimate. In the meantime one could test parameter set II which has yet to be used in the Monte Carlo program.

The Metropolis Monte Carlo method was used to calculate the average potential energy, azimuthal angle φ, and polar angle θ for monolayer and multilayer systems at a number of temperatures.

The following can be concluded from these studies.

i) The monolayer system has a stable $p(2\times1)$ structure and forms a herringbone-like pattern. There are two CO_2 molecules in each unit cell which are related via a glide plane. The average potential energy is temperature dependent and was found to obey the equation: $E_{1K}+5k_B\Delta T/2$, where the value of the potential energy at 1 K was calculated to be E_{1K}=-8.457 kcal/mol. The molecules were found to tilt with respect to the surface normal by θ =60°. These results are in good agreement with experiment.

ii) The bilayer system also has a stable $p(2\times1)$ herringbone-like structure with the direction of the pattern reversing in the second layer. The average potential energy is temperature dependent was found again to obey the equation $E_{1K}+5k_B\Delta T/2$ with E_{1K} = -7.116 kcal/mol. The CO_2-CO_2 interaction energy for the bilayer is -4.049 kcal/mol which is less than 2/3 of the cohesive energy of a bulk CO_2 crystal (-6.8356 kcal/mol); a lesser value is expected because the bilayer structure differs from the $c(2\times2)$ structure of bulk CO_2. The molecules in both layers were found to tilt by an angle of θ = 60° from surface normal.

iii) The trilayer system does not have a stable $p(2\times1)$ structure for all layers; the first layer maintained an ordered $p(2\times1)$ structure but the overlayers showed a significant amount of disorder. The third layer began to collapse into the second layer down and there was evidence of the formation of the more condensed $c(2\times2)$ structure. Four, five and higher layer systems were tested and were found to be unstable.

The Monte Carlo method gave a good description of the structure and interaction energies of monolayer and multilayers of CO_2. The potential energy functions used yielded results which were in good agreement with experiment. However, there is still room for improvement of the surface potential parameters. In particular, a refined surface potential which better mimics the surface diffusion barrier energy should be developed.

5. REFERENCES

[1]. A. Lakhlifi and C. Girardet; Surface Science **241** (1991) 400; J. Chem. Phys. **94** (1991) 688.

[2]. Y. Kozirovski and M. Folman, Trans. Faraday soc. **62** (1966) 1431.

[3]. T. Hayakawa, Bull. Chem. soc. Japan **30** (1957) 124, 236, 243, 332.

[4]. Otto Berg and George E. Ewing, Surface Science **220** (1989) 207 - 229.

[5]. Wei Chen and William L. Schaich, Surface Science **220** (1989) L733- L739.

[6]. J. Heidberg, E.Kampshoff, R. Kühnemuth and O. Schönekäs, Surface Science **251/252** (1991) 314-320.

[7]. J. Heidberg, E.Kampshoff, R. Kühnemuth and O. Schönekäs, Surface Science **272** (1992) 306- 312.

[8]. J. Heidberg, E.Kampshoff, R. Kühnemuth and O. Schönekäs, Journal of Electron Spectroscopy and Related Phenomena, **64/65** (1993) 341-350.

[9]. J. Heidberg, E.Kampshoff, R. Kühnemuth and O. Schönekäs, Journal of Electron Spectroscopy and Related Phenomena, **64/65** (1993) 803 - 812.

[10]. Gany- Yu Liu, Gary N. Robinson, Giacinto Scoles, Surface Science **262** (1992) 409-421.

[11]. G. Brusdeylins, R. Bruce Doak, and J. Peter Toennies, Phy. Rev. B **27** (1983) 3663 -3685.

[12]. G. Lange, D. Schmicker, J. P. Toennies, R. Vollmer, and H. Weiss, J. Chem. Phys. **103** (1995) 2308-2319.

[13]. Keith J. Laidler and John H. Meiser, *Physical Chemistry* (the Benjamin / Cummings Publishing Company, Inc. 1982).

[14]. S. Picaud, P.N.M. Hoang, C. Girardet, Surface Science **294** (1993) 149-160.

[15]. A. Lakhifi and C. Girardet, Surface Science **241** (1991) 400-415.

[16]. A.Zangwill,*Physics At Surfaces* (Cambridge University Press 1988).

[17]. M. Rigby, E. Brian Smith and William A. Wakeham, *The Forces Between Molecules* (Oxford Science Publications1986).

[18]. V. J. Barclay, D. B. Jack, J. C. Polanyi, and Y. Zeiri, J. Chem. Phys. **97** (1992) 9458-9467.

[19]. J. C. Polanyi and R.J. Williams J. Chem. Phys. **94** (1991) 978-996.

[20]. W. A. Steele, *the Interaction of Gases with Solid Surfaces* (Great Britain by Bell and Bain LTD, Glasgow, 1974).

[21]. J. E. Lennard-Jones and B. M. Dent, Trans. Faraday Soc. **24**, 92 (1928).

[22]. P. M. Blass, R. C. Jackson, J. C. Polanyi, and H. Weiss, J. Chem. phys. **94**, 7003 (1991).

[23]. K. T. Tang and J. P. Toennies, J. Chem. Phys. **80**, 3726 (1984).

[24]. T. L. Gilbert, J. Chem. Phys. **49** (1968) 2640.

[25]. T. L. Gilbert, O. C. Simpson, and M. A. Williamson, ibid **63** (1975) 4061.

[26]. F. T. Smith, Phys. Rev. A **5** (1972) 1708.

[27]. William R. busing, *WMIN, A Computer Program to Model Molecules and Crystals in terms of Potential Energy Functions* (Oak Ridge National Laboratory Oak Ridge, Tennessee 37830, 1981).

[28]. A. D. Buckingham and R. L. Disch, Proc. R. Soc. A, **273** (1963) 275.

[29]. István Náray - Szabó, *Inorganic Crystal Chemistry* (Akadémiai Kiadó . Budapest 1969)

[30]. C. S. Murthy, S. F. O'Shea and I. R. McDonald Molecular Physiocs, **50**, No. 3 (1983) 531-541.

[31]. A. J. Stone and M. Alderton Molecular Physics, **56** , No. 5, (1985) 1047-1064.

[32]. L.Miglio,F.Quasso, and G.Benedek, J. Chem. Phys. **83**, (1985) 417.

[33]. K. T. Tang and J. P. Toennies Z. Phys. D-Atoms, Molecules and Clusters **1**, (1986) 91-101.

[34]. A. J. Stone, Molecular Physics, Vol. **56**, No. 5, (1985) 1065 -1082.

[35]. Amos, R. D., 1984, CADPAC: The Cambridge Analytical Derivatives Package, publication CCP1/84/4. Science & Engineering Research Council, Daresbury Laboratory, Daresbury, Warrington WA4 4AD England.

[36]. F. Mulder, G. F. Thomas, and W. J. Meath, Molecular Physics, Vol. **41**, No. 2, (1980) 249 - 269.

[37]. P. W. Fowler and N. C. Pyper, Mol. Phys. **59** (1986) 317-326.

[38]. P. W. Fowler and N. C. Pyper, Proc. R. Soc. A **398** (1985) 377.

[39]. M. J. Allen and D.J. Tidesley, *Computer Simulation of Liquids* (Oxford Science Publications, 1987).

[40]. J. M. Haile *Molecular Dynamics Simulation* (A Wiley-Interscience Publication, 1992).